Localization, Dynamics and Functions of the Coronavirus Envelope Protein

by

Pavithra Venkatagopalan

A Dissertation Presented in Partial Fulfillment
of the Requirements for the Degree
Doctor of Philosophy

Approved April 2012 by the
Graduate Supervisory Committee:

Brenda G. Hogue, Chair
Petra Fromme
Bertram Jacobs
Robert Roberson

ARIZONA STATE UNIVERSITY

May 2012

ABSTRACT

Coronaviruses are a medically significant group of viruses that cause respiratory and enteric infections in humans and a broad range of animals. Coronaviruses assemble at the internal membranes of the endoplasmic reticulum-Golgi intermediate compartment (ERGIC). While there is a basic understanding of how viruses assemble at these membranes, the full mechanistic details are not understood. The coronavirus envelope (E) protein is a small multifunctional viroporin protein that plays a role in virus assembly but its function is unknown. The two goals of this study were : 1. To identify and analyze the localization of MHV E and 2. To identify the functions of conserved residues in the tail of the E protein. This study closely examined the localization, dynamics and mobility of the mouse hepatitis virus (MHV) E protein to gain insight into its functions. The results from the first aim of this study showed that the MHV E protein localizes at the site of assembly in the ERGIC-Golgi region based on analysis by immunofluorescence and correlative electron microscopy. A novel tetra-cysteine tagged MHV E protein was used to study the dynamics of the protein in cells. A recombinant MHV E Lumio virus was used to study the trafficking and mobility of the E protein. Live cell imaging and surface biotinylation confirmed that the E protein does not traffic to the cell surface. Fluorescence recovery after photo-bleaching (FRAP) analyses revealed that the E protein is mobile at the site of localization. As a part of the second aim, conserved prolines and tyrosine in the tail of the protein were targeted by site directed mutagenesis and analyzed for functionality. While none of the residues were absolutely essential for localization

or virus production, the mutations had varying degrees of effect on envelope formation, protein stability and virus release. Differential scanning calorimetry data suggests that the proline and tyrosine residues enhance interaction with lipids. A wild type (WT) peptide contained the conserved residues was also able to significantly reduce the hexagonal phase transition temperature of lipids, whereas a mutant peptide with alanine substitutions for the residues did not cause a temperature shift. This suggests that the peptide can induce a negative curvature in lipids. The E protein may be playing a role as a scaffold to allow membrane bending to initiate budding or possibly scission. This data, along with the localization data, suggests that the E protein plays a mechanistic role at the site of virus assembly possibly by remodeling the membrane thereby allowing virus budding and/or scission.

ACKNOWLEDGMENTS

Dear Appa and Amma, this is for you. You gave me all the freedom to choose whatever it is I chose to do. You were there every time I needed you. You both taught me to fight the fight. Appa, you were always being painfully logical, no matter how upset I was. Amma, you always reasoned with me, no matter how angry I was. Thank you.

Dear Yogi, you have a way of explaining things- A way that is uniquely yours. Talking to you always made me feel better. Thank you.

I am incomplete without my family. I am incredibly thankful that you all have been with me through this intense journey. You reminded me that we don't get to choose the lessons we learn. You helped me stand up and keep my head high when all I wanted to do was lie down. There are so many of you! Thank you.

Kaushik, I came here to be with you. The 5 years we spent together was incredible. The little weekend vacations, the many hikes and every ordinary night and day was memorable. You know my darkest secrets and my deepest struggles with myself. You accepted me for who I am. You always remind me of my dreams and help me get to them. You have supported every one of my crazy ideas without judgement. Thank you.

Dr. Hogue, thank you for accepting me in good faith. I am sure, you have never had or you hope to never have such a "colorful" student. As improbable as it seemed quite often, we are at the end of this journey. I have learnt many lessons- some related to graduate work, some related to life itself. I am also indebted to you for convincing me to get a cat. Through your lab, I have met

people who have changed the path I had so carefully planned for myself. Thank you.

Dear Ariel and Kelly, I miss you both. Every single day I walk into the lab, I miss your warm presence. I miss your feedback about my work. I miss our lunches. I miss the dirty jokes and inappropriate comments that only you understood. You remind me everyday of the good things I can look forward to. Thank you.

Lisa, Yaralid and Blake, you taught me the importance of good food. All the members of the Hogue lab, you have all taught me little things that have taken me a long way. Rob, you were a surprise. Just when I thought I was alone, you came along and cheered me up. Thank you.

Dr Jacobs, Dr. Roberson, and Dr. Fromme, you have all been wonderfully supportive. I am incredibly lucky to have found a committee like this. You each helped me identify a weakness and helped me correct it. Thank you.

Maneesha and Val, I only wish I had met you earlier. I had a wonderful time with you both in my last year of teaching. You pushed me to be a better teacher and it was the time I enjoyed most in grad school. Thank you.

TABLE OF CONTENTS

Page

LIST OF TABLES viii

LIST OF FIGURES ix

INTRODUCTION xi

CHAPTER.....Page

1 LITERATURE REVIEW 1

2 CORONAVIRUS ENVELOPE PROTEIN REMAINS AT THE SITE OF ASSEMBLY. 30

ABSTRACT 30

INTRODUCTION.....31

MATERIALS AND METHODS.....35

RESULTS 44

DISCUSSION.....60

ACKNOWLEDGEMENTS.....70

3 CONSERVED RESIDUES IN THE TAIL OF THE CORONAVIRUS ENVELOPE PROTEIN MAY CAUSE MEMBRANE CURVATURE..... 71

ABSTRACT 71

INTRODUCTION.....73

MATERIALS AND METHODS.....78

RESULTS 86

DISCUSSION.....98

ACKNOWLEDGEMENTS.....108

4 SUMMARIZING DISCUSSION 109

References 116

Appendix

A OPTIMIZATION OF THE USE OF THE TETRA CYSTEINE TAGGED E FOR USE IN CORRELATIVE LIGHT ELECTRON MICROSCOPY (CLEM) AND LIVE CELL IMAGING.....137

LIST OF TABLES

Table Page

1. Coronavirus classification, hosts and infections 4

2. Primers used for generation of mutant viruses 79

LIST OF FIGURES

Figure Page

1. Coronavirus classification and evolution 5
2. Coronavirus virion schematic 8
3. The Envelope Protein 14
4. Coronavirus genome and replication 21
5. Coronavirus Lifecycle 25
6. MHV E localizes in the ERGIC and Golgi 42
7. MHV E does not traffic beyond the site of assembly 47
8. MHV E localizes to membranes around assembled virions 49
9. Characterization of TC-tagged E and recombinant MHV with tagged E 52
10. MHV E Lumio virus allowed live cell imaging of the E protein during infection 55
11. CLEM of TC-tagged E in infected cells 59
12. Schematic illustration of E protein potential roles at its localization in ERGIC/Golgi membranes during infection 66
13. Alignment of tail of the E protein 75
14. Characterization of mutant viruses 87
15. Mutations do not affect virion morphology 89
16. Mutations affect virus release and protein stability 93
17. WT peptide interacts with lipids 96

18. Secondary structure prediction of E proteins 102

19. Mechanism of action of the E protein 106

20. Mechanistic role of E in driving virus assembly..... 113

21. Protocol for Correlative Live Imaging and Electron Microscopy...140

INTRODUCTION

Coronaviruses are medically significant viruses that cause a variety of respiratory and enteric diseases in humans and a broad range of domesticated animals. Roughly 30% of upper respiratory infections that cause common cold like symptoms in humans are caused by coronaviruses and they have relatively mild symptoms. Before 2002, coronaviruses were mainly studied because of the devastating effects they had on the cattle and poultry industry. In 2002, the emergence of a new virus - the severe acute respiratory syndrome (SARS) demonstrated the lethality of coronavirus infections in humans. The virus caused significant economic and social disruption. Two novel human coronaviruses – HKU1 and NL63, have been discovered since. The identification of SARS-like coronaviruses in various animal reservoirs allows the potential for re-emergence. Thus it is essential to understand these viruses to better facilitate the development of vaccines and anti virals. The focus of this dissertation, virus assembly, is a good target for development of antiviral reagents.

Coronaviruses are single stranded positive sense RNA viruses with a genome size of up to 31kb. These viruses belong the *Coronaviridae* family in the *Nidovirales* order. The viral envelope contains three main structural proteins. The spike (S) protein decorates the viral envelope giving the virus the classic crown like appearance (*corona* in Latin). The membrane (M) protein is the most abundant protein in the viral envelope. M interacts with itself and other structural proteins to form the virus lattice and organizes assembly. The singe stranded

RNA genome is encapsidated by the nucleocapsid (N) protein to form a helical nucleocapsid. The envelope (E) protein is a minor component of the viral envelope but previous studies indicate that it plays an important role in virus assembly.

The coronavirus E protein is a small viroporin protein ranging from 12-15kD. There is very low sequence homology among the coronavirus E proteins, but the overall structure of the proteins remains the same. There is a short amino terminus, followed by a long hydrophobic domain, and a long highly charged carboxy tail. The protein is palmitoylated and membrane associated. The minimal requirements for the formation of MHV virus like particles (VLPs) are the expression of the E and M proteins. Coronavirus assembly occurs at the internal membranes of the endoplasmic reticulum Golgi intermediate compartment (ERGIC) and Golgi. This study closely examined the localization of the MHV E protein. The E protein was found to localize at the ERGIC-Golgi membranes. This was the first study to determine the dynamics of the E protein using a novel tetracysteine tagged system. Correlative light electron microscopy (CLEM) was established and the localization of the E protein was further confirmed to be the in the Golgi. The tail of the E protein has two highly conserved prolines and tyrosine. We hypothesized that these conserved residues play a critical role in the function of the E protein. Results from this study suggest that the tail of the E protein may play a role in inducing membrane curvature at the site of assembly. We identified that these residues played a critical role in the membrane interaction of the E protein and likely affects virus assembly.

Chapter 1

LITERATURE REVIEW

History and classification of Coronaviruses

Viruses are intracellular parasites that have evolved and co-existed with all life forms. The first non-bacterial infectious agent was described in 1892 and the first virus - Tobacco Mosaic Virus was described in 1898 (Lustig and Levine 1992). Since then, more than 5000 viruses have been discovered. Viruses can manifest in a wide range of ways, ranging from asymptomatically co-existing in their host or replicate aggressively, destroying the host cells in the process. Viruses have co- evolved with every life form.

Coronaviruses were first discovered in the 1930's (Schalk & Hawn 1931). The first identified coronavirus was from poultry, called avian infectious bronchitis virus (IBV) followed by murine hepatitis virues (MHV) and transmissible gastroenteritis virus (TGEV) found in pigs (Beaudette 1950; Bailey et al. 1949; Doyle and Hutchings 1946). The first human coronavirus was identified in the 1968 from fecal matter (Tyrrell, Bynoe, and Hoorn 1968). The coronavirus genus was defined based on the crown-like appearance produced by the surface glycoprotein, and thus resulting in the name *corona* which is Latin for crown (Lecce, King, and Mock 1976).

Coronaviruses are in the order *Nidovirales* along with *Arteriviridae* and *Roniviridae*. All viruses in this order have an RNA genome and carry out RNA synthesis using a discontinuous negative stranded synthesis mechanism for transcription (S. G. Sawicki and Sawicki 1990). They all produce a 3'-co-terminal

nested set of subgenomic mRNAs. Coronaviruses are in the *Coronaviridae* family along with the Torovirus genus. While they have similar genome organization and replicate using similar strategies, the torovirus genome is smaller, at about 28 kb (Cavanagh et al. 1993). The viral replicase gene encodes the key functions required for coronavirus RNA synthesis. The gene comprises more than 20,000 nucleotides and encodes two replicase polyproteins, pp1a and pp1ab, that are proteolytically processed by viral proteases (Flint, Enquist, and Racaniello 2009). The replicase genes are encoded by two-thirds of the genome. All the viral structural proteins are translated from the subgenomic mRNAs (Lecce, King, and Mock 1976; Cavanagh 1997; Cavanagh et al. 1990).

Evolution of Coronaviruses

Coronaviruses are separated into four groups based on various serological assays including antibody cross reactivity, neutralization from sera of infected hosts (Siddell 1995; Dea, Verbeek, and Tijssen 1990; Flint, Enquist, and Racaniello 2009) (Fig. 1) Each group is further characterized according to their host and diseases which they cause (F. Li 2012). Coronaviruses infect a wide range of animals and humans. Since the identification of the first coronavirus in the 1930's, several new coronaviruses have been identified in both animals and humans. Coronaviruses mainly cause respiratory and enteric infections in humans and domesticated animals (Table 1). Evolution of different strains of coronaviruses among various hosts have also been studied using sequence analysis of different viral genes (Siddell 1995).

Until recently, a large emphasis on understanding coronavirus infection was to develop vaccines against viruses that infected pets and cattle. Severe infections in humans were not identified even though up to 30% of all common colds have been attributed to coronaviruses (Hamre and Procknow 1966; McIntosh et al. 1967; Tyrrell, Bynoe, and Hoorn 1968; El-Sahly et al. 2000). However, a novel coronavirus emerged in 2003 and was named severe acute respiratory syndrome coronavirus (SARS-CoV). The emergence of SARS of epidemic not only had significant impact on global economics and trade but caused up to 40% mortality in children and elderly people (Kienzle et al. 1990; Ksiazek et al. 2003). The World Health Organization (WHO) estimated that 8000 cases were confirmed with 10% mortality rate (Parry 2003). SARS-CoV causes more severe disease then other previously known human coronaviruses and results in atypical pneumonia, fever, and shortness of breath (Lewicki and Gallagher 2002; Ksiazek et al. 2003). It was originally thought SARS-CoV originated exotic trade in China but it has now been identified from sequencing data that the reservoir is likely bats (Gagneten et al. 1995; Lau et al. 2005; W. Li et al. 2005). Although the epidemic died out naturally and controlled by careful health practices, the identification of SARS-like coronaviruses in bat reservoirs keeps the possibility of re-emergence of SARS-CoV or SARS like viruses alive (Thorp et al. 2006; Tong et al. 2009). Since the emergence of SARS, two new human coronaviruses have been isolated- HKU-1 and NL-63. Both HKU-1 and NL-63 coronaviruses infect infants but only cause mild respiratory diseases compared to SARS-CoV infection (Lau et.al 2006; Sloots et.al 2006).

Group	Virus	Host	Respiratory	Enteric	Hepatitis	Neurologic	Other*
Alpha	HCoV-229E	Human	X				
	HCoV-NL63	Human	X				
	TGEV	Pig	X	X	X		
	CCoV	Dog		X			
	FIPV	Cat	X	X	X	X	X
	RbCoV	Rabbit			X		
Beta	HCoV-OC43	Human	X				
	SARS-CoV	Humans	X	X			
	HCoV-HKU1	Humans	X	X			
	MHCoV	Mouse	X	X		X	
	HECoV	Pig	X	X			
Gamma	IBV	Chicken	X		X		X
	TCV	Turkey	X	X			
Delta #		Wild aquatic birds					

* Infectious peritonitis, immunological disorders, nephritis, pancreatitis, etc

Suggested new group

Table 1: Coronavirus classification, hosts and infections

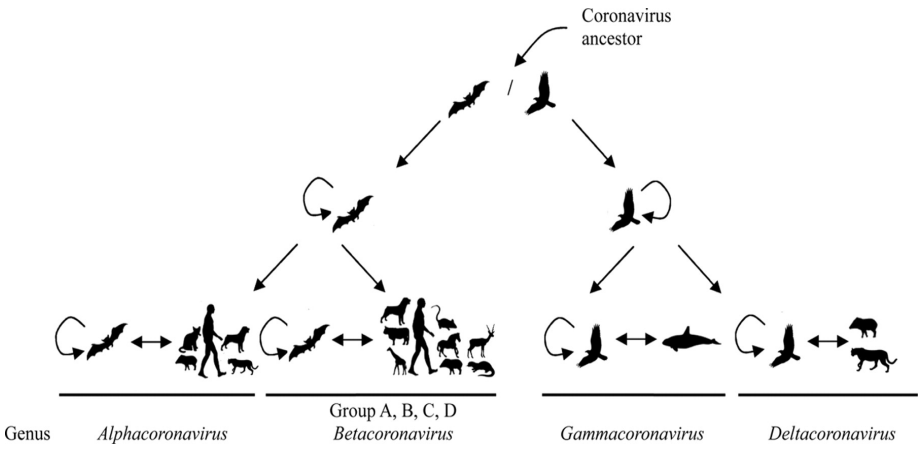

Figure 1: Evolution of Coronaviruses:

Currently, coronaviruses are classified into four groups. Classification into each group depends on immunogenicity of the spike proteins on the virus. Viruses can recombine with each other when co-infected in a host to give rise to new strains.

Woo P C Y et al. J. Virol. 2012; 86: 3995-4008

Reproduced with permission from Journal of Virology

Coronaviruses infections in cattle and domesticated animals have a significant impact on the global poultry, cattle and swine industries. TGEV infections are highly transmissible and can cause large-scale fatal diarrhea in pigs (Lecce, King, and Mock 1976). IBV infections cause wide spread death in poultry farms. Canine coronavirus infections are vaccine preventable (Pratelli et al. 2003) whereas feline coronavirus infections are fatal.

Virion morphology and structure

Coronaviruses are enveloped viruses with a single stranded positive sense RNA genome. They have the largest known RNA genome ranging from 27-31kb. The viruses are pleomorphic and range from 100- 120 nm in size (Flint, Enquist, and Racaniello 2009; Lai and Cavanagh 1997). The large genome is bound by the nucleocapsid (N) protein to form a helical nucleocapsid (Flint, Enquist, and Racaniello 2009). The viral envelope is derived from host membranes. Three main structural proteins, the spike (S), membrane (M), and envelope (E) proteins are anchored in the envelope (Fig. 2). Some coronaviruses also contain the hemagglutinin esterase (HA) protein in the viral envelope (Kienzle et al. 1990) .

Structural Proteins

Spike (S) Protein

The spike (S) protein is present in the virion envelope, and protrudes to give the characteristic crown like appearance to the virus (Fig. 2). The S protein initiates infection by binding to cellular receptors. Neutralizing antibodies are

produced against the S protein during infection(Jiménez et al. 1986) . The S protein is a large glycoprotein that is roughly 150-180kD in size and is thought to form trimers in the viral envelope (Cavanagh 1983; Luytjes et al. 1988; Lewicki and Gallagher 2002; Delmas and Laude 1990). The S protein is a type I membrane protein that has a short C terminal endo-domain, followed by a transmembrane domain and a large N terminal domain that extends outside the virion. The protein is highly glycosylated and during maturation of the S protein in the cell, it is cleaved by cellular proteases to form S1 and S2 regions that remain non-covalently associated (Sturman et.al. 1990). The globular S1 region binds to host cell receptor and there is a lot of variability in the S1 sequence among coronaviruses giving a wide range of hosts for coronaviruses to infect. The S2 region constitutes the stalk region of S and is not exposed to the immune system. There are two conserved heptad repeats in the S2 region and they are thought to form a coiled-coil structure (Siddell 1995; Gagneten et al. 1995). Once the S1 binds to the cellular receptor, the S2 region is important for mediating fusion between viral and host membranes (Fleming et al. 1983; Thorp et al. 2006; Ziebuhr 2005; Z. Luo and Weiss 1998). For SARS, cleavage of S1 and S2 occurs during entry by an unknown mechanism (Cavanagh 1997; Sturman and Holmes 1977; Hsieh et al. 2005). However, the S proteins of group I coronaviruses are not cleaved (De Haan et al. 2008; de Groot et al. 1989).

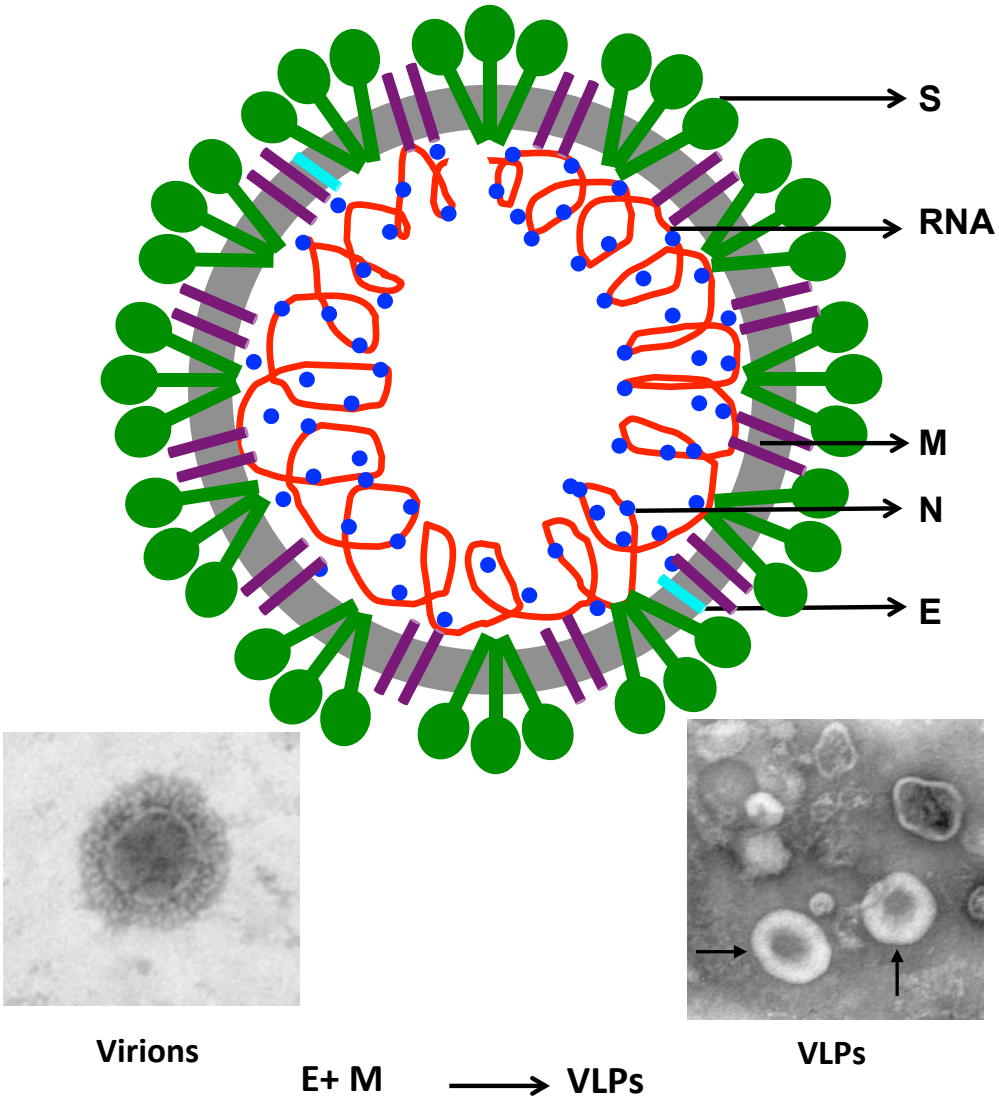

Figure 2: Coronavirus virion schematic

The virus envelope is depicted in gray. The viral envelope proteins spike (S), membrane (M) and envelope (E) are shown in green, purple and cyan respectively. The RNA genome (red) is encapsidated by the nucleocapsid (N) protein shown in blue.

The S protein initiates the coronavirus infection. S is highly immunogenic and is recognized by many monoclonal neutralizing antibodies (Shih et al. 2006). The S2 region mediates extensive fusion between viral and cell membranes and cell to cell membranes (Gombold, Hingley, and Weiss 1993; Routledge et al. 1991). This causes a cytopathic effect which is characteristic of betacoronavirus infection (Gombold, Hingley, and Weiss 1993). The S protein traffics to the cell surface in the absence of the M protein and mediates cell-to-cell fusion. Crystal structures N terminal domain of S, along with the MHV receptor have been obtained (Peng et al. 2011).

Hemagglutinin-esterase (HE) protein

The HE glycoprotein is found on the virion of some beta and gamma coronaviruses (Siddell 1995). Coronaviruses lacking the HE protein do not have a significant effect in virulence in vivo and the HE gene is frequently lost in viruses passaged in cell culture. It has been proposed that a co-infection of a host with a coronavirus and Influenza C virus allowed a recombination to incorporate HE into the coronavirus genome (Luytjes et al. 1988). It is a 65 kD glycoprotein that forms short spikes in the viral envelope. It associates with the S and M proteins in infected cells. It exists as disulfide linked dimers and has both heagglutinating and esterase activity (Siddell 1995; Hogue, Kienzle, and Brian 1989). It is unknown whether the protein plays a role in virus entry or release or both. However, by itself, it cannot initiate infection and S protein is required for this process (Fleming et al. 1983; Ziebuhr 2005). The HE protein is not essential for virus replication and assembly in cell culture. Upon repeated passaging, the

HE protein is deleted or mutated in the genome (Cavanagh 1997). In some strains of MHV, the HE protein increases neurovirulence in mice (Kazi et al. 2005).

Membrane (M) Protein

The M protein is the most abundant protein in the viral envelope (Fig. 2). It is a type III membrane protein and is about 25 kD in size (Locker et al. 1992). It has a short amino terminus followed by three membrane-spanning domains and a long carboxy tail located inside the virion (Locker et al. 1992). For alphacronaviruses like TGEV both amino and carboxy ends of the M protein are possibly located on the outside of the virion (Risco et al. 1995). M localizes in the Golgi region when expressed alone (Klumperman et al. 1994; Krijnse-Locker et al. 1994). The amino terminus is O- or N-linked glycosylated depending on the virus classification (Voss et al. 2009; Niemann et al. 1984; S. A. Tooze, Tooze, and Warren 1988; Niemann et al. 1984; Lai and Cavanagh 1997; Oostra et al. 2006). While glycosylation does not appear to be important for correct localization of the protein or virus production, it has been implicated to play a role in interferon induction (de Haan et al. 2003; de Haan et al. 1998). The M protein and its interactions with viral and host proteins drives virus assembly (Wang et al. 2009). M molecules interact with each other to form a lattice and M also interacts with the S protein and nucleocapsid during virus assembly (de Haan et al. 1999; de Haan, Vennema, and Rottier 2000; Escors et al. 2001; Kuo and Masters 2002; Nguyen and Hogue 1997; Opstelten et al. 1995). The S protein and a small number of E molecules are interspersed in the M protein lattice in mature virions. The M-N interaction involves the carboxy end of both M and N proteins and it

occurs in the absence of the S and E proteins (Hurst et al. 2005; Kuo and Masters 2002; H. Luo et al. 2006; Narayanan et al. 2000; Verma et al. 2006). The M protein also interacts directly with the RNA packaging signal further increasing the specificity of packaging only of nucleocapsids associated with full length genomic RNA (Narayanan and Makino 2001). Coronavirus M proteins also interact with host proteins. For example, specific domain in the IBV M have been shown to interact with beta-actin (Wang et al. 2009) and results suggest this interaction may be important for virus assembly and budding.

Nucleocapsid (N) protein

The N protein is a highly basic nucleic acid binding protein rich in lysines and arginines. It is approximately 55kD and is phosphorylated (Wilbur et al. 1986; Molenkamp and Spaan 1997; White, Yi, and Hogue 2007). The protein can be divided into three domains (Parker and Masters 1990). The amino and central domains have an overall positive charge and the carboxy domain has an overall negative charge (Parker and Masters 1990). The sequences in between the domains are highly variable. Specific phosphorylation sites have been identified for TGEV, MHV, SARS-CoV and IBV and the sites are clustered around the amino- central domains and at the carboxy domain (Calvo et al. 2005; H. Chen et al. 2005; White, Yi, and Hogue 2007). The primary function of the N protein is encapsidation of the genomic RNA (Fig.2). This forms a flexible helical nucleocapsid (Narayanan, Kim, and Makino 2003; Baric et al. 1988; Chang and Brian 1996; Macneughton and Davies 1978). The domains required for RNA binding are different in different viruses. In IBV and SARS N, the RNA binding

region is the amino terminal (Zhou and Collisson 2000). For MHV, the RNA binding domain is the central domain (Q. Huang et al. 2004). The sequence specificity of RNA binding to N is unknown, but the N protein does specifically binds to the packaging signal (Cologna, Spagnolo, and Hogue 2000). The conserved SR- rich region has been identified for N multimerization and cellular localization (H. Luo et al. 2005). The N protein may also play a role in inhibiting host cell translation (Tsui-Yi Peng, Lee, and Tarn 2008). The N protein can non specifically bind to the genomic RNA, as well as the 5' leader, 3' untranslated region (UTR) and the packaging signal (Cologna and Hogue 2000; Masters 1992; Molenkamp and Spaan 1997; Nelson and Stohlman 1993; Nelson, Stohlman, and Tahara 2000). The N protein may also function as an RNA chaperone, playing a role in RNA synthesis, stability and increase the efficiency of replication (Almazán, Galán, and Enjuanes 2004; Chang and Brian 1996; Schelle et al. 2005; Yount, Curtis, and Baric 2000; Yount et al. 2002). It may play a role in template switching during transcription. The N protein also plays a role in virus assembly and is an important structural protein. The interaction of the N protein with the M protein likely results in the envelopment of the nucleocapsid into the viral particle. Specific residues in the carboxy domain of the M and N proteins are required for M-N interactions (Verma et al. 2006; Verma et al. 2007). The N protein may also function as an interferon antagonist (Ye et al. 2007).

Envelope (E) Protein

The E protein is present in low abundance in the virion envelope It is 9-12 kD in size is the focus of this dissertation. All coronavirus E proteins share similar

conserved characteristics. These include a short amino terminus, a long hydrophobic transmembrane region, and a cysteine-rich region after the hydrophobic domain, conserved prolines, and a highly charged carboxy terminal domain. Two topologies have been reported for E proteins where it spans the membrane once or twice depending on the virus strain (Maeda et al. 2001; Arbely et al. 2004). The SARS E protein has been shown to localize at the membranes of ERGIC/Golgi (Cohen, Lin, and Machamer 2011). The MHV E protein is predicted to have two membrane topologies, with the carboxy tail always in the cytoplasm. (Fig. 3) (Maeda et al. 2001). The hydrophobic domain of the E protein is predicted to form an amphipathic helix and affecting the pitch of the helix impacts the ion channel activity of the protein and virus production and release (Ye and Hogue 2007). The transmembrane domain of IBV E protein can be replaced with the transmembrane domain from VSV-G, with effects on VLP formation and protein localization (Ruch and Machamer 2011). The transmembrane domain of IBV E may affect trafficking of host protein in the cells (Ruch and Machamer 2011). Additionally, E is palmitoylated on cysteine residues in the cysteine-rich region for several coronaviruses. The palmitoylation of the cysteine residues are important for protein stability and virion trafficking (Boscarino et al. 2008; Lopez et al. 2008). It has been proposed that the insertion of the palmitic acid modifications can anchor the protein in the membrane by insertion into the membrane (Lopez et al. 2008)

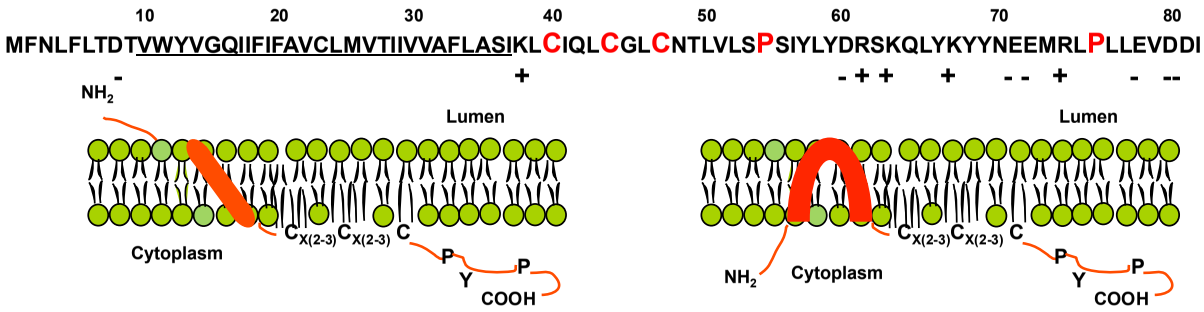


```
Group I
TGEV     MTFPRALTVIDDNGMVINIIFWFLLIIILILLSIALLNIIKLCMVCCNLG-RTVIIVP----AQHAYD---AYKNFMRIKAYNPDGALLA----------- 82
FeCoV    MTFPRAFTIIDDHGMVVSVFFWLLLIIILILFSIALLNVIKLCMVCCNLG-KTIIVLP----ARHAYD---YKTFMQTKAYNPDEAFLV----------- 82
229E     -MF---LKLVDDHALVVNVLLWCVVLIVILLVCITIIKLIKLCFTCHMFC-NRTVYGP----IKNVYH---IYQSYMHIDPF-PKRVIDF---------- 77
NL63     -MF---LRLIDDNGIVLNSILWLLVMIFFFVLAMTFIKLIQLCFTCHYFF-SRTLYQP----VYKIFL---AYQDYMQIAPV-PAEVLNV---------- 77

Group II
MHV    --MFNLFLTDTVWYVGQIIFIFAVCLMVTIIVVAFLASIKLCIQLCGLC-NTLVLSP----SIYLYDRSKQLYKYYNEEMRLPLLEVDDI---------- 83
BCV    MFMADAYFADTVWYVGQIIFIVAICLLVIIVVVAFLATFKLCIQLCGMC-NTLVLSP----SIYVFNRGRQFYEFYN-VKPPVLDVDDV---------- 84
OC43   MFMADAYLADTVWYVGQIIFIVAICLLVTIVVVAFLATFKLCIQLCGMC-NTLVLSP----SIYVFNRGRQFYEFYN-DIKPPVLDVDDV---------- 84
HEV    MFMADAYLADTVWYVGQIIFIVAICLLVIIVVVAFLATFKLCIQLCGMC-NTLVLSP----SIYVFNRGRQFYEFYN-VKPPVLDVDDV---------- 84
SARS   MYSFVSEETGTLIVNSVLLFLAFVVFLLVTLAILTALRLCAYCCNIV---NVSLVKP----TVYVYS---RVKNLNSSEGV-PDLLV---------- 76
HKU 1  ---MVDLFFNDTAWYIGQILVLVLFCLISLIFVVAFLATIKLCMQLCGFCNFFIISP----SAYVYKRGMQLYKSYSEQVIPPTSDYLI---------- 82


Group III
IBV-MTNILSKSLEENGSFLTAVYIFVGFLAFYLLGRALQAFVQAADACCLFW-YTWVVVPGAKGTAFVYN--HTYGKKLNKPELEAVIVNEFPKNGWNNKSPANFQYDGKLHT 107
```

Figure 3: The Envelope protein

The envelope protein has a small amino end followed by a long transmembrane domain that spans the lipid bilayer once. The conserved cysteines are palmitoylated. The tail is highly charged and is oriented towards the cytoplasm or inside the virion. The cysteines are at residues 40, 44 and 47. The conserved prolines are at residues 54 and 76.

Adapted from Lopez et.al., J Virol. 2008 Mar;82(6):3000-10.

When charged residues within the carboxy domain of E were mutated to neutrally charged alanines, virions displayed an aberrant morphology and low thermo-stability (Fischer et al. 1998). A putative localization signal has been identified in the tail of the E protein that is predicted to form a helix-turn helix .(Cohen, Lin, and Machamer 2011). The MHV M and E proteins are sufficient and required for budding of virus-like particles (VLPs) (de Haan, Vennema, and Rottier 2000). However, when expressed alone the E protein is released from transfected and infected cells in the form of vesicles (J. Maeda, Maeda, and Makino 1999). Therefore, it is thought that the E protein triggers virus assembly. The E protein also causes local membrane modifications in the cell called tubular bodies (Ulasli et al. 2010; Raamsman et al. 2000). The exact role of E has not been elucidated but it has been shown to play an important role in virus production. Deletion of the E protein from the viral genome results in a varying phenotype that is strain dependent. Absence of TGEV E results in a lethal phenotype whereas deletion of E from SARS-CoV causes only a marginal decrease in virus production that is cell type dependent (Ortego et al. 2007; DeDiego et al. 2007). Even though MHV E can be deleted from the genome and viruses are viable, these mutants grow to titers several logs lower compared to WT. Additionally, coronavirus E proteins have been shown to have ion channel activity which presumably plays a role in viral entry and/or budding (Wilson, Gage, and Ewart 2006; Wilson et al. 2004; Ye and Hogue 2007). NMR data of the transmembrane region has helped identify critical pore lining residues in the E protein (Pervushin et al. 2009). SARS E protein has been shown to be

ubiquitinated, interacts with nsp3 and members of the cellular cytoskeleton (Alvarez et al. 2010). This may be playing a role in directing virus trafficking in cells. SARS E has also been shown to interact with PALS 1 at tight junctions in cells (Teoh et al. 2010). SARS-CoV deleted of the E protein has been shown to be effective as a SARS vaccine. This mutant virus causes a much milder infection but induces a robust immune response including cytokine response suggesting that the E protein may function as a virulence factor (Dediego et al. 2007; Dediego et al. 2007; Dediego 2008).

Coronavirus Genome and Nonstructural Proteins

Viral Genome

Coronavirus genome consists of a single stranded, positive sense RNA. The genome is a 5' 7-methyl guanosine capped and a 3' poly (A) tailed, resembling a large cellular mRNA (Schochetman, Stevens, and Simpson 1977). Purified genome is infectious (Lai and Cavanagh 1997). There is a leader sequence at the 5' end of the genome and is 65-98 nucleotides in length. This leader is also located at the 5' ends of all the subgenomic mRNAs. There are untranslated regions (UTRs) that are about 300 nucleotides at both the 5' and 3' ends of the genome, which play important roles in RNA replication and transcription (Lai and Cavanagh 1997; Spagnolo and Hogue 2000) . Translation begins immediately upon virus entry, since the genome is infectious. The first two thirds of the genome contain open reading frame (ORF) 1, which encodes ORF1a and ORF1b. ORF 1a and ORF1b encode all the proteins necessary for transcription and replication. Translation of ORF 1b occurs after ribosomal

frame-shifting at a region between the two ORFs (Brierley et al. 1987; Lai and Cavanagh 1997).The last one third of the genome encodes all the structural genes. The order of translation is always 5' S-E-M-N-3'(de Haan et al. 2002). Several group specific nonstructural genes are present interspersed among the structural ORFs. The function of the nonstructural proteins is peripheral and is not required for replication in cell culture. Deletion of these accessory genes has an impact on viral replication in animals, such as MHV replication in mice (de Haan et al. 2002). Analysis of the SARS-CoV genome revealed the presence of the largest number of nonstructural genes identified so far and none of them were essential for growth in cell culture (Yount et al. 2005). It is possible that these accessory genes contributed to the increased virulence of SARS-CoV.

Nonstructural Proteins (nsps)

The largest non-structural protein is translated from the first two- thirds of the genome. The ORF1a/ b proteins are translated as a large polyprotein which are then proteolytically cleaved into the proteins necessary for transcription and replication. ORF1 encodes for up to sixteen nonstructural proteins (Ziebuhr 2005; Ziebuhr, Snijder, and Gorbalenya 2000). All coronaviruses encode for papainlike and chymotrypsinlike proteases from ORF1a (Lai and Cavanagh 1997) . These proteases then completely process the ORF1 polyprotein through various processing intermediates (Xu et al. 2001; Ziebuhr and Siddell 1999; Stobart et al. 2012). These proteases are critical for coronavirus replication and many drugs have been developed against SARS-CoV proteases (Ramajayam, Tan, and Liang 2011). Since ORF1a encodes for many proteins, most have not been

characterized. One of the most well studied non-structural proteins is nsp3. It has an ADP-ribose 1'-phosphatase activity and a cylindrical structure. It may have a single stranded RNA binding domain and may be important for virus replication (Egloff et al. 2004; Saikatendu et al. 2005). ORF1b encodes for the viral RNA dependent RNA polymerase (RdRp) (nsp12) and a helicase (nsp13). The nsp13 also has other enzymatic activities including NTPase, dNTPase, and 5'-triphosphatase activities.(Seybert et al. 2000) ORF1b also encodes a 3'-to-5' exonuclease (ExoN), a uridylate-specific endoribonuclease (N endoU). In addition, the nsp10/nsp16 complex function as an mRNA capping enzyme 2'-O-methyltransferase (Snijder et al. 2003). The ORF1 proteins localize to regions of intracellular membranes. Extensive membrane modification occurs during replication (Ulasli et al. 2010). Some of the nonstructural proteins such as nsp6 have been implicated in the process, which produce autophagosome utilizing membranes of the ER (Cottam et al.2011). Proteins of the replicase complex localize to double membrane vesicles (DMVs) around the perinuclear region in MHV and SARS CoV (Snijder et al. 2006; Gosert et al. 2002). ORF 8a of SARS CoV encodes for an ion channel protein (Chen et al.2011).

Viral Life Cycle

Attachment and Entry

Coronavirus infection is initiated with the virion attaching to susceptible host cell receptors (Fig. 4). This interaction is very specific. The S protein is the virus attachment protein that binds to specific receptors found on the cell surface. Different coronaviruses use different receptors to initiate infection. Several such

receptors of coronavirus infection have been identified. The S- receptor determines host specificity and cellular tropism. The receptor for MHV infection is a biliary glycoprotein in the carcinoembryonic antigen family, Ig superfamily (CEACAM1) (Dveksler et al. 1991; Williams, Jiang, and Holmes 1991). The MHV S protein binds to the extracellular Ig-like loops of the CEACAM1a receptor. CEACAM1 molecules are expressed in the liver and gastrointestinal tract, on macrophages, dendritic cells, B cells, and activated T cells in mice (Lai and Cavanagh 1997; Nakajima et al. 2002; Turner et al. 2004).

Alphacoronaviruses utilize a host specific cell membrane-bound metalloprotease called aminopeptidase N (APN) as their receptor (Lai and Cavanagh 1997; Benbacer et al. 1997). APN is distributed in respiratory and intestinal epithelium and on neuronal cells as well as at synaptic junctions (Shapiro et al. 1991).

Betacoronaviruses use the N-acetyl-9-O-acetylated sialic acid as their receptor on host cells (Schultze and Herrler 1992; Künkel and Herrler 1993). The host cell receptor for SARS-CoV and HCoV-NL63 is the angiotensin-converting enzyme 2 (ACE2) (Hofmann et al. 2005; W. Li et al. 2003). ACE2 is expressed in several tissues including the heart, lung, kidney and small intestine (Hamming et al. 2004).

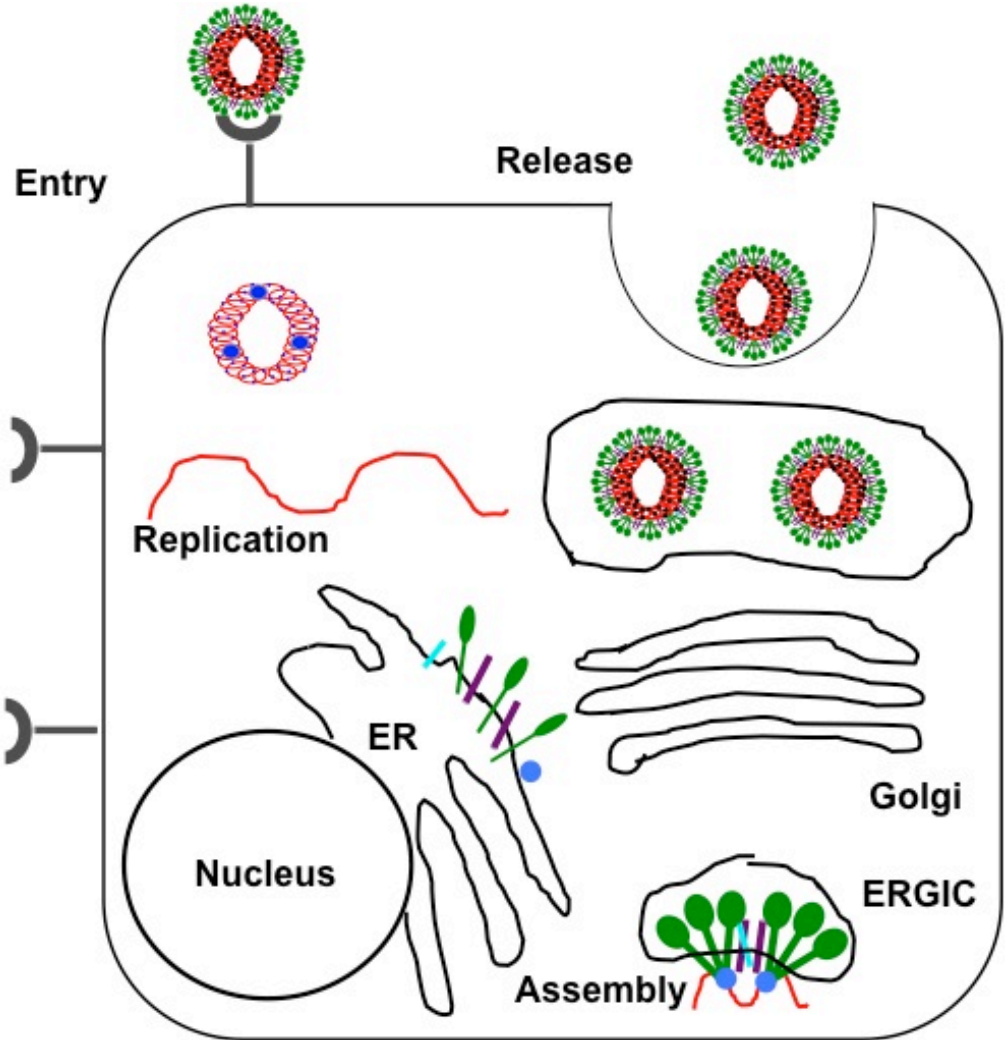

Figure 4: Coronavirus lifecycle

Coronavirus entry is initiated by receptor- mediated endocytosis. Virus replication occurs in the cytoplasm, assembly takes place at the membranes of the ERGIC and Golgi. Assembled virions traffic out to the cell surface as cargo in large vesicles.

Once the S protein binds to the host cell receptor, it undergoes a conformational change that allows fusion of viral and host membranes (Zelus et al. 2003) (Fig. 4). MHV, BCoV, and IBV induce fusion optimally at a neutral or slightly alkaline pH, which suggests these viruses fuse directly with the plasma membrane ((Zelus et al. 2003; Payne and Storz 1988; Lai and Cavanagh 1997). Some MHV strains appear to enter cells by utilizing the pH dependent endosomal pathway (Gallagher and Buchmeier 2001). For some strains of MHV, infectivity is reduced in the presence of acidifying drugs suggesting that they enter the cells by utilizing the pH dependent endosomal pathway (Gallagher, Escarmis, and Buchmeier 1991). Upon entry, the nucleocapsid protein- RNA complex is released into the cytoplasm. In order for the translation machinery to access the genome, the RNA is then stripped off the N protein. The process of release and uncoating of the genomic RNA is likely regulated by the phosphorylation of the N protein (Spencer et al. 2008). The N protein is a highly basic protein that can be phosphorylated, imparting it an overall negative charge. It is possible that phosphorylation by virus and host kinases that may lead to the disassociation of N from RNA (Mohandas and Dales 1991). Cholesterol is essential for virus entry and reduction of cholesterol from the plasma membrane severely inhibits virus entry (Choi, Aizaki and Lai 2005). Cellular factors may also be involved in coronavirus entry (Asanaka and Lai 1993).

Transcription and replication

Upon entry, the RNA-nucleocapsid is released into the cytoplasm. The RNA is then uncoated, making it accessible to the cellular translation machinery.

Once the translation of the ORF 1a and ORF 1b takes place. The polyprotein is then proteolytically processed to generate all proteins required for virus transcription and replication (Flint, Enquist, and Racaniello 2009). In order to make mRNAs for the structural genes, the replicase-transcriptase complex generates sub-genomic negative-strand RNA molecules (Fig. 5). These are used for transcription of subgenomic mRNAs. A 3' co-terminal nested set of subgenomic mRNAs are produced during viral infection. Each subgenomic mRNA contains the leader sequence at the 5' end, identical to the leader as is present on the 5' end of the genome (Lai and Cavanagh 1997). Therefore, they all contain the same 5' and 3' ends but are of varying lengths. Although, each subgenomic mRNA contains more than one ORF, only the most 5' ORF gets translated. Intergenic or transcription-regulatory sequences (TRSs) are present on the genomic RNA in between each structural ORF. These TRSs play a role in regulation of subgenomic mRNA transcription. There is a sequence similarity between the TRS and the 3' end of the leader sequence. This may play a role in template switching to create the 3' co- terminal nested subgenomic RNAs. A model of discontinuous transcription mechanism was proposed since each subgenomic mRNA contains the leader sequence as well as TRSs (Lai et al. 1984; Baric, Stohlman, and Lai 1983; Spaan et al. 1983). Coronavirus replication is thought to adapt a discontinuous transcription mechanism during negative-strand synthesis. This model proposes that subgenomic mRNA transcription occurs during negative-strand RNA synthesis (S. G. Sawicki and Sawicki 1990). The polymerase would stall at the TRS sequences and then switch to the 3' end of the

leader that contains homologous sequence to the TRS, to continue transcription. This is called template switching (S. G. Sawicki and Sawicki 2005). This results in negative-strand subgenomic mRNAs these would serve as template for the synthesis positive-strand mRNAs. Full-length positive-and negative-strand genomic RNAs are also made during infection. The RNA secondary structures of the 5' and 3' UTRs as well as may play a role in the modulation between replication and transcription (Thorp and Gallagher 2004; Hsue and Masters 1997; Goebel et al. 2004).

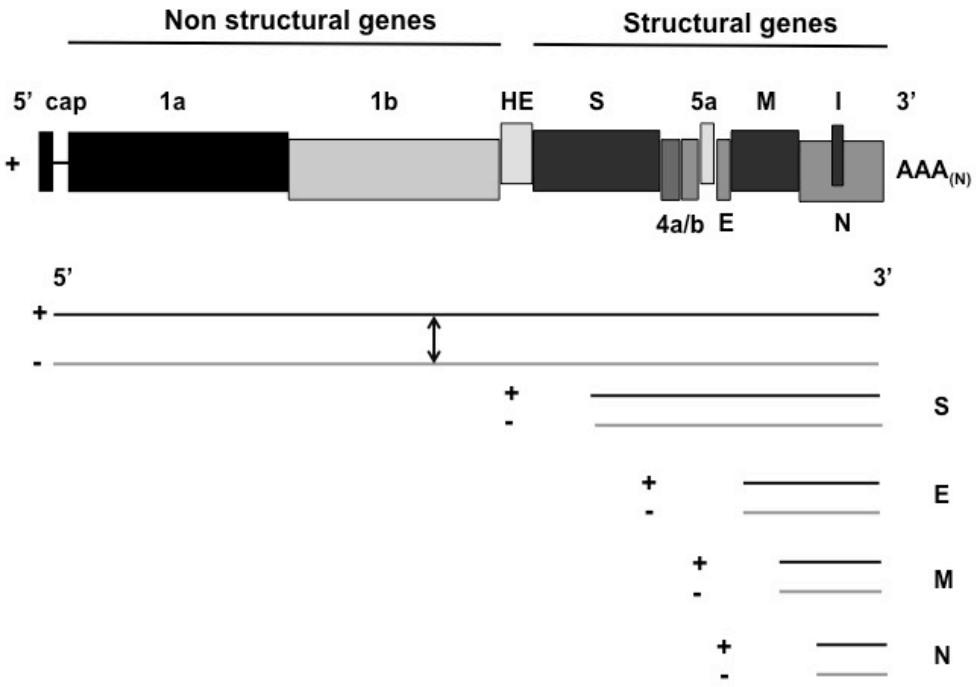

Figure 5: Coronavirus genome and replication

The coronavirus genome is a single stranded – positive sense RNA. The full length genome is replicated into a full length negative strand. This serves as template for the production of more full length positive sense genome. A 3' co-nested set of discontinuous negative stranded subgenomic RNA is generated. This serves as template for monocistronic mRNAs that encode the structural proteins.

Translation

The full-length coronavirus genome is 5' capped and 3' poly A tailed and resembles a large mRNA (Schochetman, Stevens, and Simpson 1977).

The cellular translation machinery immediately recognizes it and ORF1 is translated immediately after infection as one large polyprotein about 800 kD in size. ORF1 contains ORF1a and 1b that are in different reading frames. Translation of ORF1b occurs after a ribosomal frameshifting takes place during the translation of ORF 1a (Brierley et al. 1987). The ORF1 gene encodes all the proteins in the transcriptase-replicase complex. The structural proteins are translated off the subgenomic mRNAs. Translation is initiated by a traditional cap-dependent mechanism because all the subgenomic RNAs are 5' capped and 3' poly-A tailed. Even though the subgenomics contain more than one ORF, typically only the most 5' ORF is translated Cavanagh 1991). The only exception is the MHV E protein, which is encoded on subgenomic mRNA 5, is translated from the second ORF (Thiel and Siddell 1994). Translation of the E protein occurs through a cap-independent internal ribosomal entry site (IRES) (Jendrach, Thiel, and Siddell 1999) .

Assembly and Release

Most enveloped viruses assemble at the plasma membrane. Coronaviruses, flaviviruses and bunyaviruses derive their envelope from the internal membranes. Very little information is known about the factors driving virus budding at internal membranes. Virus assembly takes place at the ER/Golgi intermediate compartment (ERGIC) and Golgi membranes (Fig. 4). At lower temperatures like

30 ^{0}C, virus assembly has been observed at the ER (Holmes, personal communication). The viral structural proteins are localized to the site of assembly. The S protein is co-translationally inserted into the rough ER (RER). It is highly glycosylated and a portion of the protein is transported to the plasma membrane through the secretory pathway (Klumperman et al. 1994). During infection or co- expression with M, a large portion of the S protein is retained at the site of assembly (McBride and Machamer 2010). The M protein is also co-translationally inserted into the ER membrane and localizes primarily in the ERGIC/ Golgi in infected cell (Klumperman et al. 1994). At the site of assembly, the M protein organizes the other structural proteins and drives assembly. The E protein localizes at the site of the assembly in the ERGIC/ Golgi region (Cohen, Lin, and Machamer 2011). The N protein is soluble and is found in two components in the cells- free floating and membrane associated (Verheije et al. 2010). Replication takes place on double membrane vesicles (DMVs) that are generated early in infection. Various non-structural proteins localize to these membranes early in infection. N also localizes to the DMVs. It is unknown which component of N is associated with the RNA that is then encapsidated into the virion.

The virus assembly process generates various membranous structures in the cells that have recently been systematically analyzed (Ulasli et al. 2010). This system used peptides to prevent S mediated fusion inside the cells. So all the structures observed were due to the replication and assembly processes. The first structures to the identified are the DMVs. Following this, convoluted membrane

(CM) structures appear, that connect the membranes of the ER with the DMVs. The function of this connection is unknown. Nucleocapsid and replicase proteins localize to these structures. The viral structural proteins interact with each other to form assembly complexes that help facilitate the assembly and budding process. Once replication occurs, virions appear. Virions bud into structures described as large virion containing vacuoles (LVCV). Virus structural proteins and ERGIC/ Golgi proteins localize to this structure (Fig. 4) Virions traffic out to the cell surface in these vesicles. At later times post infection, rare membrane modifications occur in the cells. These include tubular bodies (TB) and cubic membrane structures (CMS). The functions of these modifications are unknown(Ulasli et al. 2010).

The E protein plays a major role in virus budding and trafficking. Although all these protein interactions must take place for efficient assembly of infectious particles, the M and E proteins are the minimal requirements for envelope formation for MHV, IBV, and BCoV, as they form virus-like particles (VLPs) (Vennema et al. 1996).Therefore, it is thought these two viral proteins are crucial for assembly of virions. Most enveloped viruses require the nucleocapsid for assembly so coronaviruses are unique as they utilize nucleocapsid independent assembly. Since the M protein alone cannot drive the assembly process, it is thought the E protein plays an important role in assembly and release. Studies have suggested that E may induce membrane curvature or could be involved in the pinching off of budding virions. Additionally, when E is expressed alone, vesicles are produced and released from cells(Raamsman et al. 2000). While E

proteins can substitute for one another in virus assembly with minor changes, the exact role of the E protein in each virus strain may different (Kuo, Hurst, and Masters 2007). Immediately upon infection, organelle identity is lost. One of the hallmarks of MHV infection is the disassembly of the Golgi architecture (Oshiro, Schieble, and Lennette 1971). This has been attributed to the E protein and its ion channel activity (Ruch and Machamer 2011). The implication of such a disassembly for virus assembly is unknown.

Chapter 2

CORONAVIRUS ENVELOPE PROTEIN REMAINS AT THE SITE OF ASSEMBLY.

ABSTRACT

Coronavirus (CoV) assembly at endoplasmic reticulum Golgi intermediate compartment (ERGIC) membranes and egress is not completely elucidated, but the envelope (E) protein clearly influences the process. Mouse hepatitis CoV A59 E protein localization and dynamics were investigated to further understanding of its functions. E protein localizes in the ERGIC and Golgi with the amino and carboxy ends in the lumen and cytoplasm, respectively. The protein does not traffic to the cell surface. The transmembrane (TMD) domain is not required for targeting to intracellular membranes. A genetically engineered MHV with a tetracysteine (TC) tag appended to the carboxy end of E was used for real-time imaging during infection. Fluorescence recovery after photobleaching (FRAP) showed that E is not highly mobile in the ERGIC/Golgi region and correlative light electron microscopy (CLEM) confirmed its presence in Golgi cisternae. Altogether, these results provide strong support for a primary role of E at the site of budding/assembly.

INTRODUCTION

Coronaviruses are medically important enveloped, positive stranded RNA viruses that infect humans and a broad range of animals. At least three proteins are present in the lipid envelope, the membrane (M), spike (S) and envelope (E) proteins. The envelope surrounds the ~30 kb RNA genome that is encapsidated by the phosphorylated nucleocapsid (N) protein as a helical nucleocapsid. The viral components assemble at intracellular membranes in the ERGIC compartment where they bud into the lumen and are subsequently transported out of the cell by exocytosis in cargo vesicles (Palokangas et al. 1998; J. Tooze and Tooze 1985). The roles of the M and S proteins are well defined. The M protein with its three transmembrane domains and ~100 amino acid endodomain tail forms a lattice network that makes up the bulk of the envelope. Through interactions with itself, S and the nucleocapsid, M plays a required role in organizing the envelope for particle assembly. The S protein is interspersed in the M lattice and extends from the envelope to form the characteristic spikes that function to bind cellular receptors and facilitate entry during infection. Only a few molecules of the E protein are actually present in virus particles, even though it is expressed well during infection. The function(s) of E during virus assembly are much less well defined than for the other protein, but it is well established that the protein plays an important role(s) in coronavirus production (Bos et al. 1996; Corse and Machamer 2000; Vennema et al. 1996).

E proteins are small (~8-10 kDa) hydrophobic viroporins (Wilson et al. 2004; Wilson, Gage, and Ewart 2006). They are expressed well during infection,

despite being underrepresented in the viral envelope. All coronavirus E proteins contain two distinct structural domains, a longer than typical hydrophobic domain and a charged cytoplasmic tail, but the proteins exhibit amino acid sequence variability. E proteins from other coronaviruses can replace MHV E when its gene is deleted, suggesting that the proteins provide a common function that is interchangeable among the viruses (Kuo, Hurst, and Masters 2007). Surprisingly, a truncated variant of the M protein was recently shown to enhance the growth of MHV lacking the E gene (Kuo and Masters 2010). Thus, it is apparent that much remains to be understood about the mechanistic role(s) coronavirus E proteins.

E and M proteins are sufficient and necessary for virus-like particle (VLP) production for most coronaviruses, even though addition of the N protein can enhance VLP output in some cases (Bos et al. 1996; Corse and Machamer 2000; Vennema et al. 1996; Siu et al. 2008; Boscarino et al. 2008; Arndt, Larson, and Hogue 2010). Severe acute respiratory syndrome coronavirus (SARS-CoV) VLP production appears to be most efficient when M, N and E proteins are co-expressed (Siu et al. 2008). However, expression of only M and N or M and E have both been reported to be sufficient for SARS-CoV VLP release from cells and expression of M alone has been reported to form extracellular vesicles that are less dense than VLPs (Y. Huang et al. 2004; Hatakeyama et al. 2008; Hsieh et al. 2005; Tseng et al. 2010). Deletion of the E gene from the viral genome results in variable decrease in virus yields that ranges from almost no virus output in the case of MHV to only modest reduction that is cell type dependent in the case of SARS-CoV (Ortego et al. 2007; Kuo and Masters 2003; DeDiego et al. 2007).

When E is deleted from transmissible gastroenteritis coronavirus (TGEV) virions assemble, but are blocked as immature particles in the secretory pathway (Ortego et al. 2007).

A number of coronaviruses E proteins have been shown to form ion channels in lipid bilayers that transport cations (Na^+ or K^+) (Wilson et al. 2004; Wilson, Gage, and Ewart 2006) and recently ion channel activity was measured in transfected cells expressing SARS-CoV E (Pervushin et al. 2009). The relevance of presumed ion channel activity during virus infection remains to be shown, but consistent with a possible role of the activity, disruption of the hydrophobic domain of MHV E or replacement of the transmembrane domain (TMD) of infectious bronchitis virus (IBV) with a heterologous TMD results in decreased virus production and defects in release of virions from cells (Ye and Hogue 2007; Ruch and Machamer 2011). All Coronavirus E proteins are presumed to oligomerize since they form ion channels in lipid bilayers. Computational modeling of SARS-CoV E hydrophobic domain and subsequent nuclear magnetic resonance (NMR) analysis indicates that the domain forms pentameric alpha-helical bundles (Liao et al. 2006; Torres et al. 2006; Pervushin et al. 2009).

E proteins have been reported to localize in the ER, ERGIC and Golgi, as well as on the cell surface (Raamsman et al. 2000; Corse and Machamer 2000; Lim and Liu 2001; Teoh et al. 2010; Tseng et al. 2010). Since E is significantly underrepresented in mature virus particles, yet expressed well during infection, we sought to better define its localization and expression dynamics to help further our understanding of its mechanistic role(s) in virus assembly and egress or other

roles that it may play during infection. We show that MHV E localizes both in the ERGIC and Golgi and that the protein does not traffic to the cell surface. The protein is oriented with its carboxy end on the cytoplasmic side of the membranes and the amino end on the luminal side. Using a recombinant genetically engineered MHV that expresses a TC tagged E, the protein was monitored in real-time during infection to determine that it is not highly mobile in ER/ERGIC membranes. Additionally, CLEM analysis allowed E to be visualized directly in Golgi stacks. The results strongly support the notion that E function(s) at the intracellular site of assembly. This is the first report to describe live-cell imaging of a coronavirus E protein that expands opportunities to analyze interplay between E and cells to help further our understanding of its functions during infection.

MATERIALS and METHODS

Cells and viruses. Mouse 17 clone 1 (17Cl1) and L2, baby hamster kidney (BHK-21) and human 293T cells were maintained as previously described (Arndt, Larson, and Hogue 2010). Wild type (WT) and recombinant MHV A59 virus stocks were grown in 17Cl1 cells at specified multiplicities of infection (MOI) and virus titers were determined in L2 cells.

Generation of TC-tagged E proteins. MHV E and tagged forms of the gene were expressed in the pCAGGS vector under the control of the chicken β-actin promoter as described previously (Lopez et al. 2008). pCAGGS E-Lumio was constructed by PCR amplification using pCAGGS E as the template and appropriate primers that included the coding sequence for the tetracysteine tag (CCPGCC) and two preceding codons for alanine and serine in the reverse primer. The chimeric E – VSV TMD Lumio construct was generated by replacing the TMD of MHV E (QIIFIFAVCLMVTIIVVAFLASI) with the TMD of VSV G (SSIASFFFIIGLIGLFLVL) by serial PCR with appropriate primers.

Construction of recombinant MHV with TC tagged E. Recombinant MHV E Lumio was made by reverse genetics using a MHV A59 clone (Yount et al. 2002). The coding sequence for WT E was replaced in the G clone with TC-tagged E as described above by three-way ligation of PCR amplified fragments covering the E gene locus and flanking regions. Following sequence confirmation of the subcloned region between *Sbf* I and *Nde* I restriction sites and junctions after ligation into the G clone, a full-length cDNA genomic clone was assembled, transcribed and electroproated into BHK-MHVR cells as described previously

(Verma et al. 2006). Viruses were recovered, plaque purified, passaged and stability of the TC tag was confirmed after at least five passages.

Indirect Immunofluorescence. Mouse 17Cl1, hamster BHK-21 or human 293T cells were plated either on Nunc Lab-Tek chamber slides or coverslips (No. 1.5) in multiwell plates 1 day prior to use. Cells were infected at the specified MOIs or transfected using *Trans*IT-LT1 transfection reagent (MirusBio LLC, Madison, WI). At the specified times cells were washed with phosphate-buffered saline (PBS) and fixed with 100% methanol for 15 min at -20° C for internal staining. Cells were washed with PBS and blocked with 0.2% gelatin in PBS for 1 h at room temperature (RT) or overnight at 4° C. For surface staining cells were washed two times with PBS and fixed in freshly prepared 3% paraformaldehyde in PBS for 15 min at RT, followed by quenching with 10mM glycine for 15 min. Cells were permeabilized with 0.1 % Triton X-100 in PBS for 3 min for parallel internal staining, followed by washing and blocking with gelatin as described above. For digitonin permeabilization, cell chamber slides were placed on ice and rinsed in KHM buffer containing 110mM potassium acetate, 20 mM HEPES (pH 7.2) and 2 mM magnesium acetate. Cells were permeabilized with 25 μg/ml of digitonin in KHM buffer on ice for 5 min, followed by two washes in PBS. Cells were fixed in 3% paraformaldehyde and quenched as described above.

Cells were incubated with appropriate primary antibodies for 2 h at RT, washed multiple times with 0.2% gelatin in PBS before incubation with Alexa Fluor-labeled secondary antibodies (Invitrogen). Cells were washed several times

in PBS containing 0.2% gelatin, once with PBS alone and mounted in ProLong Gold antifade reagent (Invitrogen). In most cases nuclei were stained with 4,6-diamino-2-phenylindole (DAPI) prior to mounting. Images were viewed using an epifluorescence Nikon inverted microscope (Nikon Inc., Melville, NY) with MetaMorph imaging software (Universal Imaging Corporation, Downingtown, PA). Image processing was performed using Adobe Photoshop. Laser scanning confocal microscopy was done using the Zeiss LSM 510 META microscope and software (Carl Zeiss, Inc., Thornwood, NY). Images were processed using Image J software (Rasband WS 1997-2011; Abramoff, M.D., Magalhaes, P.J. and Ram, S.J 2004).

Primary antibodies used in this study included rabbit polyclonal 9410 generated in the Hogue Lab against the carboxy terminal 21 amino acids of MHV E coupled to keyhole limpet hemocyanin (KLH). Mouse monoclonals J1.3 and 2.7 were previously described and polyclonal antibody A04 against MHV S was kindly provided by Kathryn Holmes, University of Colorado Health Sciences.

Biotinylation of surface proteins. Mouse 17Cl1 cells were plated on 60mm cell culture dishes (BD Biosciences) 1 day prior to use. Cells were infected at a MOI of 0.1. At 8, 12 and 16 h p.i. the media was aspirated and cells were washed twice in PBS. Cells were incubated on ice with 1 mg/ml biotin (Thermo Fisher Scientific) for 1 h. Cells were washed twice in PBS and biotin was quenched with 50mM glycine in PBS for 5 min. Cells were lysed in biotinylation lysis buffer containing 10mM HEPES (pH 7.2), 0.2 % NP-40, 150mM NaCl containing protease inhibitor cocktail (Sigma, St. Louis, MO) at 0°C for 10 min. Lysates

were clarified at 16,000 X g for 10 min at 4ºC.Streptavidin agarose resin (ThermoFisher Scientific) was equilibrated in biotinylation lysis buffer and added to the cell lysate. Binding was carried out at 4ºC with constant rotation. The Streptavidin agarose resin was pelleted at 4,000 X g for 10 min at 4ºC. Biotinylated surface proteins were eluted from the agarose resin in Laemmli sample buffer by heating at 100º C. Ten percent of the intracellular fraction and 40% of the surface fraction were loaded onto SDS-PAGE gels and subsequently analyzed by Western blotting.

Immunogold labeling: Mouse 17cl1 cells were infected at an MOI of 5. Cells were fixed at 6 h p.i. in 2% formaldehyde and 2% glutaraldehyde in 0.1 M phosphate buffer pH 7.6 for 1 hour at room temperature. Cells were scraped into a pellet and processed for immunogold labeling. The pellet was serially dehydrated in increasing concentrations of ethanol and embedded in increasing concentrations of LR White resin (London Resin Company). The pellet was sealed in a plastic bullet in the absence of air and allowed to polymerize at 55^0C for 48 hours. The pellet was excised from the plastic bullet, trimmed and serially sectioned into 70 nm sections. Sections were collected on formvar coated Nickel grids. Grids were then incubated with a rabbit anti E antibody (1:50 dilution) for 2 hours in PBS with 0.5 % gelatin. The grids were incubated further with a secondary antibody (Goat anti rabbit IgG conjugated to 10 nm gold beads-Sigma). After the incubation with the antibodies, the grids were stained with 0.5 % uranyl acetate for 30 seconds and observed under the transmission electron microscope.

Live cell imaging. Mouse 17Cl1 cells were grown in glass bottom 35 mm dishes (MatTek) and subsequently infected at a MOI of 0.1 with MHV E Lumio virus. At 7 h p.i.cells were washed in serum free Opti-MEM and labeled with 200 nMLumio Green (FlAsH) reagent (Invitrogen) in Opti-MEM for 30 min at 37° C in the presence of CO_2. Cells were washed thoroughly with Opti- MEM, re-fed with 1X MEM without phenol red, plus 200 nM disperse blue for background reduction and allowed to recover for 30 min at 37° C. Cells were monitored and imaged using a Zeiss LSM 510 META Confocal Microscope with the 488 nm laser at 5% power in a humidified chamber supplied with CO_2 and equipped with a heated stage and objective. Images were captured every 10 min over a 3 h 20 min time course with Z-sections of 0.5 μm.

Fluorescence recovery after photobleaching (FRAP). Mouse 17cl1 cells were grown in glass bottom 35mm dishes (MatTek) and infected with MHV E Lumio virus at a MOI of 0.1. Cells were stained with 200 nM Lumio Green (FlAsH) reagent (Invitrogen) and imaged as described above. Individual cells were selected for FRAP analysis. Selected regions were photobleached with a 488 nm laser at 100% power and recovery was measured every 5 sec for 5 min. Initial signal intensity was set as 100% and signal recovery was calculated accordingly. Mobility fraction was calculated as the percentage of fluorescence recovery from what was measured immediately following photobleaching.

Correlative light electron microscopy (CLEM). Mouse 17Cl1 cells were grown on 35 mm gridded glass bottom dishes (MatTek). Cells were infected with MHV E Lumio virus at a MOI of 0.5 pfu/cell. At 8 h p.i. cells were washed twice with

Opti-MEM and labeled with 200 nM Lumio Red (ReAsH) reagent (Invitrogen) in Opti-MEM. Cells were incubated for 30 min in the presence of CO_2. After washing, cells were refed with Opti-MEM containing 0.5 μM 2,3-dimercapto-1-propanol plus 20 mM DTT and incubated in the presence of CO_2 for an additional 30 min. Cells were washed to remove all traces of DTT and refed with 1 ml of 1:1 DMEM:Opti-MEM containing 2.5% fetal calf serum. Cell images were collected using a Zeiss LMS 510 META Confocal Microscope.

For photoconversion after labeling with ReAsH, cells were fixed with 2% glutaraldehyde in 100mM sodium cacodylatebuffer (pH 7.4) and incubated for 30 min at 37ºC. Cells were rinsed in 100mM cacodylate buffer and treated for 5 min with blocking buffer (100mM cacodylate buffer (pH 7.4) supplemented with 10mM potassium cyanide, 10mM aminotriazole, 0.01% hydrogen peroxide and 50mM glycine). After rinsing with blocking buffer a solution of 1 mg/ml diaminobenzidine in 100mM cacodylate buffer (pH 7.4) was added to cells. Photoconversion was performed using intense illumination (75 W xenon lamp without neutral density filters) focused through the 10X microscope objective. Cells of interest for further electron microscopy analysis were identified by their location on the gridded coverslips.

Cells were washed with 0.1 M phosphate buffer (pH 7.4) before being fixed with a mixture of 1% osmium tetroxide and 0.8% potassium ferricyanide in distilled water for 1 h at 4ºC. Cells were stained with 2% uranyl acetate in water for 1 h and dehydrated through a series of increasing concentrations of acetone for 10 min each at RT. Resin infiltration with epoxy TAAB 812 (Electron Microscopy Sciences, Hatfield, PA) was

carried out by increasing the resin to acetone ratio from 25% to 100% and polymerization at 60º C for 48 h. Previously selected cells were sectioned at 70 nm and collected on formvar coated copper grids. Images were collected on a Philips 80kV STEM microscope and processed using ImageJ software (Rasband WS 1997-2011; Abramoff, M.D., Magalhaes, P.J. and Ram, S.J 2004).

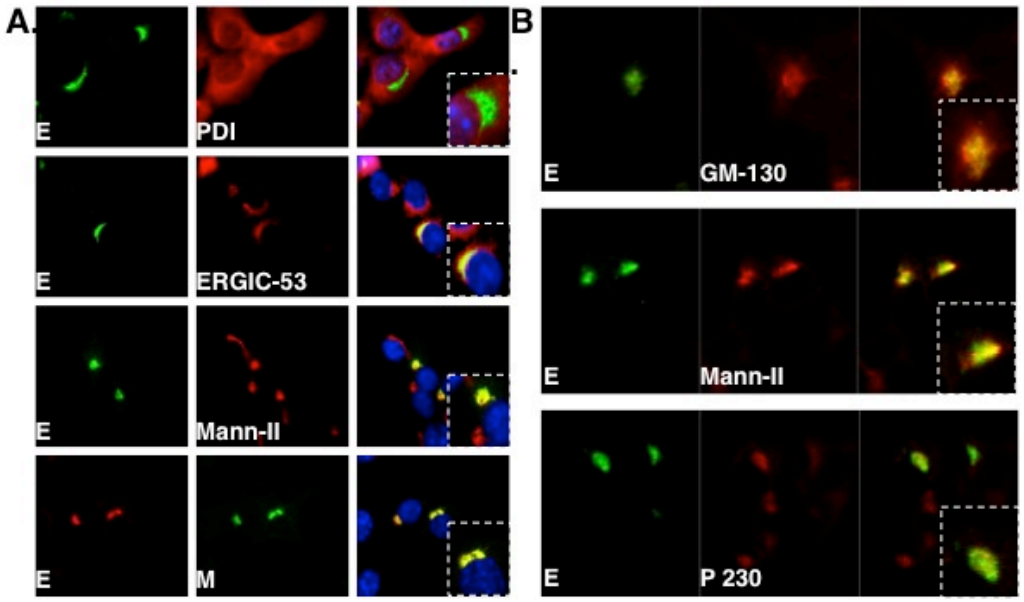
A.
E
PDI
E
ERGIC-53
E
Mann-II
E
M
B
E
GM-130
E
Mann-II
E
P 230

Figure 6: MHV E localizes in the ERGIC and Golgi.

Mouse 17cl1 cells were infected with MHV A59 at a MOI of 1 and analyzed at 6 h p.i. (A) Cells were processed for dual-label immunofluorescence detection of E and protein disulfide isomerase (PDI) (Alexis), ERGIC-53(Alexis), or mannosidase II (Mann-II) (Covance), as ER, ERGIC, and Golgi markers, respectively. The bottom panels were probed for M and E proteins using rabbit polyclonal anti-E 9410 and mouse monoclonal J1.3 and J2.7 antibodies, respectively. Alexa fluorophore tagged secondary antibodies (Molecular Probes) were used to counter stain the primary antibodies. Merged images are shown in the far right column, with enlarged insets of selected cells. Epifluorescence images were taken using a 60X objective. (B) Cells were processed for dual-label immunofluorescence detection using antibodies specific for E (9410) andcis Golgi GM 130 (Santa Cruz Biotechnology Inc.), medial Golgi Mann-II (Covance) or trans Golgi p230 (GE Healthcare). Confocal images were taken with a 100X objective.

Data in panel A was generated by Dr. Lisa A. Lopez and submitted by LL to Arizona State University in partial fulfillment for the requirememts of the PhD in Molecular Cellular Biology.

RESULTS

MHV-A59 E localizes in the ERGIC and Golgi. To identify the cellular localization of E protein in infected cells, 17Cl1 mouse cells were infected with WT MHV A59. During infection, as early as 6 h p.i. , MHV E exhibited compact localization adjacent to the nucleus that clearly did not overlap with the ER marker, protein disulfide isomerase (PDI) (Fig. 6A). Instead, the protein co-localized with markers of both the ERGIC and Golgi structures (middle two panels). Cells dual labeled for M and E exhibited complete overlap of the signals from the two proteins (lower panels).

To determine the distribution of the E protein in the Golgi, colocalizations with *cis*-Golgi GM-130, medial-Golgi Mann–II and *trans*-Golgi p230 were examined (Fig. 6B). E colocalized most extensively with the *cis*- and medial-Golgi markers and less so with the *trans*-Golgi marker p230. Altogether these results clearly define MHV E localization during infection in both the ERGIC and Golgi, with it being concentrated primarily in the *cis* and medial regions of the latter.

MHV E does not traffic to the cell surface. To further address localization and trafficking of E, protein expression was examined in cells during a time course following infection. S and M proteins were analyzed in parallel. At 8h p.i. E and M continued to colocalized as we had observed at 6h p.i. (Fig. 7A). Interestingly, by 12h p.i. the M protein was localized in areas of the cell distant from the ERGIC/Golgi region, whereas E remained localized at perinuclear sites. Additionally, E did not localize with the M or S proteins distant to the perinuclear

sites when all three proteins were analyzed at 12 h p.i. (data not shown). By 16 h p.i., and more prominently at 24 h p.i., a large portion of the M protein was visualized throughout the cytoplasm, presumably as virus output increased. In contrast, at the late time points E continued to remain localized primarily in the ERGIC/Golgi region. Only a few small punctate dots were seen outside of these regions, presumably due to the extensive fusion that is characteristic of MHV A59 infected cells at late times after infection. These results indicate that E and M colocalize at the ERGIC/Golgi assembly site early during infection and E remains there at later times as virions and S traffic toward the cell surface.

Previous reports suggested that coronavirus E proteins localize to the cell surface during infection. To further examine this, cells infected or transiently expressing E were analyzed for surface expression (Fig. 7B). The S and M proteins were monitored in parallel as positive and negative controls, respectively, for surface expression. Two approaches were used to monitor surface expression. First, 17cl1 cells were infected with WT MHV A59 and proteins on the cell surface were biotinylated at 8, 12, and 16 h p.i. Surface and intracellular fractions were then analyzed by Western blotting for the viral proteins. As expected, S was detected in both the intracellular and surface fractions, characteristic of a protein that transports through the exocytic pathway. The M protein was also detected in both fractions at later time points, whereas E was detected only in the intracellular fraction at all times.

Surface staining was also analyzed by immunoflouresence (Fig. 7C). Again, 17cl1 cells were infected with MHV and probed with specific antibodies

for S, M or E proteins after cells were permeabilized with digitonin or TX-100 to reveal the cytoplasmic or both luminal and cytoplasmic epitopes, respectively. The amino end of the M protein was recognized by monoclonal antibody J1.3 in the perinuclear region after cells were permeabilized with TX-100, but not with digitonin, consistent with the orientation of the protein at intracellular membranes and its known localization. The E protein was not detected in a perinuclear region in both TX-100 and digitonin treated cells when probed with antibody 9410 that recognizes the carboxy terminus. This indicates that the carboxy end is located on the cytoplasmic side of internal membranes. No signal was thus visible in non-permeabilized cells. Since antibodies that recognize the amino were not available, we made use of a construct with a Strep tag appended on the amino end to determine if the protein traffics to the cell surface (Fig. 7D). VLPs can be assembled with the Strep-tagged E (data not shown), thus we reasoned that it would provide a relevant assessment for whether the amino end is accessible at the cell surface. BHK-21 cells were transfected with the pCAGGS vector containing the Strep-tagged E gene. The amino and carboxy ends of E were detected with Strep tag-specific or 9410 antibodies, respectively. The results clearly showed that indeed the amino end is not exposed on the cell surface.

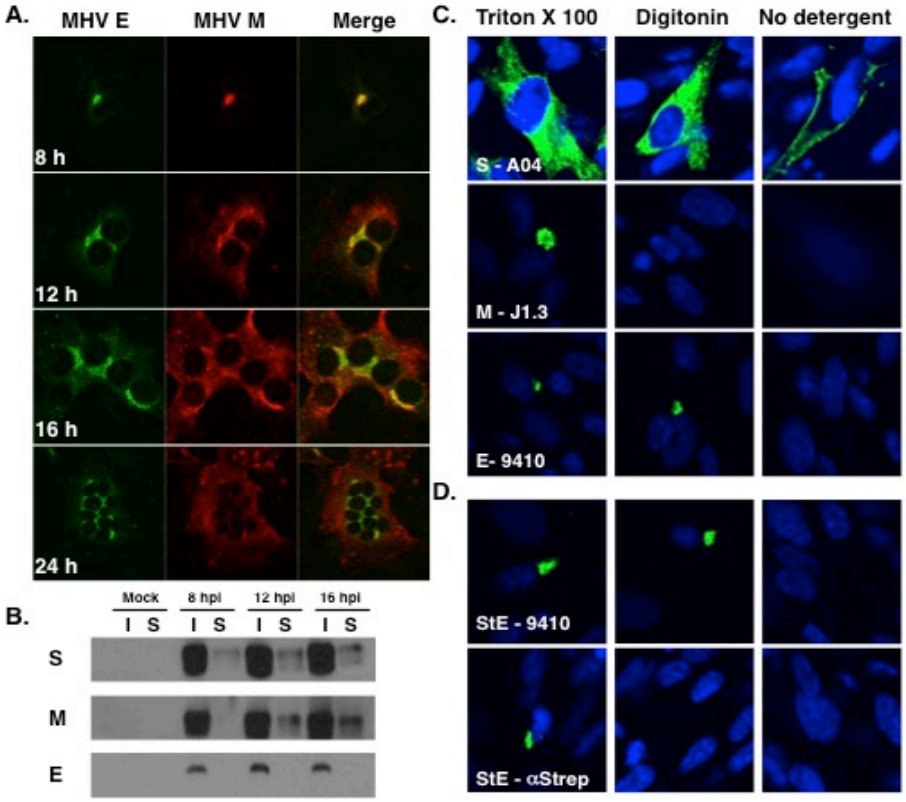
A.
MHV E
MHV M
Merge
8 h
12 h
16 h
24 h
B.
Mock
8 hpi
12 hpi
16 hpi
I S I S I S I S
S
M
E
C.
Triton X 100
Digitonin
No detergent
S - A04
M - J1.3
E- 9410
D.
StE - 9410
StE - αStrep

Figure 7: MHV E does not traffic beyond the site of assembly.

(A) 17Cl1 mouse cells were infected with MHV A59 at a MOI of 1 and fixed indicated times. Indirect immunofluorescence was used to probe for E (green) and M (red) proteins. (B) 17cl1 cells were infected with MHV at an MOI of 0.1. At 8, 12 and 16 h p.i., surface proteins were biotinylated. Surface and intra cellular proteins were analyzed for S, M and E by Western Blotting. (C) 17cl1 mouse cells were infected with MHV at an MOI of 0.1 and probed for S, M and E with digitonin or TX-100 to reveal the cytoplasmic or both luminal and cytoplasmic epitope of the protein. (D) BHK-21 cells were transfected with pCAGGS DNA expressing MHV E with a Strep- tag at the amino end. The amino and carboxy ends of E were detected with an anti-Strep monoclonal, *Strep*MAB-Classic (IBA) and rabbit anti-E 9410 antibodies, respectively.

Data in panel A was generated by Dr. Lisa A. Lopez and submitted by LL to Arizona State University in partial fulfillment for the requirememts of the PhD in Molecular Cellular Biology.

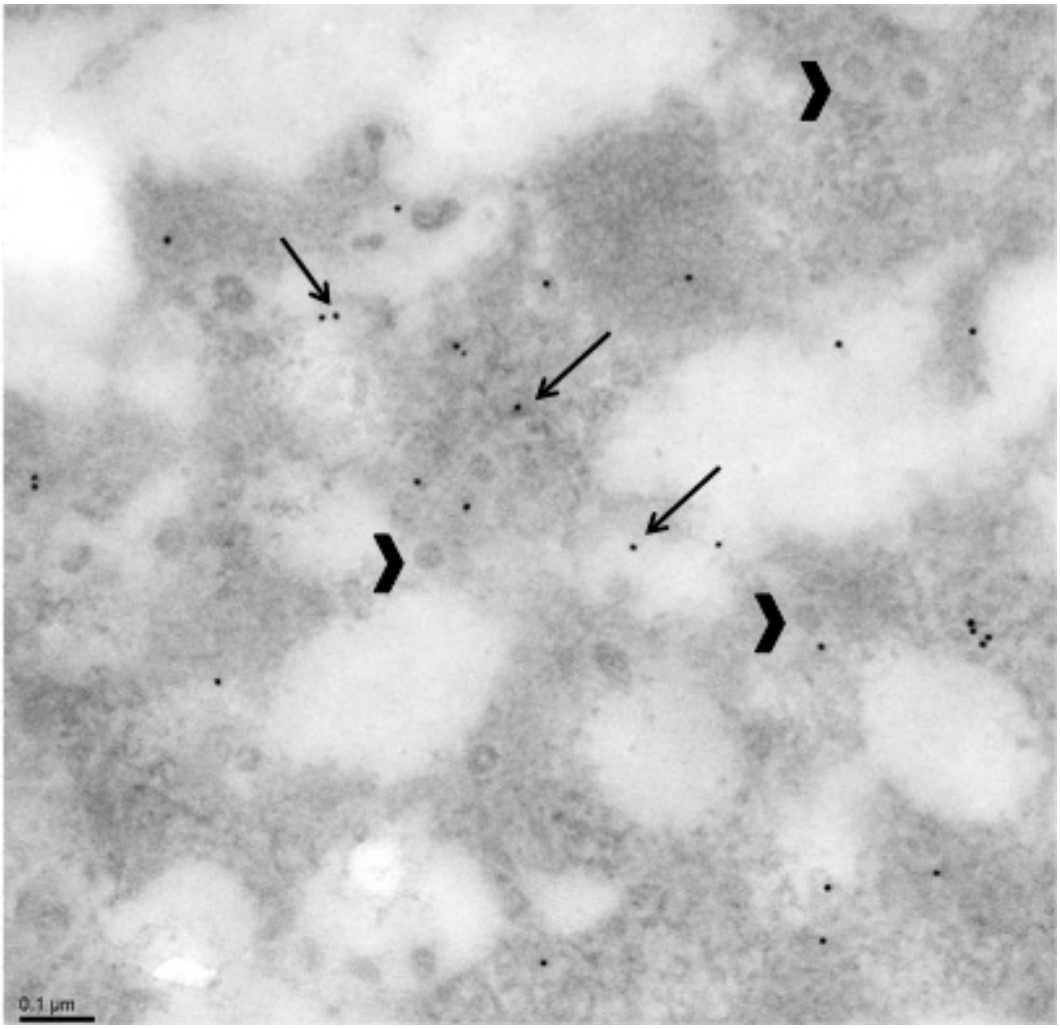

Figure 8: MHV E localizes to membranes around assembled virions

17cl1 cells were infected at an MOI of 5 and fixed at 6 h p.i. Samples were processed for immunogold labeling and stained against antibodies for E. The arrows indicate gold beads (10nm) and arrowheads indicate fully assembled virions.

MHV E localizes to membranes around assembled virions. To identify the ultrastructural localization of E in infected cells, we performed immunogold labeling on cells infected with the MHV A 59 virus. We infected cells at a high MOI and fixed it at an early time post infection. This would prevent the extensive membrane remodeling that occurs at late times post infection. We were able to detect antibodies against E consistently localizing to membranes around fully assembled virions (Fig 8). This was consistent with previously known information about E, where very few molecules of E are present on assembled virions with the majority of E present in membranes at the region of assembly.

Generation of MHV with a tetracysteine (TC)-tagged E protein. To investigate the dynamics of E expression in live cells, we constructed a recombinant E protein with a TC tag (CCPGCC) appended at the carboxy end. TC tags form hairpin structures that bind small, membrane-permeable fluorescein derivatives such as the fluorescein arsenical hairpin binder (FlAsH) or a variant, resorufin arsenical hairpin binder (ReAsH), a red-shift analog. The biarsenicals are fluorescent when they bind to TC tags. We initially confirmed that the tagged E could support VLP formation (data not shown) and that the protein localized correctly in the ERGIC/Golgi (Fig. 9A). A chimeric TC-tagged E with the TMD replaced by that of VSV G was previously constructed for other purposes, thus we took advantage of the opportunity to determine where it localized as well. The chimeric protein also localized in the ERGIC and Golgi like the WT protein, which suggests that the signal for intracellular localization is likely in the carboxy

terminal domain of E, even though contribution of the short nine residue amino terminus cannot be ruled out (Fig. 9B)

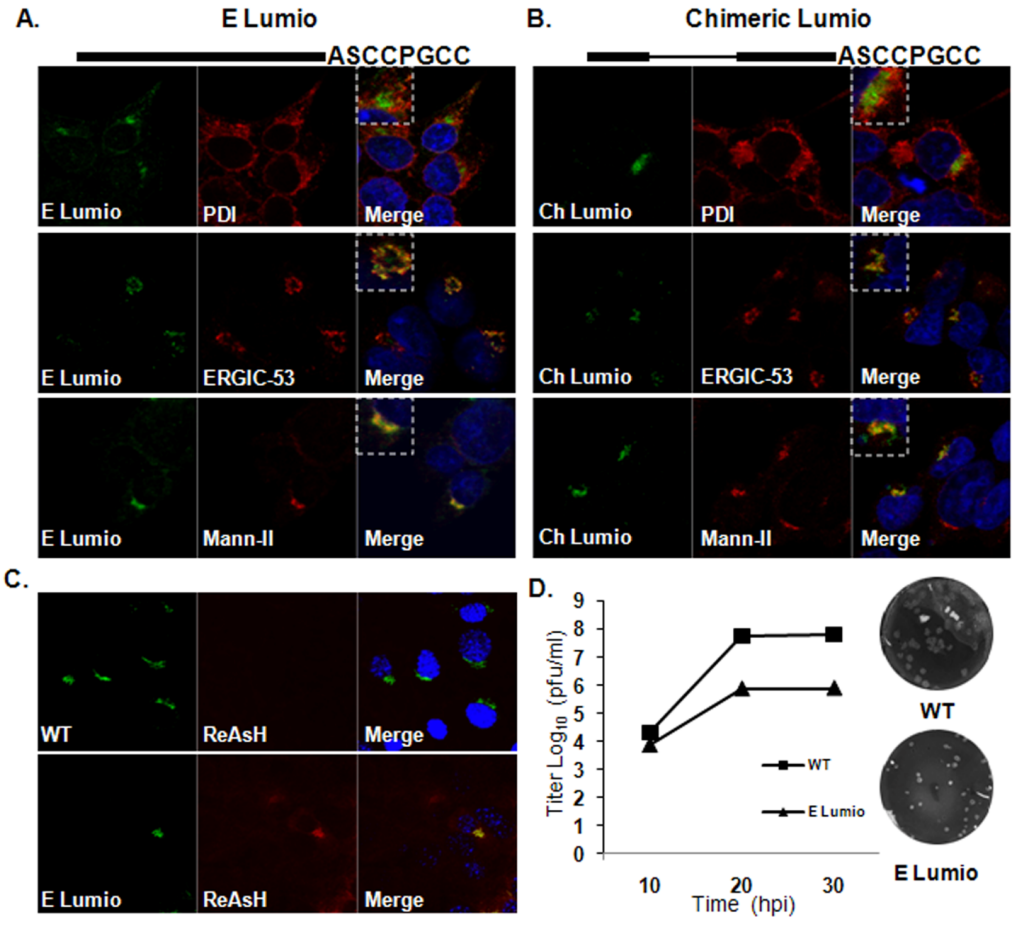
A.
E Lumio
ASCCPGCC
E Lumio
PDI
Merge
E Lumio
ERGIC-53
Merge
E Lumio
Mann-II
Merge
B.
Chimeric Lumio
ASCCPGCC
Ch Lumio
PDI
Merge
Ch Lumio
ERGIC-53
Merge
Ch Lumio
Mann-II
Merge
C.
WT
ReAsH
Merge
E Lumio
ReAsH
Merge
D.
Titer Log10 (pfu/ml)
Time (hpi)
WT
E Lumio
WT
E Lumio

Figure 9: Characterization of TC-tagged E and recombinant MHV with tagged E.

Schematics indicate location of TC tag at the carboxy ends of WT E or a chimeric E gene with the TMD replaced by the TMD of VSV G protein. (A) 293T cells were transfected with pCAGGS-MHV-E Lumio, fixed at 8 h post transfection and processed for indirect immunofluorescence to detect E (green), and ER, ERGIC or Golgi (red) markers as indicated in middle images. Yellow in the merged panels indicates co-localization of signals from the two channels. (B). 293T cells were transfected with pCAGGS vector containing the E-VSV TMD chimeric gene, fixed at 8 h after transfection and processed for indirect immunofluorescence as described above. (C). 17Cl1 mouse cells were infected with WT (top) or E Lumio (bottom) viruses at a MOI of 1. Cells were labeled with Lumio Red (ReAsH) at 8 h p.i., fixed and stained for E. Yellow in the merged panels indicates co-localization of ReAsH and E. Inserts show magnified images of a representative cell. (D). Growth kinetics and plaque characteristics of WT and E Lumio viruses were analyzed in 17Cl1 mouse cells infected at a MOI of 0.01. Titers were determined by plaque assay on L2 cells at the indicated times.

Having determined that the tag does not interfere with localization of the protein, we then constructed a recombinant MHV A59 with the WT E gene replaced by the TC-tagged form. The recombinant virus, designated as MHV E-Lumio was easily recovered. Colocalization with the anti-E antibody in infected cells demonstrated specificity of the ReAsH staining. The TC-tagged E from the virus co-localized specifically with the signal produced by anti-E recognition of the protein (Fig. 9C). However, the E-Lumio virus did produce smaller plaques and growth kinetic analysis showed that the virus grew slower, yielding titers that were ~100-fold less than the WT untagged virus by 20 h p.i. (Fig. 9D). Nonetheless, the tag was stably retained when analyzed through five passages. This indicated that MHV E Lumio was replication and assembly-competent and thus, a good model to study, for the first time, the dynamics of the protein in live infected cells.

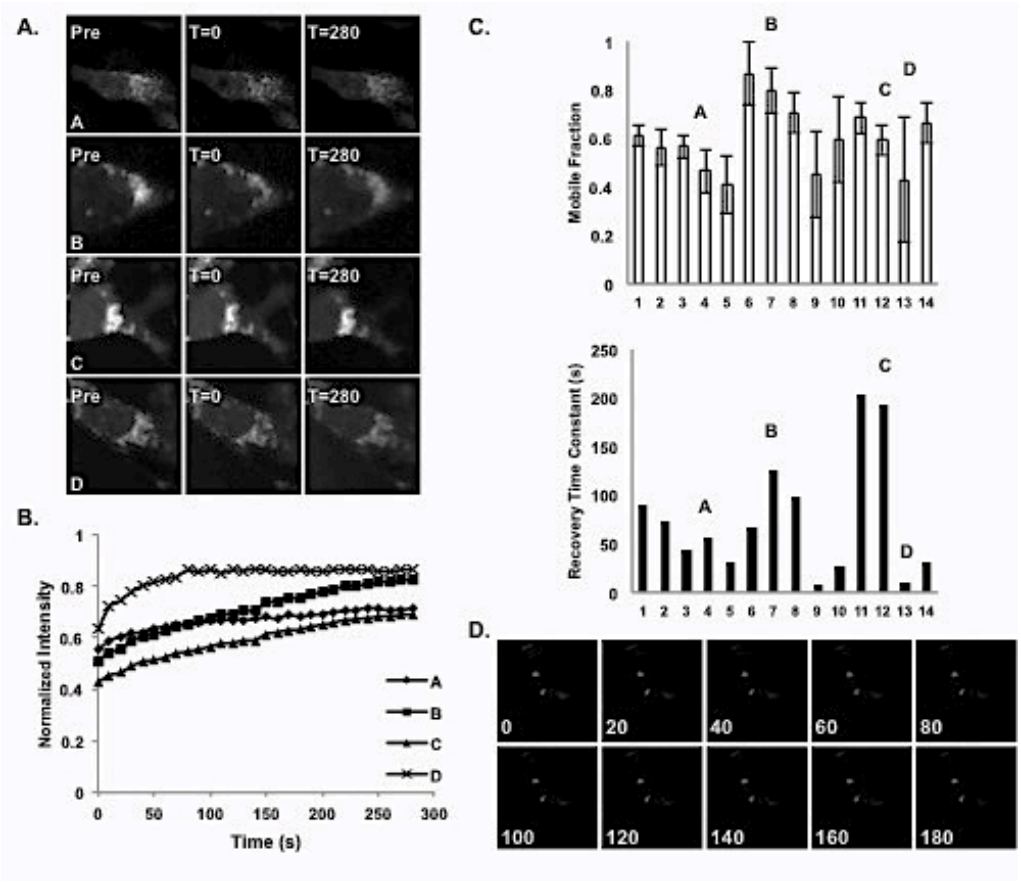
A.
Pre
T=0
T=280
A
B
C
D
B.
Normalized Intensity
Time (s)
A
B
C
D
C.
Mobile Fraction
Recovery Time Constant (s)
D.
0
20
40
60
80
100
120
140
160
180

Figure 10: MHV E Lumio virus allowed live cell imaging of the E protein during infection.

FRAP was performed on MHV E Lumio in 17cl1 cells at 8 h p.i. FRAP analysis revealed that the E protein was dynamic in the membrane and among all the cells observed, four different recovery trends were observed (n= 14). An example of each recovery trend along with the corresponding images are shown in Figures 10B and 10A. The E protein has a wide range of mobility fractions ranging from 41- 87% with an average of 61% (n= 14) (10C- top). While the mobility fraction revealed that the E protein was mobile, the rate of recovery was wide, ranging from 10 s to 200 s (10C bottom). The mobility fraction and time constant of recovery for the four shown images are indicated on the graphs. Long-term analysis (200 min) of the dynamics of the E protein revealed that the protein remained at the site of assembly and further suggested that the E protein did not traffic to the cell surface.

Live-cell imaging of E protein in infected cells. MHV E Lumio virus allowed live cell imaging of the E protein during infection. Flourescence Recovery After Photobleaching (FRAP was performed on MHV E Lumio in 17cl1 cells at 8 h p.i. FRAP analysis revealed that the E protein was dynamic in the membrane and among all the cells observed, four different recovery trends were observed (n= 14). An example of each recovery trend along with the corresponding images are shown in Figures 10B and 10A. The E protein has a wide range of mobility fractions ranging from 41- 87% with an average of 61%. (n= 14) (10C- top). While the mobility fraction revealed that the E protein was mobile, the rate of recovery was wide, ranging from 10 s to 200 s (4C bottom). The mobility fraction and time constant of recovery for the four shown images are indicated on the graphs. Long term analysis (200 min) of the dynamics of the E protein revealed that the protein remained at the site of assembly and further suggested that the E protein did not traffic to the cell surface.

Correlative Light Electron Microscopy of E protein in infected cells. A TC tag allows for proteins to be imaged directly in live cells, as described above, but it also offers the advantage that following addition and photoconversion of diaminobenzidine (DAB) that the same cells can be analyzed by electron microscopy (EM). Cells infected with MHV E-Lumio were initially viewed by confocal microscopy after addition of the biarsenical reagent ReAsH (Fig. 11A). Photoexcitation of ReAsH bound to a TC tag results in release of singlet oxygen, which in turn polymerizes added diaminobenzidine (DAB). The precipitate that forms can be visualized directly by EM following osmimum tetroxide staining. In

MHV E-Lumio virus infected cells a precipitate was visible that co-localized with ReAsH labeling, as expected in a perinuclear position, consistent with the ERGIC/Golgi localization described earlier. When examined by EM the electron-dense precipitate was localized in Golgi stacks (Fig. 11B). In some cells Golgi fragmentation was evident and E was associated with~20-nm vesicles apparently derived from the stacks (data not shown).

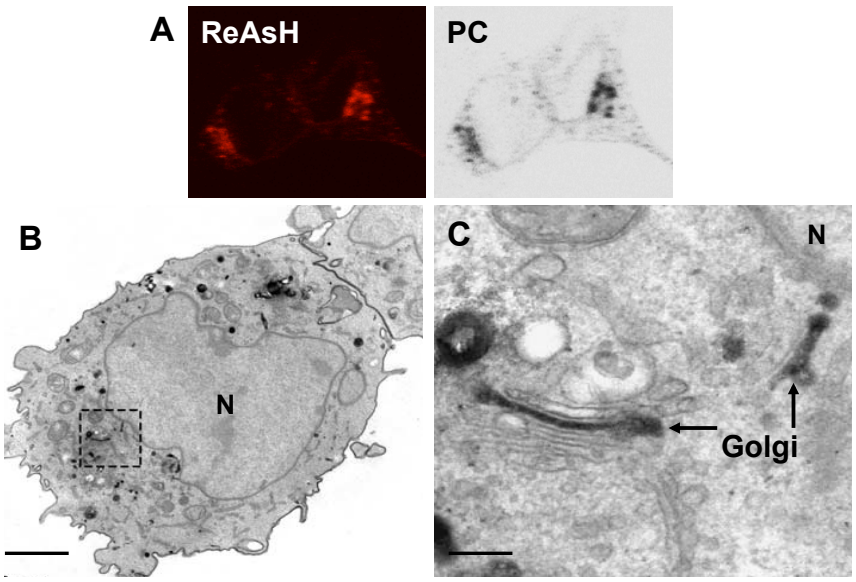

Figure 11: CLEM of TC-tagged E in infected cells.

Mouse 17Cl1 cells were infected with MHV E Lumio virus at a MOI of 1. (A) At 8 h p.i., cells were stained with ReAsH (left), followed by photo conversion (right). (B) A low-magnification electron micrograph of the cell on the lower right in A is shown after photo conversion. The electron dense region corresponding to the Golgi region is boxed. (C) Higher magnification shows electron density in Golgi stacks indicated by the arrows adjacent to the nucleus (N). Scale bars = 1 μm and 50 nm, respectively, for B and C images.

DISCUSSION

Coronavirus E proteins are clearly important for virus assembly and egress, but their mechanistic role(s) is still not understood. Genetic approaches have been used to examine contributions of various conserved residues and domains to gain insight about the function of the protein. Many of the alterations significantly impact virus production and transport out of the cell. The interchangeable nature of the E proteins, at least in the context of MHV, supports the idea that sequence-specific interactions are not required for E to function during infection. This raised questions about the localization of E relative to the other viral proteins, particularly the M protein, during virus infection.

Earlier work concluded that MHV E accumulates in pre-Golgi membranes, based on its presence in electron-dense convoluted membrane structures that co-localized with Rab-1, a marker characteristic of ER and ERGIC compartments. Our confocal imaging, in parallel with a full panel of exocytic pathway cellular markers, clearly shows that MHV E is not in the ER, but is present in both the ERGIC and Golgi, primarily in the *cis* and medial cisternae of the latter, early during infection. Based on the apparent similar roles that the E proteins play in virus assembly, it stands to reason they likely share common localization characteristics. IBV and SARS-CoV E proteins were previously reported to localize in the ER and/or Golgi. Tagged constructs, over expression and limited parallel localization with cellular marker proteins were used to draw conclusion in some of these studies. Recent studies have more clearly and definitively shown that SARS-CoV E co-localizes with ERGIC-53 in infected

cells and also when expressed transiently. Strong transient expression of SARS-CoV E in the *cis*-Golgi, but hardly any expression in the ERGIC and trans-Golgi was also recently reported. We previously showed as well that HA-tagged SARS-CoV E localized in both the ERGIC and Golgi during transient expression. Collectively, it appears that we can conclude that coronavirus E proteins are expressed in both ERGIC and Golgi compartments, though the distribution may vary depending on the virus and cell type.

Targeting information was previously mapped to the cytoplasmic tails of both IBV and SARS-CoV E proteins using chimeric proteins in which the ectodomains and TMDs were replaced by that of VSV G protein. Our result with a similar chimeric protein also suggests that the cytoplasmic tail of MHV E contains targeting information. However, since only the TMD was replaced in our chimera, we cannot exclude the possibility that additional targeting information is present in the amino-terminal region of MHV E. The presence of additional targeting information was also suggested when only the cytoplasmic tail of SARS-CoV E was replaced by that of VSV-G and the chimeric protein still targeted to the Golgi.

Previous studies reported that coronavirus E proteins traffic to the cell surface. In addition to surface immunofluorescence, cellular permeabilization by E proteins and whole-cell patch clamp measurement of ion channel activity in cells expressing SARS-CoV E were also suggestive of surface expression. We did not detect MHV E on the surface of non-permeabilized transfected or infected cells. This is consistent with the recent report, which clearly demonstrated that

SARS-CoV E is not present at the plasma membrane. Our confocal microscopy analysis over a time course following infection strongly illustrates that E remains in its perinuclear location even late during infection. Results from our live-cell and CLEM imaging also support the conclusion that MHV E remains at the site of assembly in ERGIC/Golgi membranes and does not transport to the plasma membrane. Our surface expression results yielded additional information confirming that MHV E assumes an orientation with the amino end located in the lumen and the cytoplasmic tail in the cytoplasm, consistent with the recently described topology SARS-CoV E. The cytoplasmic tail of MHV E was previously determined to reside in the cytoplasm, but with a flag tag placed at the amino end it was suggested that the protein spans the lipid bilayer twice with both the amino and carboxy ends in the cytoplasm.

Live-cell imaging was only recently used to follow trafficking and dynamics of coronavirus proteins. Fluorescent tags, such as GFP or mCherry were appended to nsp2, nsp4 or N proteins to study replication-transcription complexes and their relationship to formation of membrane structures in virus infected cells. Results from our live cell imaging and FRAP analysis of MHV E Lumio show that TC tagged E is mobile at internal membranes of infected 17Cl1 cells. The average mobility (M_f = 61%) of E is similar to what was measured for nsp4 in ER membranes. Nsp4 is a nonstructural integral membrane protein that localizes to the ER, but the protein is recruited during infection to replication complex structures that are interconnected with ER membranes, where its mobility (M_f = 33%) is apparently restricted. The mobility of GFP tagged N and

nsp2, both soluble cytoplasmic proteins, were also analyzed in cells infected with recombinant MHVs expressing the tagged constructs. The N protein (M_f = 40.4%) is dynamically associated with replication-transcription complexes, whereas nsp2 (M_f = 9.9%) is thought to be immobilized through protein-protein interactions in the complexes in infected cells.

The E protein displayed a range of motilities (M_f = 41 – 87%) at 6 h p.i., the point at which virus assembly is actively ongoing. Several factors may account for the M_f range. The population of E molecules that are actively involved in assembly maybe associated with other structural proteins or possibly host factors that differently restrict lateral diffusion in membranes. The E protein assembles into oligomeric ion channels that could affect the proteins mobility. Possibly only a fraction of molecules exists as a component of the channels. The E protein is palmitoylated. We do not know if all potential cysteine residues are modified at any given time or if possibly the protein undergoes dynamic palmitoylation/ depalmitoylation cycling during infection. The conserved cysteines are located adjacent to the transmembrane domain, which when palmitoylated may influence interaction of the protein tail with membranes and thus, its diffusion. The HA protein of influenza virus is a transmembrane protein that is both palmitoylated and myristoylated. Recent data shows that YFP tagged HA has different diffusion coefficients that vary based on the acylation state of the protein. WT HA- YFP has a diffusion coefficient of 0.14um/s^2 while an unacylated mutant has a diffusion coefficient of 0.30um/s^2. The acylation greatly reduces the mobility of the protein. The E protein has been shown to be

palmitoylated at three possible cysteine sites. Depending on the number of sites palmitoylated, the E protein may have different mobilities. Also, the E protein localizes at the ERGIC- Golgi region- an active site of assembly. It is possible that the region undergoes rapid changes in the membrane affecting the dynamics of the E protein.

Fluorescently labeled SARS-CoV structural proteins were also expressed to study VLP production and trafficking in live cells. VLPs were assembled with chimeric N and S proteins containing a fluorescent protein (cyan – eCFP or green – eGFP) tag fused at their carboxy termini, but similarly tagged M protein could not be incorporated. Data was not shown, but the authors indicated that the E protein did not tolerate addition of the large fluorescent protein tags. Our study highlights the utility and tolerance of the smaller TC tag since we were able to generate a recombinant virus with the tag fused to the carboxy end of E. Other recombinant RNA viruses, including VSV, HIV, influenza virus and flockhouse virus, with TC tagged proteins have also been described recently.

Assembly of coronaviruses at intracellular ERGIC membranes was established sometime ago. More extensive and higher resolution views of ultrastructural changes that occur during replication and assembly were recently described. Three membranous structures, including large virion-containing vacuoles (LVCVs), tubular bodies (TBs) and cubic membrane structures (CMSs), were associated with virus assembly/release. The E protein was present with two of these structures, the LVCVs that are derived from ERGIC/Golgi membranes and TBs thought to form late in infection as a result of excess protein self-

aggregation. The latter are thought to be equivalent to previously described smooth tubular membranous structures that are induced by E protein expression late during coronavirus infection. During the time frame in which our CLEM studies were conducted, we did not detect these tubular structures. We did find E associated with Golgi cisternae and in some cells association with Golgi fragmentation was noted. Golgi fragmentation has been observed by confocal microscopy in cells infected with MHV or TGEV and also when IBV E was overexpressed. Golgi disruption was not observed in cells infected with a recombinant TGEV lacking the E gene, but fragmentation occurred when E was provided in *trans*, thus providing strong support for contribution of the protein to this process. Our CLEM results illustrate the potential to follow E during infection and to monitor changes at the ultrastructural level that are associated with the protein, a direction that will be pursued further in future studies.

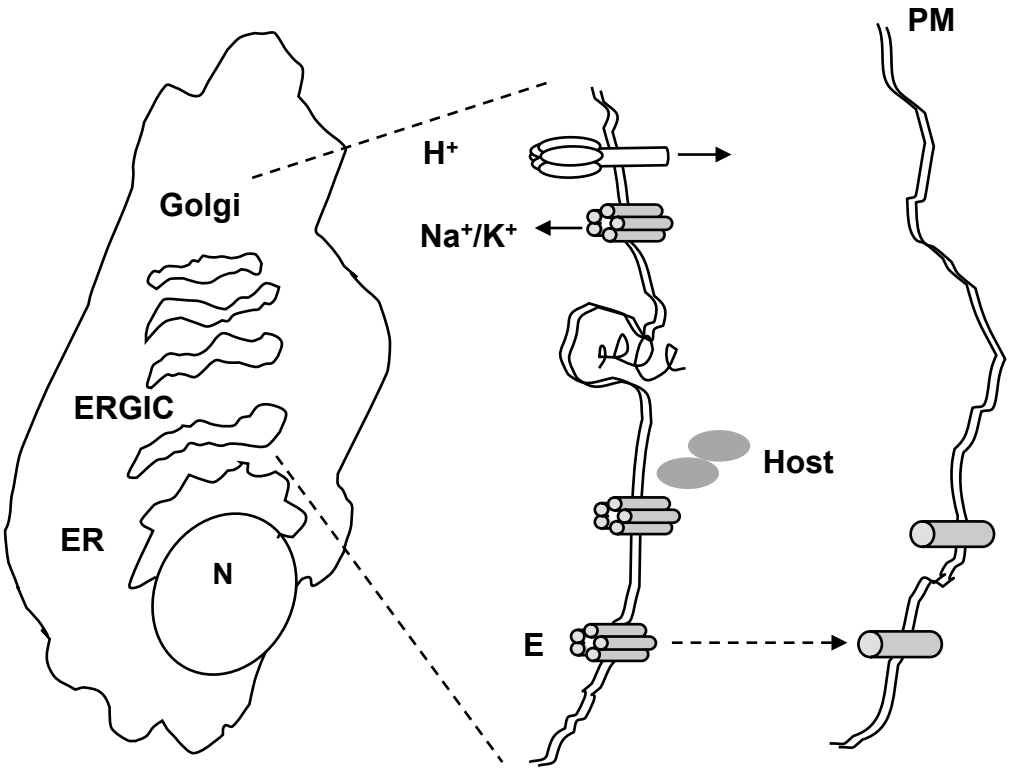

Figure 12: Schematic illustration of E protein potential roles at its localization in ERGIC/Golgi membranes during infection.

Possible roles include (1) alteration of the luminal environment through ion channel activity, (2) alteration of membrane curvature and/or scission, (3) interactions with host proteins involved in assembly and/or transport and (4) signaling to the plasma membrane (PM) as a result of host protein interactions or through ion channel activity.

The accumulation of E in ERGIC/Golgi membranes and the fact that only a few molecules are incorporated into virions suggests that E likely provides a function(s) that is peripheral to or limited at most in the area where virion particles bud. We previously proposed a model for potential mechanisms that E may play based on its accumulation in ERGIC/Golgi membranes and our overall understanding of E that has accumulated from many studies to date in the field (Hogue, B.G. et al., presented at The ninth International Symposium on Positive-Strand RNA Viruses, Atlanta, GA, 2010; Dolezal, K.A., S.M. Daskalova, B.G. Hogue, presented at American Society for Virology 29th Annual Meeting, Montana State University, Bozeman, Montana, 2010). Lack of E trafficking to the cell surface during infection lends additional support for the protein's participation in virus assembly and morphogenesis and possible other roles during infection from its position in the internal membranes as we illustrate in Fig. 12. At these membranes E may, through its ion channel transport of cations directly influence the immediate microenvironment in the ERGIC lumen by alteration of Na+ or K+ concentration that could in turn result in luminal pH changes that are balanced by activation of vacuolar H^+ATPase. The ERGIC does contain an active H^+ATPase that has been suggested to be possibly involved in directional transport and concentration of cargo molecules. A second, previously suggested, possibility is that E plays a role in helping mediate membrane curvature or scission. Influenza M2, a well-characterized multifunctional small integral membrane protein with proton-selective ion channel activity, plays a significant role in entry during infection, but it is also involved in virus assembly. Recently

M2 was shown to mediate membrane curvature and scission during budding. Coronavirus E proteins could play a similar role. Thirdly, coronavirus E proteins may, through interactions with host proteins, facilitate virus budding or vesicular transport. A large number of host proteins co-purify with SARS virions and recently host and viral proteins that interact with E were identified. Finally, E ion channel activity at internal membranes may result in signaling that activates ion channel activity at the cell surface. While the latter is only speculative at this point, measurement of ion channel activity at the surface of cells expressing SARS-CoV E might reflect a response to such signaling and while such activity might be less likely to play a role in virus assembly and transport of LVCVs, such activity could impact a role of the protein as a possible virulence factor during infection. SARS-CoV lacking the E gene is attenuated in animal models, thus the protein, at least for this virus, may be a virulence factor.

Evidence for disruption of protein trafficking by overexpression of IBV during MHV infection was recently described. Based on IBV E modification of the secretory pathway, potential roles and mechanisms that the protein may provide were discussed, some of which are similar to possibilities we outlined above. It is clear that E protein residence in the ERGIC/Golgi region impacts the local cellular environment, which may be linked to possibly multiple roles that it plays in virus assembly/release, as well as pathogenesis. The ability to monitor E directly in live cells and to extend this to ultrastructural studies using CLEM should expand the opportunities to analyze interactions between the protein and

the cell during infection to help increase our understanding of its role(s) and mechanistically how it functions.

ACKNOWLEDGEMENTS

The Strep tagged E construct used in Figure 7D was generated by Kelly A. Dolezal. The tetracysteine tagged WT and chimeric E constructs used in Figure 9 were generated by Dr. Sasha Daskalova. The MHV E Lumio virus described in Figure 9 was generated by Kelly A. Dolezal, with assistance from Dr. Sasha Daskalova.

Chapter 3

CONSERVED RESIDUES IN THE TAIL OF THE CORONAVIRUS ENVELOPE PROTEIN MAY CAUSE MEMBRANE CURVATURE

ABSTRACT

Coronavirus envelope (E) proteins are small membrane viroporin proteins. Viroporins are characteristic of many RNA viruses. Few E molecules are present in mature virions, yet co-expression of E and the membrane (M) proteins is sufficient for the formation of virus-like-particles (VLPs) of most coronaviruses. The roles of E are yet to be fully understood, but it is clear that the protein is important for virus assembly and release. Multiple domains, including the transmembrane domain, the charged carboxy end and conserved cysteines are recognized contributors to these processes. One important domain contains conserved proline and tyrosine resides. The domain is located adjacent to the conserved membrane proximal palmitoylated cysteine domain. This strongly suggests that the conserved proline residues are important and may contribute to the overall structure of the protein that is important for its function(s). We have shown that alanine substitutions at these positions in mouse hepatitis CoV (MHV) A59 E results in and significant reduction in virus-like particle assembly and production of infectious virus particles. However, these mutants are viable in the context of infection and produce viruses that are crippled to various extents. The conserved domain we have identified may affect the interaction of E with membrane lipids. We were able to use peptides encompassing the conserved region and study its interaction with lipids. The WT peptide was able to interact

well with lipids, reducing their melting temperature. More over, the WT peptide was able to significantly reduce the hexagonal phase transition temperature of the lipid POPE, thereby causing a local negative membrane curvature. This may play a role to initiate or stabilize virion budding and/ or aid in virion scission.

INTRODUCTION

Coronaviruses are medically important pathogens that belong to the family *Coronaviridae* in the *Nidovirales* order. The viruses cause primarily respiratory and enteric infections in humans and a wide range of animals. The emergence of severe acute respiratory syndrome coronavirus (SARS-CoV), subsequent discovery of other previously unrecognized human and animal coronaviruses, combined with knowledge that some coronaviruses are zoonotic, has increased awareness of their medical relevance. The importance of understanding the biology of the large family of viruses and development of treatment and preventative measures is clearly warranted.

Coronaviruses are enveloped, positive-stranded RNA viruses. Minimally, virions consist of four structural proteins, the spike (S), membrane (M), envelope (E) and nucleocapsid (N). The M protein has three transmembrane domains, flanked by a short extra-virion region and a long carboxy tail that is located inside the virion. The protein forms a lattice that forms the overall membrane scaffold. S is the receptor attachment protein that mediates virus entry through fusion. The E protein is a minor component of the envelope that plays a role(s) in virus assembly and release. The N phosphoprotein encapsidates the viral genome into a helical nucleocapsid. For murine hepatitis virus (MHV), the M and E proteins are minimally required for the formation of virus like particles (VLPs) and for SARS, the E, M and N protein are required for the same.

The E protein is a small hydrophobic viroporin protein. The overall structure of all coronavirus envelope proteins is highly conserved (Fig. 13). A

short amino terminus precedes a long hydrophobic stretch, encompassing two-thirds of the protein, followed by conserved cysteines, conserved prolines and a highly charged carboxy tail. The hydrophobic domain is predicted to form an amphipathic helix and the pitch of the helix is vital for the ion channel activity of the E protein. The palmitoylation at the conserved cysteines increase protein stability. The charge to alanine clusters at the tail of the E protein affect virus morphology and thermostability. Upon close analysis of betacoronavirus E proteins, it was revealed the presence of an absolutely conserved proline and tyrosine (Fig. 13) in the tail of the E protein. Coronaviruses assemble at the membranes of endoplasmic reticulum Golgi intermediate compartment (ERGIC). The mechanism of virus assembly and budding at internal membranes is poorly understood. Also, unlike normal vesicle budding, virions assembly and bud into the lumen. It is highly likely that host factors play a role in this process. The most characterized host mechanism that allows multivesular body formation is the endosomal sorting complex required for transport (ESCRT) pathway and have been shown to play a very important role in budding and release of viruses such as HIV, Herpes, Ebola and Hepatitis C. The interaction of proteins with members of the ESCRT pathway is mediated by the presence of specific sequences called late domains, which are rich in prolines and tyrosines. The ESCRT pathway regulates protein trafficking using mono- ubiquitination. Recently, SARS E has been shown to be ubiquitinated.

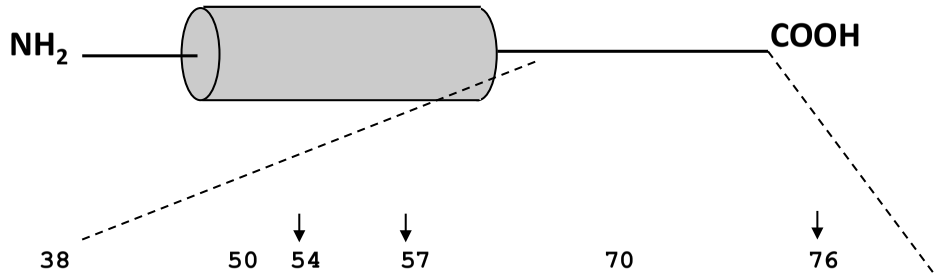


```
                38          50  54     57          70          76
MHV    -------KLCIQLCGLCNTLVLSP----SIYLYDRSKQLYKYYNEEMRL-------PLLEVDDI
BCV    -------KLCIQLCGMCNTLGLSP----SIYVFNRGRGFYEFYN-DVKP-------PVLDVDDV
OC43   -------KLCIQLCGMCNTLVLSP----SIYVFNRGRQFYEFYN-DVKP-------PVLDVDDV
SARS   -------RLCAYCCNIVNVSLVKP----TVYVYS---RVKNLNSSEGV--------PDLLV
HEV    -------KLCIQLCGMCNTLVLSP----SIYVFNRGRQFYEFYN-DVKP-------PVLDVDDV
HKU    -------KLCMQLCGFCNFFIISP----SAYVYKRGMQLYKSYSEQVIP-------PTSDYLI

TGEV   -------KLCMVCCNLGRTVIIVP----AQHAYD---AYKNFMRIKAYN-------PDGALLA
FIPV   -------KLCMVCCNLGKTIIVLP----ARHAYD---AYKTFMQTKAYN-------PDEAFLV
229E   -------KLCFTCHMFCNRTVYGP----IKNVYH---IYQSYMHIDPF--------PKRVIDF
NL63   ----KLIQLCFTCHYFFSRTLYQP----VYKIFL---AYQDYMQIAPV--------PAEVLNV

IBV    RALQAFVQAADACCLFWYTWVVIPGAKGTAFVYK--YTYGRKINNPELEAVIVNEFPKNGWNNKNPANFQDVQRDKLYS
TCoV   RVLQAFVQTADACCLFWYTWIVVPGAKGAAFVYN--YTYGKKLNKPELEAVIVNEFPKNGWNNKSPANF

                38          50  54     57          70          76
MHV    -------KLCIQLCGLCNTLVLSP----SIYLYDRSKQLYKYYNEEMRL-------PLLEVDDI

P54A                           A
Y57A                              A
P76A                                                          A
P54AY57A                       A  A
P54AP76A                       A                              A
```

Figure 13: Alignment of tail of the E protein .

A schematic of the coronavirus E protein is represented. The hydrophobic domain is indicated by the cylinder. Sequence of the MHV –A59 E protein is shown. A sequence alignment of the tails of envelope proteins from alpha, beta and gamma coronaviridae are shown. Arrows indicate conserved prolines and tyrosine of interest. Generated mutants of MHV A 59 E protein are shown, along with the mutated residues.

Previous studies have shown that the E protein is critical for virus trafficking and release. We hypothesized that the conserved proline and tyrosine may play a role in virus trafficking and release. Another proline is highly conserved in the tail of the E protein corresponding to position 76 for MHV E. This proline may be playing a role in the positioning of the tail of the E protein. The overall aim of this paper is to dissect the role of the conserved prolines and tyrosine in the tail of the E protein using site directed mutagenesis - reverse genetics approach. The paper demonstrates the significance of the conserved residue proline 54 and tyrosine 57 in virus assembly and trafficking. This paper shows the first biophysical evidence that the tail of E protein may be introducing negative curvature in lipids allowing membrane bending possibly during virion budding.

MATERIALS AND METHODS

Cells and viruses. Mouse 17Cl1 cells and L2 cells were used to grow WT and mutant MHV viruses. Cells were maintained in Dulbecco's Modified Eagle's Medium supplemented with 5% heat- inactivated fetal calf serum and 1 % glutamine, 10 % tryptose phosphate broth and the antibiotics penicillin and streptomycin. Human embryonic kidney (HEK) 293 –T (ATCC No. 112678) cells were maintained in Dulbecco's Modified Eagle's Medium supplemented with 10% heat- inactivated fetal calf serum and 1 % glutamine. BHK- 21 cells expressing the MHV receptor Bgp 1a (BHK- MHV ^{R}) were maintained in Glasgow's Modified Eagle's Medium supplemented with 5 % heat inactivated fetal calf serum, 10% tryptose phosphate broth and (amount to be added) geneticin (G418) (Dveksler et al., 1991).

Construction of alanine substitution mutants. pScript E, a pPCR- Script Amp SK (+) vector (Stratagene) vector containing the MHV A59 E gene (GenBank Accession no: AAF69347.1) was used for mutagenesis. Mutagenesis was performed using a whole plasmid PCR approach using appropriate primers, listed in table 1, with high- fidelity *Pfu* polymerase (Stratagene). Following an initial incubation at 95^0C for 5 min, 25 cycles of 95^0C for 30s, 50^0C for 60s and 72^0C for 12 minutes was applied. PCR products were DpnI treated to remove methylated template DNA and transformed into Top 10 competent cells (Invitrogen). Mutations were confirmed by sequencing the entire insert and subcloned into the MHV G clone at the EcoRV and Sbf1 restriction sites.

Name	Primer sequence	Use
MHV E P_{54}A FWD	CTTTGGTGCTGTCCGCGTCTATTTATTTGTATGATAGG	MUTAGENESIS
MHV E P_{54}A REV	CAAATAAATAGACGCGGACAGCACCAAAGTATTACATAAACC	MUTAGENESIS
MHV E P_{76}A FWD	GAAGAATTGAGACTGGCTCTATTAGAGGTGCATGATATC	MUTAGENESIS
MHV E P_{76}A REV	CACCTCTAATAGAGCCAGTCTCATTTCTTCATTATTATA	MUTAGENESIS
MHV E Y_{57}A FWD	GTGCTGTCCCCTTCTATTGCTTTGTATGATAGGAGTAAGCAG	MUTAGENESIS
MHV E Y_{57}A REV	CATACAAAGCAATAGAAGGGGACAGCACCAAAGTATTACATAAACCGAAAG	MUTAGENESIS
MHV E $P_{54}AY_{57}$A FWD	GTGCTGTCCGCCTCTATTGCTTTGTATGATAGGAGTAAGCAG	MUTAGENESIS
MHV E $P_{54}AY_{57}$A REV	CATACAAAGCAATAGAGGCGGACAGCACCAAAGTATTACATAAACCGCAAAG	MUTAGENESIS
MHV EM (+)	CAGAACTGTCCAACAGGCCGTTAGCAAG	RT-PCR (+) strands
MHV EM (-)	GCAACCCAGAAGACACCTTCAATGC	RT-PCR (-) strands
MHV MN (+)	CCACCTCTACATGCAAGGTGTTAAGC	RT-PCR (+) strands
MHV MN (-)	GGTCTGCCACAACCTTCTCTATCT	RT-PCR (-) strands
MHV E Reverse	CGGTACCTTTCATATCTATAC	Sequencing E gene
MHV 4 Reverse	AGTCTGCTTTGGCTGATTCCTTC	Sequencing M gene
MHV 6 Reverse	TTCCTGAGCCTGTCTACG	Sequencing M gene
MHV 7 Reverse	ATTCTGGTGGTGCTGATGAACCGGC	Sequencing N gene
MHV 8 Reverse	GGCAGAAGCTCCTCTGTAAACC	Sequencing N gene
PS PCR Forward	TATTGACGTGTGCTGGACTCAC	Packaging signal
PS PCR reverse	CATAACCAGGTTTCCAGTCAGC	Packaging signal

Table 2: Primers used for mutagenesis, reverse transcription and sequencing

Generation of mutant viruses. E protein mutants were introduced into the full-length infectious clone for MHV A- 59. The full- length cDNA clone for wild type (WT) and mutant viruses were assembled, *in- vitro* transcribed and electroporated into BHK- MHV^R cells as described previously.The cells were overlaid with L2 cells to enhance virus production. Cells were monitored for cytopathic effects (CPE) 24- 36 hours post electroporation. An aliquot of the supernatant was taken and used to infect fresh L2 cells. The electroporated cells were harvested to extract total RNA using RNaqueous- 4PCR extraction kit (Ambion). The extracted RNA was DNase treated to remove any extraneous DNA and used as a template for reverse transcription (RT) using an oligo dT primer (Superscript, Invitrogen). The RT product was used as a template to amplify the E and M genes with the forward and reverse primers (EM+/-) for 30 cycles using the SuperTaq plus kit (Ambion). The PCR product was purified using Qiagen's minielute columns and directly sequenced. Supernatant from the electroporated cells was used to purify viruses and passaged five times on 17Cl1 mouse cells. RNA was extracted from passages 1 and 5, reverse transcribed and amplified for the E and M genes. This was further sequenced to confirm the presence and stability of the introduced mutations. The mutant viruses also carried a silent change in the codon for alanine at residue 22. This was also confirmed from sequencing information.

Growth Kinetics. Growth kinetics analysis was performed in duplicate for all WT and mutant viruses by infecting 17Cl1 cells at a multiplicity of infection (MOI) of 0.01. Supernatant was harvested at indicated times post infection. Titers

were determined by standard plaque assay on L2 cells. At 72 hours post infection, the agarose/ medium overlay was removed and the cells were fixed and stained with crystal violet in ethanol. Plaques were counted and virus titer at each time point was determined. All data was collected in duplicate.

Generation of pCAGGS constructs. pScript E containing WT and mutant E proteins were used as a template to subclone WT and mutant E proteins into pCAGGS expression vector **.** The E gene was amplified using the forward (GGG CCA AAT TCG AAA GAA ATG) and reverse (GCA TCG ATT TAG ATA TCA TCC ACC TCT AAT AG) primers to introduce EcoRI and ClaI restriction enzyme sites flanking the E gene for subcloning. The product was resolved on an agarose gel and the 250 base pair product was extracted using Qiaquick gel extraction kit (Qiagen). The eluted product was co- digested with EcoRI and ClaI (New England Biolabs) and purified by Qiaquick nucleotide removal kit (Qiagen) and ligated into alkaline phosphatase treated pCAGGS vector digested with EcoRI , ClaI. Ligation was confirmed by restriction digestion and direct sequencing of the E gene. pCAGGS vectors expressing WT M was constructed as previously described.

Negative staining of virions. Ten T- 150 cell culture flasks of 17cl1 mouse cells were infected at an MOI of 0.01 with WT and mutant viruses. Viruses were harvested at different times post infection ranging from 22- 40 hours post infection. Supernatant was clarified at 7500 X g for 10 minutes. Viruses were concentrated at 90,000 X g for 2 hours onto a 60% sucrose cushion in TMEN (50mM Tris –maleate pH 6.0, 0.1 M NaCl, 1mN EDTA). The concentrated

sample was isopycnically centrifuged on an 30 ml 20- 60 % (wt/wt) sucrose gradient in TMEN for 4.5 hours at 90,000 X g. Upon centrifugation, fractions were collected and the density of fractions were determined using a refractometer. Fractions having a density of 1.18- 1.20 g/cm^3 were pooled together and diluted to get a final sucrose concentration of 30%. The viruses were pelleted at 90,000X g for 2.5 hours. The pellet was resuspended in 300µl TMEN. Five microliters of each virus was adsorbed onto a formvar coated 400 mesh EM grid in a humid chamber. Grids were stained by placing on a 10µl drop of 0.5% ammonium molybdate (pH 6.5) for 30 seconds. Excess liquid was drained from the side of the grid with a filter paper and air dried for five minutes. Samples were examined in a transmission electron microscope at 66,000 X magnification.

VLP analysis. 293 T cells were transfected with 1µg of pCAGGS vector expressing WT or mutant E proteins singly or in combination with 1µg pCAGGS vector expressing WT M protein using TransLT- 293 transfection reagent (Mirus) as per manufacturer's recommendation. The total amount of DNA in each transfection was normalized to 2µg using pCAGGS empty vector. At 24 hours post transfection, the supernatant was clarified at 14000 X g for 10 minutes at 4^0 C. VLPs was pelleted by centrifuging the clarified media at 4^{0}C through a 30 % sucrose cushion in a Beckman SW55Ti at 30,000 rpm for 3 hours. Pellets were directly resuspended in Laemlli sample buffer. The cells were washed gently with phosphate- buffered saline (PBS) and lysed on ice in a buffer containing 100 mM Tris, 100 mM NaCl, 0.5% Triton X-100, and 1 mM phenylmethylsulfonyl fluoride (PMSF). Nuclei were pelleted and the supernatant was stored at – 80^{0}C

for Western blot analysis. Intracellular and extracellular samples were resolved by SDS- PAGE and proteins were transferred onto polyvinylidene difluoride membranes. Extracellular fraction was probed for M using goat anti M AO3 antibody (kindly provided by Kathryn Holmes, University of Colorado Health Sciences) and E using rabbit anti E 9410 antibody. The intracellular fraction was probed for M, E and actin (mouse anti β actin antibody ab 6276 -Abcam)

E protein stability. 293 T cells were transfected with 1μg pCAGGS vectors expressing WT or mutant E proteins. At 12 hours post transfection, one set of dishes was lysed, representing "0" or starting time point. Protein translation inhibitor, cycloheximide (Sigma) was added to other dishes at 50 μg/ ml. One set of dishes was lysed at 2, 4 and 6 hours after addition of cycloheximide. Samples were analyzed by SDS- PAGE and Western Blotting. Rabbit anti- MHV E 9410 was used to detect the levels of E proteins. Mouse anti- ß actin antibody 6276 (Abcam) was used to detect intracellular actin as a loading control. Bands on the X- ray films were quantified using Image J (Rasband WS 1997-2011; Abramoff, M.D., Magalhaes, P.J. and Ram, S.J 2004). Half- life of WT and mutant E proteins were calculated assuming first- order kinetics for the degradation of E proteins.

Virus release. Mouse 17cl1 cells were infected with WT or mutant viruses at an MOI of 0.01. At 16 h p.i. , supernatant and cells were harvested separately. The supernatant containing extracellular virus was clarified to remove cell debris. An equal volume of medium was added to the cell monolayer and subjected to three freeze- thaw cycles to release intracellular virus. Both fractions were titrated on

L2 cells to determine virus titer. The percentage of virus release was determined as the percentage of extracellular virus titer over the sum of intra and extracellular virus titers.

Peptide synthesis: Two peptides were synthesized for the analysis of their interaction with different lipids: TLVLSPSIYLYDRSK (WT) and TLVLSASIALYDRSK (5476). Peptides were synthesized either at the School of Life Sciences in house facility or ordered from Genscript (New Jersey, USA). The peptides were N terminally acetylated and C terminally amidated and purified by FPLC when necessary.

Peptide: lipid interaction analysis: Peptides were dissolved in chloroform/methanol at indicated molarity. The solvent was then evaporated under a stream of nitrogen with constant rotation of a test tube so as to deposit a uniform film over the bottom third of the tube. Last traces of solvent were removed by placing the tube under high vacuum for at least three hours. The lipid film was then hydrated with 20 mM PIPES, 1 mM EDTA, 150 mM NaCl with 0.002% NaN_3, pH 7.40 and suspended by intermittent vortexing and heating to 50°C over a period of 2 minutes under argon. Peptides and lipids were mixed at indicated mole fractions. Cholesterol was added for CRAC identification at indicated molarity. Differential scanning calorimetry was performed in samples with heating and cooling cycles. Measurements were made using a Nano Differential Scanning Calorimeter (Calorimetry Sciences Corporation, Lindon, UT). Each sample was scanned with 2–3 cycles of heating and cooling between 0 and 60 °C. The scan rate was 2°C/min and there was a delay of 5 minutes between

sequential scans in a series to allow for thermal equilibration. DSC curves were analyzed by using the fitting program, DA-2, provided by Microcal Inc. (Northampton, MA) and plotted with Origin, version 5.0.The melting and phase transition temperatures were measured based on heat absorbance of the sample during the temperature scans. This analysis was performed by personnel in Dr. Richard M. Epand's laboratory at McMaster University, Hamilton, Canada.

RESULTS

Alanine substitution mutants have reduced virus output. To analyze the significance of the conserved proline and tyrosine residues alanine substitutions were introduced into the MHV-A59 genome by reverse genetics. Proline residues at positions 54 and 76 and tyrosine residue at position 57 were replaced with alanine singly and in combination (Fig. 14). For each construction, a WT control virus was assembled in parallel. Infectious viral particles were recovered for all constructs (Fig. 14). RNA was extracted from the electroporated cells and the E, M and N genes was sequenced. Sequence analysis revealed that all introduced mutations were maintained and no compensatory changes were identified in any of the genes sequenced.

Even though viruses were recovered for all introduced mutations, plaque size revealed that $P_{54}A$, $Y_{57}A$ and $P_{76}A$ produced plaques somewhat smaller than WT and $P_{54}AY_{57}A$ and $P_{54}AP_{76}A$ produced very tiny plaques (Fig. 14). This indicated that while the proline residues are not absolutely essential for virus production, replacement of the residues was compromising virus output in an unknown mechanism. Individual plaques were isolated for each virus and passaged 5 times. At the end of the 5^{th} passage, RNA was extracted from infected cells and E, M and N genes were sequenced. Sequencing confirmed that the introduced mutations were stable, with no secondary changes in E, M and N genes.

To further understand the growth properties of the mutant viruses, 17Cl1 mouse cells were infected at a low MOI of 0.01.

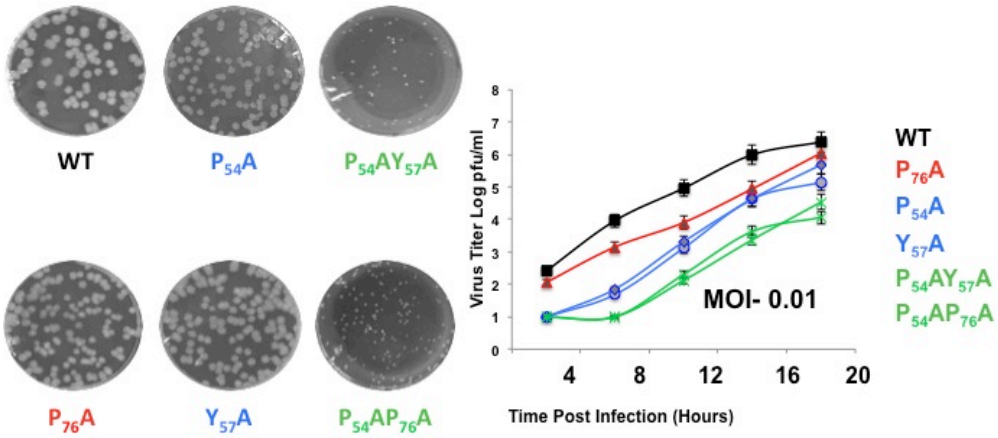

Figure 14: Characterization of mutant viruses

Recovered viruses were plaqued on L2 cells . Cells were stained with crystal violet 3 days after infection (top). 17cl1 mouse cells were infected at an MOI of 0.01. Samples were collected at indicated times post infection and virus titer was determined using a standard plaque assay.

Samples were collected over a period of 20 hours and analyzed by plaque assay on L2 mouse cells. The growth kinetics suggested that, while all mutations affect virus production, mutations in the P_{54} and Y_{57} residues had ~2 log reduction in virus output and the P_{76} residue has less than 1 log reduction in virus output. The double mutants $P_{54}AP_{76}A$ and $P_{54}AY_{57}A$ were found to be highly crippled with ~ 3 log reduction in virus output. At 20 hours post infection, the growth kinetics data indicates that the single mutants may be able to achieve WT- like titers. However, we think that this may be due to the fact that they may have more uninfected cells than in the WT infection, thereby, allowing virus production for a longer time, as compared to WT, before plateauing.

Mutations do not affect virus morphology. Previous work on residues in the tail of the E protein was identified to be critical for virus morphology. Since these residues were in the same region as previously identified residues, virus morphology of each of the mutations was studied. None of the mutations were found to have an effect on virus morphology. All viruses were found to have a WT like morphology (Fig.15).

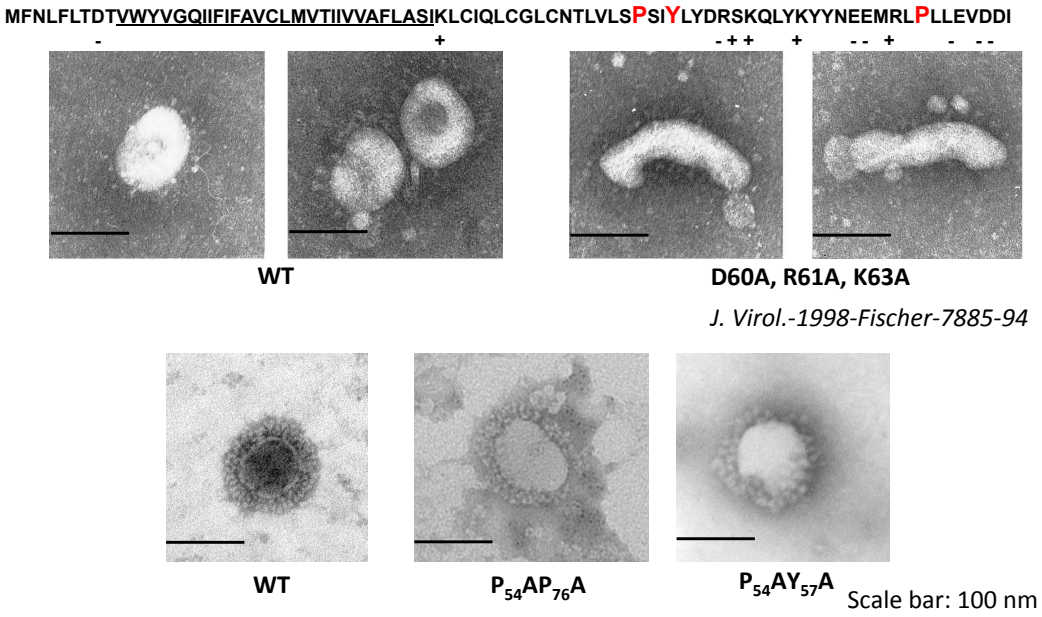

Figure 15: Mutations have no effect on virion morphology

Top panel indicates mutant viruses recovered by Samsonoff et.al., (1998). Mutant viruses were elongated and found to be thermo labile. *(Used with permission from Journal of Virology)*.

Bottom panel shows WT and mutant viruses generated and purified and stained with 0.5% ammonium molybdate. All viruses were found to have WT like morphology.

Proline at position 54 is more sensitive to changes. When expressed by itself, WT E localizes to the ERGIC- Golgi region and WT M localizes to the Golgi. However, when WT E and M are co-expressed, E localizes with M at the site of assembly in the ERGIC. To determine if the introduced mutations affect localization of the E protein BHK- 21 cells were transfected with pCAGGS vectors expressing WT and mutant E proteins alone and also in combination with a pCAGGS vector expressing the M protein. Immunofluorescence analysis of cells revealed that mutant E proteins appear to have a WT E like localization when expressed alone and also when co- expressed with M. Similar co-localization was seen upon infection (Data not shown). Previous studies have established that co- expression of E and M are the minimal requirements for envelope formation for MHV. To determine if the introduced mutations affect envelope formation, pCAGGS vectors expressing WT and mutant E proteins were transfected singly and in combination with pCAGGS vector expressing MHV M protein into HEK 293 cells. At 23 hours post transfection, cells were lysed and the media from the transfected cells were harvested and pelleted through a 30% sucrose cushion. The intracellular and extracellular fractions were analyzed by Western blotting for the E and M proteins. The presence of M in the pellet indicates envelope formation, since the protein is not transported out of the Golgi when expressed alone. All mutant E proteins except 5457 and 5476 were found to be competent for envelope formation since M was present in VLPs pelleted from the supernatant. When the E protein is over- expressed, it can be released as vesicles. Such vesicles were seen when WT and mutant E proteins were able to

generate such vesicles when expressed by singly or in combination with MHV M. Taken together these results suggest that single replacement of these residues does not alter the localization of the E protein. The loss of VLP formation by 5457 and 5476 mutants strongly indicate that these residues are required for interaction with M. (Data not shown)

Virus release is affected. In order to further determine the stage in the virus life cycle affected by these mutations in the E protein, the percentage of virus released upon infection was determined. Media from infected cells were plaqued for the extracellular virus titer and infected cells were frozen and thawed to release the intracellular virus. Virus release was calculated as a percentage of extracellular virus titer relative to total virus produced .WT virus consistently released 90 % of the virus produced, whereas all mutant viruses released around 50 % of virus produced. This clearly indicated that mutations in these residues affected virus release. While $P_{76}A$ significantly affects only virus release, $P_{54}A$ and $Y_{57}A$ affect virus production as well as release (Fig. 16- top panel).

Mutations affect protein stability. 293 cells were transfected with pCAGGS vectors expressing WT and mutant E proteins. At 12 hours post transfection, cycloheximide was added to prevent further translation. At 0, 2, 4 and 6 hours post addition of cycloheximide, cells were lysed and analyzed for the levels of E using Western Blotting. The bands were quantified and the half-life of WT and mutant E proteins were calculated using first order kinetics. WT E had a half-life of 90 min. All mutants with a proline- to – alanine change had a reduction in their

half-lives. $P_{54}AP_{76}A$ was severely unstable and had a half-life of only 10 minutes. Interestingly, $Y_{57}A$ was as stable as WT E at 91 minutes (Fig. 16 – bottom panel).

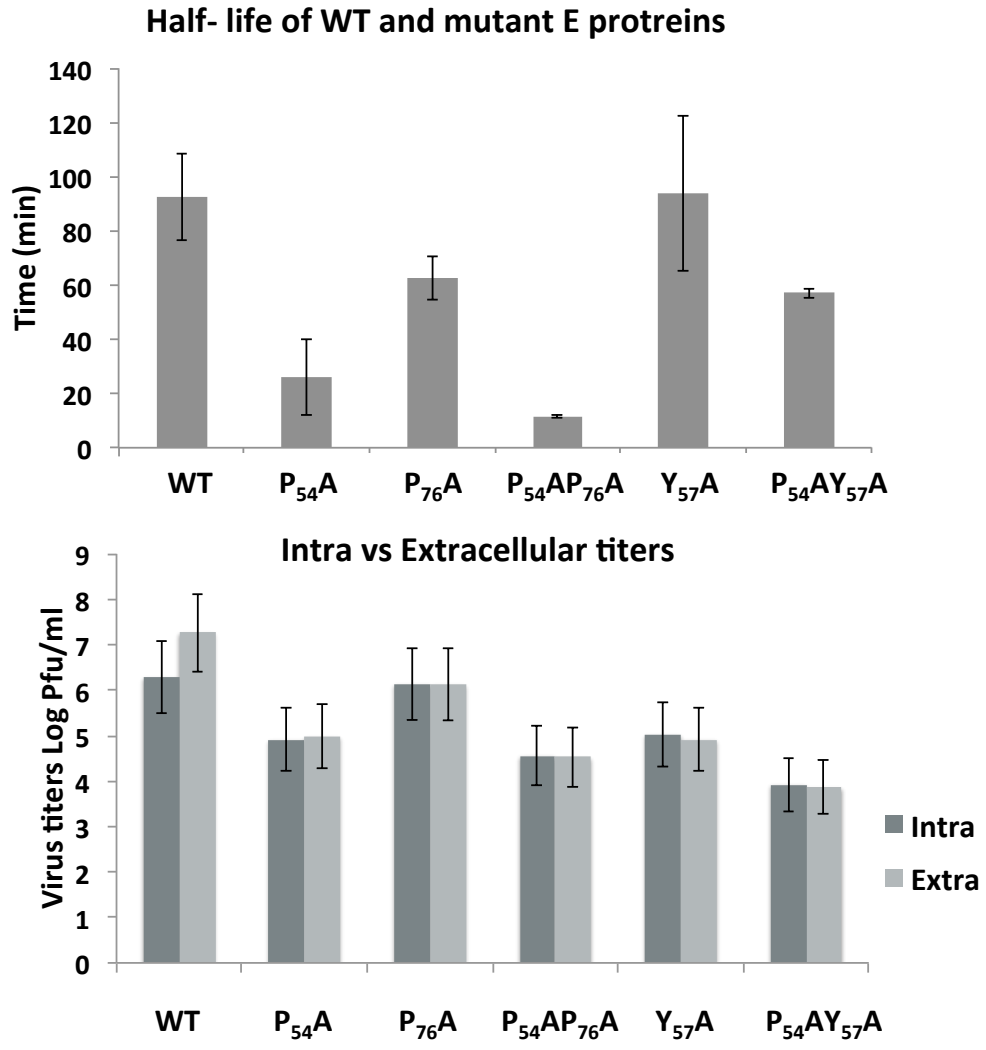
Half- life of WT and mutant E protreins
Time (min)
140
120
100
80
60
40
20
0
WT
P54A
P76A
P54AP76A
Y57A
P54AY57A
Intra vs Extracellular titers
Virus titers Log Pfu/ml
9
8
7
6
5
4
3
2
1
0
Intra
Extra
WT
P54A
P76A
P54AP76A
Y57A
P54AY57A

Figure 16: Mutations affect virus release and protein stability

17cl1 mouse cells were infected at an MOI of 0.01. At 16 hpi, the extracellular (supernatant) and intracellular (cell- associated) viruses were titered using a standard plaque assay. Bar graphs indicate virus titers. Percentage of virus release was calculated as a percentage of extracellular virus over total virus produced. Virus release percentages are indicated above the bar graphs for each mutant. 293 cells were transfected with plasmids expressing WT and mutant E proteins. At 12 hours post transfection, cycloheximide was added to prevent protein translation. At indicated times post addition of cycloheximide, cells were lysed and analyzed for E protein by Western blotting. The levels of E were quantified using Image J and were fit to a first order kinetics. The half-life of WT and E mutants were calculated from the first order kinetics reaction.

E protein does not contain a functional CRAC motif and may induce membrane curvature. Peptides encompassing residues 50- 62 of the E protein was synthesized. The WT peptide ELVLSPSIPLYDRSK and 5457 mutant peptide ELVLSASIALYDRSK were used to analyze their interaction with cholesterol and various lipids using differential scanning nanocalorimetry. Initially, differentially scanning calorimetry was performed using the peptides with the lipid SOPC in the presence and absence of cholesterol. The melting temperature (T_m) of SOPC with 40% cholesterol in the absence of WT or 5457 was 4^0 C. The melting temperature of SOPC with 40% cholesterol in the presence of WT or 5457 peptides at 15 mole fraction was also 4^0C. This suggested that both the peptides did not interact with cholesterol. However, the enthalpy of transition (ΔH) was transition was much lower for SOPC with 40% cholesterol in the presence of both WT and 5457 peptides. This suggested that both WT and 5457 peptides were able to interact with an SOPC lipid bilayer. They were able to dramatically reduce the enthalpy of phase transition in a concentration dependent manner, suggesting that they were able to get incorporated into the lipid. WT peptide was able to reduce the phase transition temperature and the enthalpy of transition of POPS as a function of mole fraction, but 5457 peptide had no effect on either. Both WT and 5457 mutant peptides had a concentration dependent interaction with POPE. WT peptide had an effect on the inverted hexagonal phase transition temperature of POPE. This indicates that the WT peptide may be promoting a negative curvature of the lipid bilayer by destabilizing the bilayer. No such effect was seen upon the addition of the 5457 mutant peptide (Fig. 17).

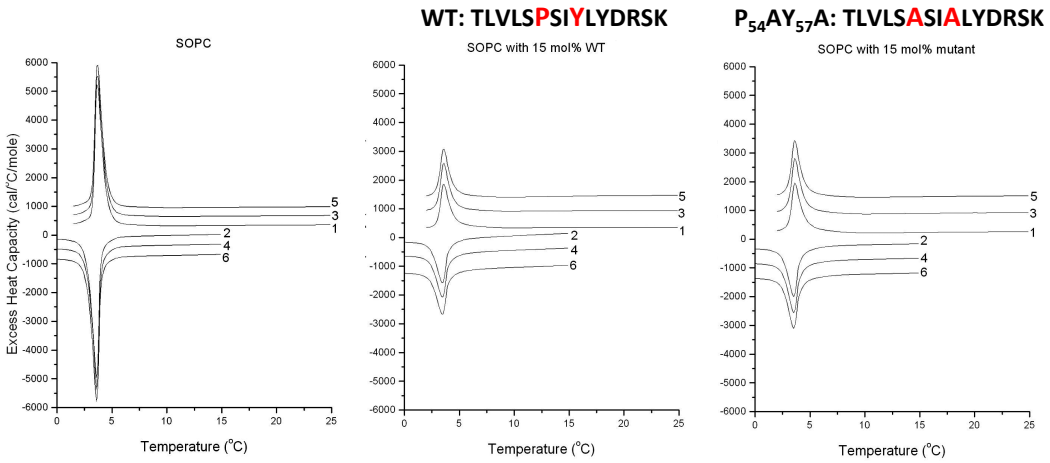
WT: TLVLSPSIYLYDRSK
P54AY57A: TLVLSASIALYDRSK
SOPC
SOPC with 15 mol% WT
SOPC with 15 mol% mutant
Excess Heat Capacity (cal/°C/mole)
Temperature (°C)
1
2
3
4
5
6

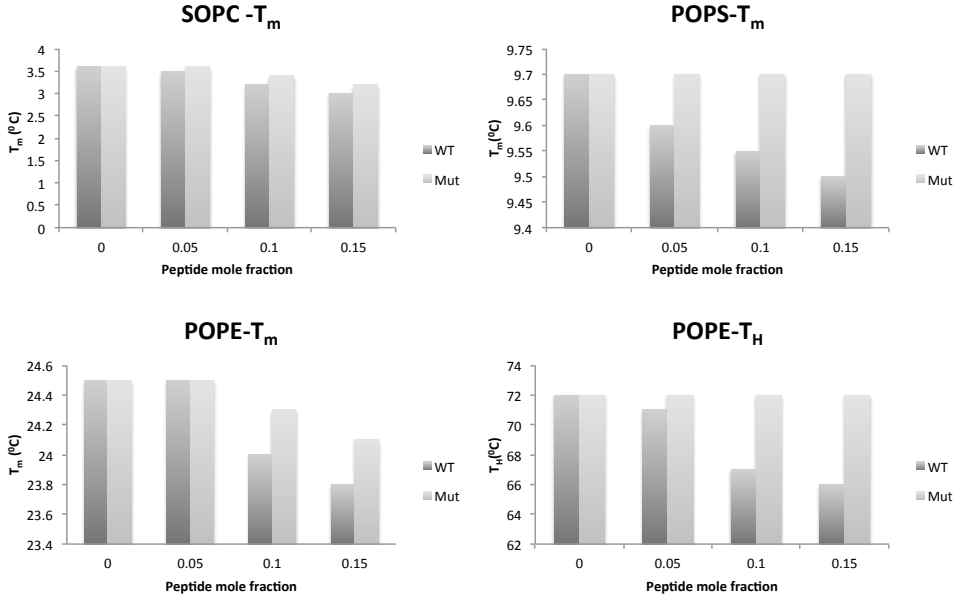
SOPC -Tm
POPS-Tm
POPE-Tm
POPE-TH
Tm (°C)
TH (°C)
Peptide mole fraction
WT
Mut
0
0.05
0.1
0.15

Figure 17: WT peptide interacts with lipids and is not a functional CRAC motif

The top three graphs describe the total enthalpy changes during differential scanning calorimetry. The melting temperature (T_m) of the lipid SOPC with 40% cholesterol is identical in the presence and absence of lipids. The bottom four graphs show the interaction of WT and 5457 peptides with various lipids.

WT (dark grey) and mutant (light grey) peptides were mixed in increasing mole fractions with indicated lipids and differential scanning calorimetry was performed. Bar graphs indicate the melting temperatures (T_m) or hexagonal phase transition temperature (T_H) from the heating cycles.

Results obtained in collaboration with Richard Epand, McMaster University

DISCUSSION

Assembly of coronaviruses at intracellular membranes is a significant area of interest. This mechanism is not clearly understood. The envelope protein, although found in low abundance in the virion, plays a pivotal role in viral assembly, trafficking and release (Kuo and Masters 2003; Boscarino et al. 2008; Ye and Hogue 2007; Ortego et al. 2007). Deletion of the E gene from various coronavirus genomes results in severely crippled or lethal phenotype (Kuo and Masters 2003; Ortego et al. 2007). In MHV, deletion of the E gene from the virus genome did not affect virus replication, but severely decreased virion production (Kuo and Masters 2003). The transmembrane domain of the MHV E protein has been shown to have an ion channel activity in context of the virus and in planar lipid bilayers *in vitro* (Wilson, Gage, and Ewart 2006; Madan et al. 2005). Our previous work showed that the E transmembrane domain is important for the protein to function efficiently during virus assembly and release (Ye and Hogue 2007). Others and we have also shown that the conserved cysteine residues following the TMD are necessary for assembly and virus (Boscarino et al. 2008; Lopez et al. 2008). An earlier study showed that charged residues at the end of the E tail are important for virus production and virion morphology (Fischer et al. 1998). This paper investigates the role of the conserved prolines and tyrosine in the tail of the E protein. Our results indicate that these residues, and the overall structure of the protein as conferred by these residues are required for efficient virus assembly, trafficking and release. However, these residues are not

absolutely essential for localization and interaction with the M protein for envelope formation.

The presence of two highly conserved proline residues in the tail of the E protein suggested that these residues may have an evolutionarily conserved function. To answer this question, site-directed mutagenesis was used to construct single and double proline to alanine substitution mutant viruses using the previously described reverse genetics system. Viruses were recovered for both single and double proline to alanine mutants. This clearly indicated that these proline residues were not required for virus assembly. However, based on the effect of the proline to alanine substitutions, it is clear that these residues play a significant role in virus production.

Upon further analysis of the recovered mutants, they were found to be stable, but viruses containing the mutations were far less robust than the wild-type virus. Growth kinetics analysis of the viruses showed that the proline to alanine double mutant was extremely crippled, whilst the single mutants were affected to different extents. The proline- 54 was found to be more sensitive to changes than proline 76, which may reflect the fact that proline 54 is conserved strictly among all coronavirus E proteins. This strongly suggests that these mutations had an effect on virus assembly.

Co-localization analysis and virus-like particle (VLP) formation along with the M protein conclusively showed that these mutants interacted like WT E to localize correctly and form the envelope. The introduced mutations did not inhibit envelope formation and correct localization of the E protein. It is

interesting to note that envelope formation is not inhibited when the mutant E proteins and M are expressed in cells, whereas virus assembly is affected significantly for some of the viruses. We attribute this to the fact that the high amount of the mutant E protein during transfection most likely overshadows the effect of the mutation on envelope formation. It should be noted that we have not quantified the VLP output. Thus, additional work is necessary to address this.

Previous data for MHV E showed that mutations in the tail affected the thermostability of the virus. The overall stability of the mutant E proteins was affected. The proline to alanine double mutant was found of have a half-life 10 times less than the WT E protein, as determined following transfection. The mutant of $Y_{57}A$ was found to be as stable as WT E but did not achieve WT- like growth characteristics. Thus, this would suggest that the structure is possibly altered.

Previous work for TGEV has shown that the deletion of the E protein results in arrest of virion trafficking (Ortego et al. 2007). Affecting the hydrophobic domain of the MHV E protein also results in reduction in virus release (Ye and Hogue 2007). In case of the proline to alanine mutants, all the mutants were affected in virus release. This can be seen in both the intracellular and extracellular titers and the virus release data. It is interesting to note that when heterologous E proteins were substituted for MHV E, they were tolerated to a large extent. Only substitution of TGEV E for MHV E resulted in various gain of function mutants. One of these mutations was $P_{57}A$, which is homologous to P_{54} in MHV E (Kuo, Hurst, and Masters 2007). The gain of function mutant was still

unable to achieve wild- type MHV characteristics. This suggests that the overall structure of the tail of E protein is crucial for interaction with other viral proteins and host proteins.

Given the highly hydrophobic nature of the E protein and challenges involved in large-scale production of the protein have prevented obtaining a crystal structure of E so far. *In silico* analysis of all the mutant E proteins using multiple prediction softwares and a consensus structure of E was obtained (npsa-pbil.ibcp.fr/). This predicted structure was used as a basis for analyzing the effect of the mutations on the structure of the E protein (Fig. 18). The tail of the E protein is predicted to have a coil-strand-coil-strand-helix conformation and $P_{54}A$ repositions the first strand to a coil conformation. $Y_{57}A$ is not predicted to induce any structural change in the protein. $P_{76}A$ is predicted to extend the last helix in the tail. $P_{54}AY_{57}A$ is predicted to disrupt the tail structure to a coil- helix- strand-helix conformation. $P_{54}AP_{76}A$ changes the conformation to coil-strand-strand-coil conformation and extends the tail helix (Fig. 18). These predicted change would explain the difference in growth properties of these mutant viruses compared to WT. While previous data indicates that the mutant E proteins may be partially functional, the stability data and structure prediction data suggests that the structure of the E protein may be affected.

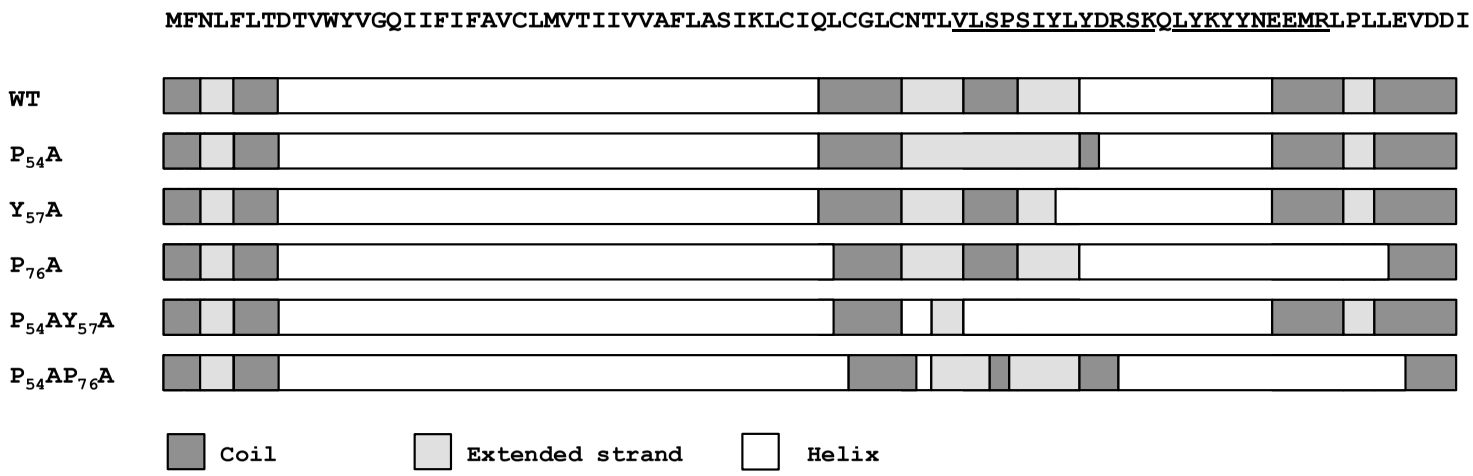
MFNLFLTDTVWYVGQIIFIFAVCLMVTIIVVAFLASIKLCIQLCGLCNTLVLSPSIYLYDRSKQLYKYYNEEMRLPLLEVDDI
WT
P54A
Y57A
P76A
P54AY57A
P54AP76A
Coil
Extended strand
Helix

Figure 18: Secondary structure prediction of E proteins.

Amino acid sequence of WT MHV E protein is shown. Multiple secondary structure prediction softwares were used to generate a consensus structure of the WT and mutant proteins. (npsa-pbil.ibcp.fr/). The two underlined areas indicate the predicted CRAC sequences. Proline to alanine mutations cause a coil- to – strand change or a coil – to- helix change. Tyrosine to alanine substitution causes a strand to helix change.

Recent work on the tail of the SARS envelope protein suggests that the proline corresponding to P_{54} in MHV E and a motif encompassing the Y_{57} may play a role in the Golgi localization of the E protein (Cohen, Lin, and Machamer 2011). However, this was tested using the tail of the SARS E protein linked to the amino and hydrophobic domains of VSV-G and the construct was tested for surface trafficking. Recently, the localization of SARS E has been defined to the ERGIC/ Golgi region and does not traffic to the cell surface (Nieto-Torres et al. 2011, Venkatagopalan et.al. Submitted 2012). We have clearly shown that MHV E does not traffic to the cell surface. The mutants generated in this paper were found to localize in the perinuclear region and the mutations had not effect on the protein localization (data not shown). The severely crippled mutants- 54-57 E and 54-76 E did not traffic to the cell surface. It is possible that the mutation in the motif affects the secondary structure of the region, thereby affecting E-E, E-M and E- host protein interactions. The highly charged tail of the E protein is likely positioned away from the lipid membrane and interacts with viral and host proteins.

The motif comprising residues 50-62 of MHV E contains of a putative cholesterol recognition amino acid consensus (CRAC) sequence (R. F. Epand, Sayer, and Epand 2005; R. M. Epand 2006). Such functional CRAC sequences have been identified in HIV gp41 and influenza M2 proteins (Greenwood et al. 2008; Stewart et al. 2010). The CRAC motif in the HIV gp41 is important for virus entry and membrane fusion. The CRAC motif in the influenza M2 protein has been suggested to play a role in virion pinching-off during virus budding

(McCown and Pekosz 2006). It was hypothesized that the CRAC motif in the tail of the E protein may be playing a role in membrane budding. However, upon testing the WT and 54-57 mutant peptide did not reveal any cholesterol binding properties (data not shown). It was also observed that the peptides themselves interacted differently with the lipids. Upon further analysis, it was found that the WT and 5457 peptides interacted differently with different lipids. The observation that the WT peptide could interact well with POPE and could reduce the inverted hexagonal phase transition temperature was a very surprising observation. The inverted hexagonal phase transition occurs when lipids bilayers are destabilized and undergo a negative curvature. This is a very significant observation because this is the first time the direct interaction of the WT E motif with lipids have been shown and the ability of the WT peptide may induce a negative curvature in the membrane. Budding of coronaviruses takes place into the lumen of the ERGIC (Bost, Prentice, and Denison 2001).The E protein localizes in the ERGIC/Golgi region. As virions bud into the lumen of the ERGIC, EM images show that the membranes undergo a negative curvature (Fig.19). The orientation of the E protein is such that the tail of the E protein is oriented in the cytoplasm. Therefore, it is mechanistically feasible for the tail of the E protein to drive forward this change in the membrane curvature. The E protein may be functioning as a direct or indirect scaffold to aid negative membrane curvature, thereby initiating budding or aid in scission of fully assembled virions (Fig.19). Future experiments will examine the effect of full length MHV E on lipid vesicles and membrane curvature.

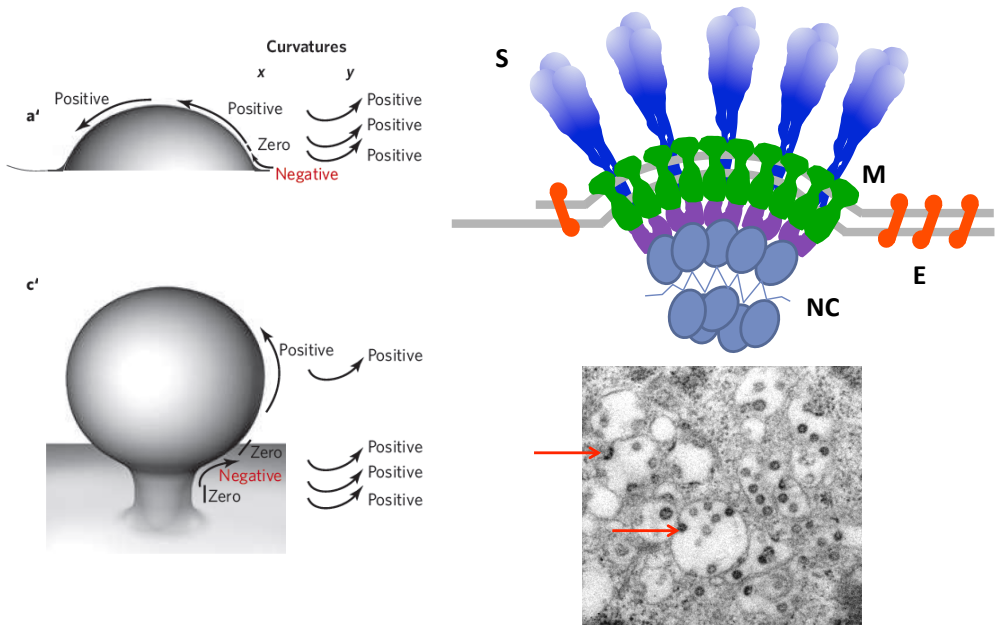

Figure 19: Mechanism of action of the E protein

The tail of the E protein may induce negative curvature in membranes. Schematic on the left shows the various membrane modifications that occur for the formation of a vesicle or a bud. Negative curvature is essential to either initiate budding or to complete bud pinch off. The E protein could be playing a role in initiating budding or virion pinching off or both. The E protein may function as a direct scaffold by directly interacting with the membranes or by interacting with other viral and host proteins.

Membrane curvature and mechanisms of dynamic cell membrane remodelling

Harvey T. McMahon & Jennifer L. Gallop. Nature 2005.

Adapted with permission from Nature publishing.

Further studies will be performed to characterize the effect of these mutants on the ion channel activity of the E protein in artificial lipid bilayers. SARS E has been predicted to form pentameric oligomers in artificial lipid bilayers (Torres et al. 2006).

We will further look into analyzing the effect of these mutations on the oligomerization of E.

ACKNOWLEDGEMENTS

Dr. Sasha Daskalova contributed to recognition and many subsequent discusions of the putative CRAC motifs in coronavirus E proteins. She selected and worked with the ASU Proteomics and Protein Chemistry Core Facility on synthesis and purification of the wild-type and mutant peptides. Dr. Zbigneiw Cichacz developed the protocol and subsequently purified the mutant peptide. The analysis of the putative CRAC motif and differential scanning calorimetry experiments were performed by personnel in Dr. Richard Epand's laboratory at McMaster University, Hamilton, Canada.

Chapter 4

SUMMARIZING DISCUSSION

The localization, dynamics and function of the coronavirus envelope (E) protein have been examined in this study. Multiple studies have examined the localization of various coronavirus E proteins using various expression systems. The results of all these studies have been inconsistent. This study examines the localization of the E protein in a relevant context of virus infection and optimal expression levels. The E protein localizes at the membranes of ERGIC and Golgi during infection and upon expression. This study also uses multiple approaches to determine that the E protein does not traffic to the cell surface, suggesting that the function of E is at the site of assembly in the ERGIC/ Golgi region. The orientation of the E protein has also been confirmed. The MHV E protein has a single pass transmembrane domain, with the amino terminus exposed to the lumen or outside the virion and the carboxy tail in the cytoplasm or inside the virion. This is the first study to successfully generate a functionally tagged MHV E protein. A small tetracysteine tag was appended to the carboxy end of the E protein (E-Lumio) and examined for localization and virion production. The E-Lumio protein localized like WT E and was functional in generating VLPs and recombinant viruses. The advantage of the tetracysteine tag is that it allowed for the visualization of E-Lumio in cells using a fluorescein/resorufin biarsenical derivative. This is the first study to follow live imaging of E using MHV E-Lumio recombinant virus. This also confirmed that the E protein did not traffic out to the cell surface. The dynamics of the E protein was studied using

flourescence recovery after photobleaching (FRAP) analysis. This data revealed that the E protein was mobile at the sight of assembly and had a wide range of mobility. This is the first study to establish and utilize correlative light electron microscopy (CLEM) to study any aspect of coronavirus infection. This challenging technique further confirmed that the E protein localized to the membranes of the ERGIC/ Golgi. This part of the study clearly demonstrated that the E protein localizes and functions at the site of assembly.

Sequence alignment of coronavirus E proteins revealed the presence of conserved prolines at positions 54 and 76 and tyrosine at position 57 for MHV. These residues were targeted for site directed mutagenesis and recombinant viruses were generated. While none of the residues were essential for the function of E, changes around residues 54 and 57 showed that they were more critical to the functions of E. Apart from affecting protein stability, all the changes affected virus release. Bioinformatics analysis suggested the presence of a cholesterol recognition amino acid consensus (CRAC) sequence in the tail of the E protein encompassing residues 54 and 57. WT and mutant synthetic peptides were used to determine any cholesterol interaction using differential scanning calorimetry. While these peptides did not interact with cholesterol, preliminary analysis suggested that the WT peptide preferentially interacted with lipids compared to mutant peptides. The WT peptide was able to reduce the melting temperature of the lipid bilayers in a concentration dependent manner. Of more significance, was the ability of the WT peptide to reduce the hexagonal phase transition temperature of the lipid phosphatidyl-oleyl phosphatidyl ethanol amine (POPE). The

hexagonal phase transition is responsible for a lipid bilayer to undergo a negative curvature. This is the first study to suggest that the E protein may be playing a mechanical role at the site of assembly by possibly inducing a local negative membrane curvature. This opens up many possibilities to the functions of E at the site of assembly.

Previous data has shown that the hydrophobic domain of E is sufficient for membrane insertion and pore formation(Wilson, Gage, and Ewart 2006; Torres et al. 2007). It is possible that the transmembrane domain, the palmitoylated cysteines and the tail may interact with the lipid bilayer differently to initiate a negative change in membrane curvature. Negative curvature plays an important role in two spatio-temporal points of any budding. The leading edge of the bud has a positive curvature, and the lagging edge of the bud has a negative curvature. When any budding occurs into the cytoplasm, cellular membrane curvature sensing protein and stabilizing proteins drive this reaction (Fig.19). The factors needed to initiate and stabilize budding into the lumen are unknown. It is possible that E plays such a role by either functioning as a direct scaffold or interactions mediated through host proteins. One of the important interactions to induce any structural change in the cell is mediated by cytoskeletal interactions. Mass spectrometry analysis shows that SARS E interacts with dynein, a cytoskeletal motor (Alvarez et al. 2010). Moreover, E and M proteins function together to release VLPs. The M protein has been shown to interact with actin. It is possible that E-M-cytoskeleton involvement drives budding. The M protein forms the lattice of the viral envelope (Bárcena et al. 2009). The E and M proteins are the

minimal requirements for MHV envelope formation. M protein has been described to be in two conformations M_{long} and M_{short} and thought to exist in equilibirium (Neuman et al. 2011). The M_{long} conformation has been associated high curvature membranes and efficient virus budding, whereas the M_{short} conformation has been associated with low membrane curvature and in inefficient budding (Neuman et al. 2011). The structural differences between these conformations are unknown, but recent work by Arndt et.al, as suggested that this change may be mediated by residues in the tail of the M protein (unpublished data from Hogue lab). Further, the mechanisms responsible for the conversion of M_{long} to M_{short} are unknown. It is possible that the membrane bending ability of the E protein may stabilize M in the M_{long} conformation. The torsional stress by a highly curved membrane may be responsible for the conversion and /or stability of the M_{long} conformation (Fig. 20). Further, at the completion of any budding, the neck region undergoes high degree of negative curvature before the vesicle pinches off. Normally, the host ESCRT pathway plays a role in this process, but there are no known late domains in any of the coronavirus structural proteins. Moreover, previous studies show that blocking the ESCRT pathway has minimal impact on virus assembly and release (Raaben et al. 2010 and unpublished data from Hogue lab). Recent data has shown that the influenza M2 protein plays a role in virion pinching off in an ESCRT independent pathway. While E protein is expressed well in infected cells, very few molecules are incorporated in virions. The E protein may play a similar role at the site of assembly and E incorporation into the virions may be incidental.

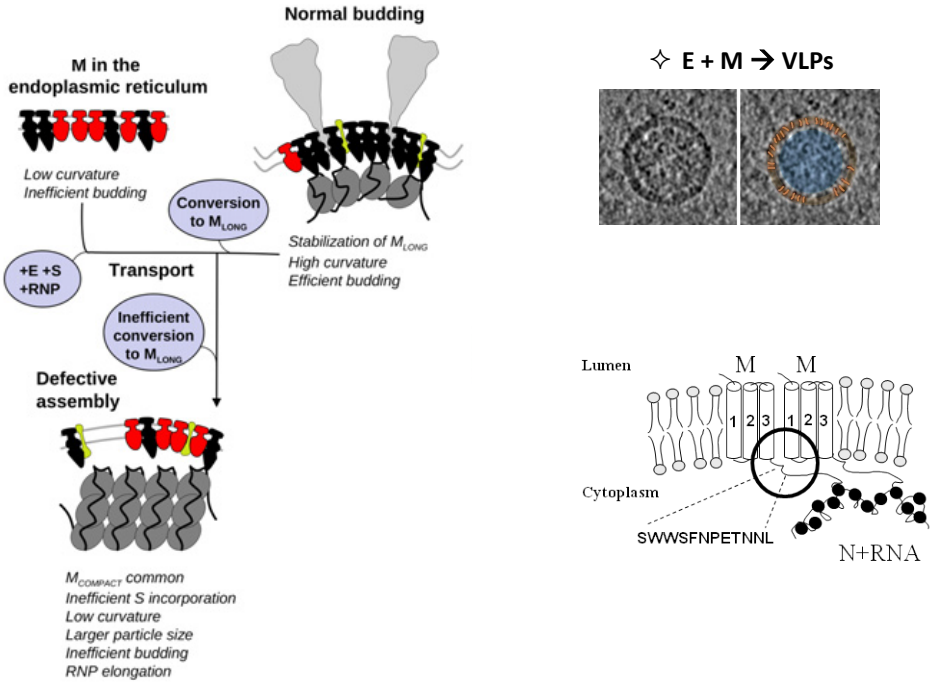

Figure 20: Mechanistic role of E in driving virus assembly

The E protein may play a role in the conversion and stabilization of M_{short} to $M_{long.}$ The E protein may induce a high degree of membrane curvature to drive efficient budding (panel- left). The M protein forms the lattice of the virus lattice. While the M protein is the main protein in maintaining the structure of the viral envelope, the E protein and the nucleocapsid play a role in driving virus assembly (panel- right).

Used with persmission from Neuman 2011, Barcena 2009, Verma 2007, Arndt 2010 unpublished

The E protein has a cation channel activity (Madan et al. 2005; Wilson, Gage, and Ewart 2006). NMR data shows that SARS E organizes pentameric bundle to form the ion channel pore in artificial lipid bilayers(Torres et al. 2006). It is possible that the membrane bending ability of the E protein may enhance or direct the formation of the ion channel. The ion channel activity of E may also change a luminal ionic concentration, which may effect the conversion of M_{short} to M_{long} form. The membrane bending ability of the E protein may also play a role in gating the ion channel activity of E. Peptides in various viral proteins have been identified that have a membrane bending ability and play a functional role in membrane fusion (Greenwood et al. 2008). Most of these are found in surface glycoproteins of various viruses. It is possible that E plays a similar role at the site of assembly.

The E protein has been suggested to be a virulence factor (DeDiego et al. 2008). This is likely due to an indirect effect of E, since the protein does not traffic out to the cell surface and plays no unknown role in virus entry. However, the E protein may cause local membrane modifications that can be sensed by cellular membrane curvature sensing molecules like TLR 4 and TLR 7 (Maier et al. 2010). Signaling through these molecules may activate pathways in the cell that may increase the pathogenicity of virus infection.

In the future, the mechanistic role of E can be analyzed using an artificial liposome based assay to directly study the effect of full length E on membrane curvature. High levels of expression of the E protein has been shown to be associated with membranes of very high curvature. While the E protein may be

making small local changes at earlier times upon infection, the accumulation of E at late times post infection may result in gross membrane modification (Raamsman et al. 2000; Ulasli et al. 2010). At the site of virus budding, there is a higher concentration of electron dense stain, likely caused by osmium tetroxide. Osmium tetroxide specifically targets unsaturated bonds in the side chains of lipids. This suggests that there is a local lipid rearrangement to allow virus budding (Lee and Ahlquist 2003). A comparative mass spectrometric analysis of the WT and mutant viruses will reveal any differences in the lipid content of the virions, which may be attributed to the differences in the E protein. The mutant proteins were not tested for their palmitoylation status. It is possible that the mutations may have prevented the E protein from being palmitoylated. Proline residues at the end of transmembrane domains play a role in ion channel gating (Choe and Grabe 2009). The predicted structural changes at the 54-57 region may have affected the gating of the MHV E ion channel. SARS E has been shown to be ubiquitinated, while the functional significance of this is not known, it is unknown whether MHV E has been ubiquitinated (Alvarez et al. 2010). Bioinformatics analysis of the E protein reveals the presence of a putative clathrin binding motif at the tail of E protein. While clathrin has not been implicated in coronavirus assembly, it is possible that the tail of the E protein may be interacting with multiple host proteins. Mass spectrometric analysis using the Strep- tagged E could be used to identify the host proteins that E may interact with.

REFERENCES

Abramoff, M.D., Magalhaes, P.J., Ram, S.J. "Image Processing with ImageJ".Biophotonics International, volume 11, issue 7, pp. 36-42, 2004.

Almazán, Fernando, Carmen Galán, and Luis Enjuanes. 2004. "The Nucleoprotein Is Required for Efficient Coronavirus Genome Replication.." *Journal of Virology* 78 (22) (November): 12683–12688.

Alvarez, Enrique, Marta L DeDiego, Jose L Nieto-Torres, Jose M Jiménez-Guardeño, Laura Marcos-Villar, and Luis Enjuanes. 2010. "The Envelope Protein of Severe Acute Respiratory Syndrome Coronavirus Interacts with the Non-Structural Protein 3 and Is Ubiquitinated." *Virology* (April 19).

Anon. "Correlative Live Video/ Electron Microscopy." *Current Protocols in Cell Biology*.

Anon. "The Order Nidovirales."

Arbely, Eyal, Ziad Khattari, Guillaume Brotons, Mutaz Akkawi, Tim Salditt, and Isaiah T Arkin. 2004. "A Highly Unusual Palindromic Transmembrane Helical Hairpin Formed by SARS Coronavirus E Protein.." *Journal of Molecular Biology* 341 (3) (August 13): 769–779.

Arndt, Ariel L, Blake J Larson, and Brenda G Hogue. 2010. "A Conserved Domain in the Coronavirus Membrane Protein Tail Is Important for Virus Assembly.." *Journal of Virology* 84 (21) (November): 11418–11428.

Asanaka, M, and M M Lai. 1993. "Cell Fusion Studies Identified Multiple Cellular Factors Involved in Mouse Hepatitis Virus Entry.." *Virology* 197 (2) (December): 732–741.

Bailey, O T, A M Pappenheimer, F S Cheever, and J B Daniels. 1949. "A Murine Virus (Jhm) Causing Disseminated Encephalomyelitis with Extensive Destruction of Myelin : Ii. Pathology.." *The Journal of Experimental Medicine* 90 (3) (August 31): 195–212.

Bárcena, Montserrat, Gert T Oostergetel, Willem Bartelink, Frank G A Faas, Arie Verkleij, Peter J M Rottier, Abraham J Koster, and Berend Jan Bosch. 2009. "Cryo-Electron Tomography of Mouse Hepatitis Virus: Insights Into the Structure of the Coronavirion.." *Proceedings of the National Academy of Sciences of the United States of America* 106 (2) (January 13): 582–587.

Baric, R S, G W Nelson, J O Fleming, R J Deans, J G Keck, N Casteel, and S A Stohlman. 1988. "Interactions Between Coronavirus Nucleocapsid Protein

and Viral RNAs: Implications for Viral Transcription.." *Journal of Virology* 62 (11) (November): 4280–4287.

Baric, R S, S A Stohlman, and M M Lai. 1983. "Characterization of Replicative Intermediate RNA of Mouse Hepatitis Virus: Presence of Leader RNA Sequences on Nascent Chains.." *Journal of Virology* 48 (3) (December): 633–640.

Beaudette, F R. 1950. "Infectious Bronchitis (Differential Characteristics From Newcastle Disease).." *Canadian Journal of Comparative Medicine and Veterinary Science* 14 (1) (January): 24–27.

Benbacer, L, E Kut, L Besnardeau, H Laude, and B Delmas. 1997. "Interspecies Aminopeptidase-N Chimeras Reveal Species-Specific Receptor Recognition by Canine Coronavirus, Feline Infectious Peritonitis Virus, and Transmissible Gastroenteritis Virus.." *Journal of Virology* 71 (1) (January): 734–737.

Bos, E C, W Luytjes, H V van der Meulen, H K Koerten, and W J Spaan. 1996. "The Production of Recombinant Infectious DI-Particles of a Murine Coronavirus in the Absence of Helper Virus.." *Virology* 218 (1) (April 1): 52–60.

Boscarino, Joseph A, Hillary L Logan, Jason J Lacny, and Thomas M Gallagher. 2008. "Envelope Protein Palmitoylations Are Crucial for Murine Coronavirus Assembly.." *Journal of Virology* 82 (6) (March): 2989–2999.

Bost, A G, E Prentice, and M R Denison. 2001. "Mouse Hepatitis Virus Replicase Protein Complexes Are Translocated to Sites of M Protein Accumulation in the ERGIC at Late Times of Infection." *Virology* 285 (1) (June 20): 21–29.

Brierley, I, M E Boursnell, M M Binns, B Bilimoria, V C Blok, T D Brown, and S C Inglis. 1987. "An Efficient Ribosomal Frame-Shifting Signal in the Polymerase-Encoding Region of the Coronavirus IBV.." *The EMBO Journal* 6 (12) (December 1): 3779–3785.

Calvo, E, D Escors, J A López, J M González, A Alvarez, E Arza, and L Enjuanes. 2005. "Phosphorylation and Subcellular Localization of Transmissible Gastroenteritis Virus Nucleocapsid Protein in Infected Cells.." *The Journal of General Virology* 86 (Pt 8) (August): 2255–2267.

Cavanagh, D. 1997. Coronavirus IBV: structural characterization of the spike protein. *The Journal of General Virology* 64 (Pt 12) (December): 2577-2583

Cavanagh, D. 1997. "Nidovirales: a New Order Comprising Coronaviridae and Arteriviridae.." *Archives of Virology* 142 (3): 629–633.

Cavanagh, D, D A Brian, M A Brinton, L Enjuanes, K V Holmes, M C Horzinek, M M Lai, H Laude, P G Plagemann, and S G Siddell. 1993. "The Coronaviridae Now Comprises Two Genera, Coronavirus and Torovirus: Report of the Coronaviridae Study Group.." *Advances in Experimental Medicine and Biology* 342: 255–257.

Cavanagh, D, D Brian, L Enjuanes, K Holmes, M Lai, H Laude, S Siddell, W Spaan, F Taguchi, and P Talbot. 1990. "Revised Nomenclature for Coronavirus Structural Proteins, mRNAs and Genes.." *Advances in Experimental Medicine and Biology* 276: 1–2.

Chang, R Y, and D A Brian. 1996. "Cis Requirement for N-Specific Protein Sequence in Bovine Coronavirus Defective Interfering RNA Replication.." *Journal of Virology* 70 (4) (April): 2201–2207.

Chen, Hongying, Andrew Gill, Brian K Dove, Stevan R Emmett, C Fred Kemp, Mark A Ritchie, Michael Dee, and Julian A Hiscox. 2005. "Mass Spectroscopic Characterization of the Coronavirus Infectious Bronchitis Virus Nucleoprotein and Elucidation of the Role of Phosphorylation in RNA Binding by Using Surface Plasmon Resonance.." *Journal of Virology* 79 (2) (January): 1164–1179.

Chen, Jing, Lin Miao, Jia-Ming Li, Yan-Ying Li, Qing-Yu Zhu, Chang-Lin Zhou, Hong-Qing Fang, and Hui-Peng Chen. 2005. "Receptor-Binding Domain of SARS-Cov Spike Protein: Soluble Expression in E. Coli, Purification and Functional Characterization." *World Journal of Gastroenterology : WJG* 11 (39) (October 21): 6159–6164.

Choe, Seungho, and Michael Grabe. 2009. "Conformational Dynamics of the Inner Pore Helix of Voltage-Gated Potassium Channels.." *The Journal of Chemical Physics* 130 (21) (June 7): 215103.

Cohen, Jennifer R, Lisa D Lin, and Carolyn E Machamer. 2011. "Identification of a Golgi Complex-Targeting Signal in the Cytoplasmic Tail of the Severe Acute Respiratory Syndrome Coronavirus Envelope Protein.." *Journal of Virology* 85 (12) (June): 5794–5803.

Cologna, R, and B G Hogue. 2000. "Identification of a Bovine Coronavirus Packaging Signal.." *Journal of Virology* 74 (1) (January): 580–583.

Cologna, R, J F Spagnolo, and B G Hogue. 2000. "Identification of Nucleocapsid Binding Sites Within Coronavirus-Defective Genomes.." *Virology* 277 (2) (November 25): 235–249.

Corse, E, and C E Machamer. 2000. “Infectious Bronchitis Virus E Protein Is Targeted to the Golgi Complex and Directs Release of Virus-Like Particles..” *Journal of Virology* 74 (9) (May): 4319–4326.

de Groot, R J, R W Van Leen, M J Dalderup, H Vennema, M C Horzinek, and W J Spaan. 1989. “Stably Expressed FIPV Peplomer Protein Induces Cell Fusion and Elicits Neutralizing Antibodies in Mice..” *Virology* 171 (2) (August): 493–502.

De Haan, C A M, B J Haijema, P Schellen, P Wichgers Schreur, E te Lintelo, H Vennema, and P J M Rottier. 2008. “Cleavage of Group 1 Coronavirus Spike Proteins: How Furin Cleavage Is Traded Off Against Heparan Sulfate Binding Upon Cell Culture Adaptation..” *Journal of Virology* 82 (12) (June): 6078–6083.

de Haan, C A, H Vennema, and P J Rottier. 2000. “Assembly of the Coronavirus Envelope: Homotypic Interactions Between the M Proteins..” *Journal of Virology* 74 (11) (June): 4967–4978.

de Haan, C A, L Kuo, P S Masters, H Vennema, and P J Rottier. 1998. “Coronavirus Particle Assembly: Primary Structure Requirements of the Membrane Protein..” *Journal of Virology* 72 (8) (August): 6838–6850.

de Haan, C A, M Smeets, F Vernooij, H Vennema, and P J Rottier. 1999. “Mapping of the Coronavirus Membrane Protein Domains Involved in Interaction with the Spike Protein..” *Journal of Virology* 73 (9) (September): 7441–7452.

de Haan, Cornelis A M, Marèl de Wit, Lili Kuo, Cynthia Montalto-Morrison, Bart L Haagmans, Susan R Weiss, Paul S Masters, and Peter J M Rottier. 2003. “The Glycosylation Status of the Murine Hepatitis Coronavirus M Protein Affects the Interferogenic Capacity of the Virus in Vitro and Its Ability to Replicate in the Liver but Not the Brain..” *Virology* 312 (2) (August 1): 395–406.

de Haan, Cornelis A M, Paul S Masters, Xiaolan Shen, Susan Weiss, and Peter J M Rottier. 2002. “The Group-Specific Murine Coronavirus Genes Are Not Essential, but Their Deletion, by Reverse Genetics, Is Attenuating in the Natural Host..” *Virology* 296 (1) (April 25): 177–189.

Dea, S, A J Verbeek, and P Tijssen. 1990. “Antigenic and Genomic Relationships Among Turkey and Bovine Enteric Coronaviruses..” *Journal of Virology* 64 (6) (June): 3112–3118.

DeDiego, Marta L, Enrique Alvarez, Fernando Almazán, María Teresa Rejas,

Elaine Lamirande, Anjeanette Roberts, Wun-Ju Shieh, Sherif R Zaki, Kanta Subbarao, and Luis Enjuanes. 2007. "A Severe Acute Respiratory Syndrome Coronavirus That Lacks the E Gene Is Attenuated in Vitro and in Vivo." *Journal of Virology* 81 (4) (February 1): 1701–1713.

Delmas, B, and H Laude. 1990. "Assembly of Coronavirus Spike Protein Into Trimers and Its Role in Epitope Expression.." *Journal of Virology* 64 (11) (November): 5367–5375.

Doyle L P, and L M Hutchings. 1946. "A Transmissible Gastroenteritis in Pigs.." *Journal of the American Veterinary Medical Association* 108 (April): 257–259.

Dveksler, G S, M N Pensiero, C B Cardellichio, R K Williams, G S Jiang, K V Holmes, and C W Dieffenbach. 1991. "Cloning of the Mouse Hepatitis Virus (MHV) Receptor: Expression in Human and Hamster Cell Lines Confers Susceptibility to MHV.." *Journal of Virology* 65 (12) (December): 6881–6891.

Egloff, Marie-Pierre, François Ferron, Valérie Campanacci, Sonia Longhi, Corinne Rancurel, Hélène Dutartre, Eric J Snijder, Alexander E Gorbalenya, Christian Cambillau, and Bruno Canard. 2004. "The Severe Acute Respiratory Syndrome-Coronavirus Replicative Protein Nsp9 Is a Single-Stranded RNA-Binding Subunit Unique in the RNA Virus World.." *Proceedings of the National Academy of Sciences of the United States of America* 101 (11) (March 16): 3792–3796.

El-Sahly, H M, R L Atmar, W P Glezen, and S B Greenberg. 2000. "Spectrum of Clinical Illness in Hospitalized Patients with 'Common Cold' Virus Infections.." *Clinical Infectious Diseases : an Official Publication of the Infectious Diseases Society of America* 31 (1) (July): 96–100.

Epand, Raquel F, Brian G Sayer, and Richard M Epand. 2005. "The Tryptophan-Rich Region of HIV Gp41 and the Promotion of Cholesterol-Rich Domains." *Biochemistry* 44 (14) (April 12): 5525–5531.

Epand, Richard M. 2006. "Cholesterol and the Interaction of Proteins with Membrane Domains." *Progress in Lipid Research* 45 (4) (July 1): 279–294.

Escors, D, J Ortego, H Laude, and L Enjuanes. 2001. "The Membrane M Protein Carboxy Terminus Binds to Transmissible Gastroenteritis Coronavirus Core and Contributes to Core Stability.." *Journal of Virology* 75 (3) (February): 1312–1324.

Fischer, F, C F Stegen, P S Masters, and W A Samsonoff. 1998. "Analysis of

Constructed E Gene Mutants of Mouse Hepatitis Virus Confirms a Pivotal Role for E Protein in Coronavirus Assembly.." *Journal of Virology* 72 (10) (October): 7885–7894.

Fleming, J O, S A Stohlman, R C Harmon, M M Lai, J A Frelinger, and L P Weiner. 1983. "Antigenic Relationships of Murine Coronaviruses: Analysis Using Monoclonal Antibodies to JHM (MHV-4) Virus.." *Virology* 131 (2) (December): 296–307.

Flint, S Jane, L W Enquist, and Vincent R Racaniello. 2009. *Principles of Virology (2 Volume Set)*. 3rd ed. ASM Press.

Gagneten, S, O Gout, M Dubois-Dalcq, P Rottier, J Rossen, and K V Holmes. 1995. "Interaction of Mouse Hepatitis Virus (MHV) Spike Glycoprotein with Receptor Glycoprotein MHVR Is Required for Infection with an MHV Strain That Expresses the Hemagglutinin-Esterase Glycoprotein.." *Journal of Virology* 69 (2) (February): 889–895.

Gaietta, Guido M, Ben N G Giepmans, Thomas J Deerinck, W Bryan Smith, Lucy Ngan, Juan Llopis, Stephen R Adams, Roger Y Tsien, and Mark H Ellisman. 2006. "Golgi Twins in Late Mitosis Revealed by Genetically Encoded Tags for Live Cell Imaging and Correlated Electron Microscopy.." *Proceedings of the National Academy of Sciences of the United States of America* 103 (47) (November 21): 17777–17782.

Gallagher, T M, and M J Buchmeier. 2001. "Coronavirus Spike Proteins in Viral Entry and Pathogenesis.." *Virology* 279 (2) (January 20): 371–374.

Gallagher, T M, C Escarmis, and M J Buchmeier. 1991. "Alteration of the pH Dependence of Coronavirus-Induced Cell Fusion: Effect of Mutations in the Spike Glycoprotein.." *Journal of Virology* 65 (4) (April): 1916–1928.

Gombold, J L, S T Hingley, and S R Weiss. 1993. "Fusion-Defective Mutants of Mouse Hepatitis Virus A59 Contain a Mutation in the Spike Protein Cleavage Signal.." *Journal of Virology* 67 (8) (August): 4504–4512.

Gosert, Rainer, Amornrat Kanjanahaluethai, Denise Egger, Kurt Bienz, and Susan C Baker. 2002. "RNA Replication of Mouse Hepatitis Virus Takes Place at Double-Membrane Vesicles.." *Journal of Virology* 76 (8) (April): 3697–3708.

Greenwood, Alexander I, Jianjun Pan, Thalia T Mills, John F Nagle, Richard M Epand, and Stephanie Tristram-Nagle. 2008. "CRAC Motif Peptide of the HIV-1 Gp41 Protein Thins SOPC Membranes and Interacts with Cholesterol." *Biochimica Et Biophysica Acta* 1778 (4) (April 1): 1120–1130.

Hamming, I, W Timens, M L C Bulthuis, A T Lely, G J Navis, and H van Goor. 2004. "Tissue Distribution of ACE2 Protein, the Functional Receptor for SARS Coronavirus. a First Step in Understanding SARS Pathogenesis.." *The Journal of Pathology* 203 (2) (June): 631–637.

Hamre, D, and J J Procknow. 1966. "A New Virus Isolated From the Human Respiratory Tract.." *Proceedings of the Society for Experimental Biology and Medicine. Society for Experimental Biology and Medicine (New York, N.Y.)* 121 (1) (January): 190–193.

Hatakeyama, Seisuke, Yusuke Matsuoka, Hidehiro Ueshiba, Nobukazu Komatsu, Kyogo Itoh, Shigeki Shichijo, Takao Kanai, et al. 2008. "Dissection and Identification of Regions Required to Form Pseudoparticles by the Interaction Between the Nucleocapsid (N) and Membrane (M) Proteins of SARS Coronavirus." *Virology* 380 (1) (October 10): 99–108.

Hofmann, Heike, Krzysztof Pyrc, Lia van der Hoek, Martina Geier, Ben Berkhout, and Stefan Pöhlmann. 2005. "Human Coronavirus NL63 Employs the Severe Acute Respiratory Syndrome Coronavirus Receptor for Cellular Entry.." *Proceedings of the National Academy of Sciences of the United States of America* 102 (22) (May 31): 7988–7993.

Hogue, B G, T E Kienzle, and D A Brian. 1989. "Synthesis and Processing of the Bovine Enteric Coronavirus Haemagglutinin Protein.." *The Journal of General Virology* 70 (Pt 2) (February): 345–352.

Hsieh, Ping-Kun, Shin C Chang, Chu-Chun Huang, Ting-Ting Lee, Ching-Wen Hsiao, Yi-Hen Kou, I-Yin Chen, Chung-Ke Chang, Tai-Huang Huang, and Ming-Fu Chang. 2005. "Assembly of Severe Acute Respiratory Syndrome Coronavirus RNA Packaging Signal Into Virus-Like Particles Is Nucleocapsid Dependent.." *Journal of Virology* 79 (22) (November): 13848–13855.

Huang, Qiulong, Liping Yu, Andrew M Petros, Angelo Gunasekera, Zhihong Liu, Nan Xu, Philip Hajduk, Jamey Mack, Stephen W Fesik, and Edward T Olejniczak. 2004. "Structure of the N-Terminal RNA-Binding Domain of the SARS CoV Nucleocapsid Protein.." *Biochemistry* 43 (20) (May 25): 6059–6063.

Huang, Yue, Zhi-yong Yang, Wing-pui Kong, and Gary J Nabel. 2004. "Generation of Synthetic Severe Acute Respiratory Syndrome Coronavirus Pseudoparticles: Implications for Assembly and Vaccine Production.." *Journal of Virology* 78 (22) (November): 12557–12565.

Hurst, Kelley R, Lili Kuo, Cheri A Koetzner, Rong Ye, Bilan Hsue, and Paul S

Masters. 2005. “A Major Determinant for Membrane Protein Interaction Localizes to the Carboxy-Terminal Domain of the Mouse Coronavirus Nucleocapsid Protein..” *Journal of Virology* 79 (21) (November): 13285–13297.

Jendrach, M, V Thiel, and S Siddell. 1999. “Characterization of an Internal Ribosome Entry Site Within mRNA 5 of Murine Hepatitis Virus..” *Archives of Virology* 144 (5): 921–933.

Jiménez, G, I Correa, M P Melgosa, M J Bullido, and L Enjuanes. 1986. “Critical Epitopes in Transmissible Gastroenteritis Virus Neutralization..” *Journal of Virology* 60 (1) (October): 131–139.

Kazi, Lubna, Arjen Lissenberg, Richard Watson, Raoul J de Groot, and Susan R Weiss. 2005. “Expression of Hemagglutinin Esterase Protein From Recombinant Mouse Hepatitis Virus Enhances Neurovirulence..” *Journal of Virology* 79 (24) (December): 15064–15073.

Kienzle, T E, S Abraham, B G Hogue, and D A Brian. 1990. “Structure and Orientation of Expressed Bovine Coronavirus Hemagglutinin-Esterase Protein..” *Journal of Virology* 64 (4) (April): 1834–1838.

Klumperman, J, J K Locker, A Meijer, M C Horzinek, H J Geuze, and P J Rottier. 1994. “Coronavirus M Proteins Accumulate in the Golgi Complex Beyond the Site of Virion Budding..” *Journal of Virology* 68 (10) (October): 6523–6534.

Krijnse-Locker, J, M Ericsson, P J Rottier, and G Griffiths. 1994. “Characterization of the Budding Compartment of Mouse Hepatitis Virus: Evidence That Transport From the RER to the Golgi Complex Requires Only One Vesicular Transport Step..” *The Journal of Cell Biology* 124 (1-2) (January): 55–70.

Ksiazek, Thomas G, Dean Erdman, Cynthia S Goldsmith, Sherif R Zaki, Teresa Peret, Shannon Emery, Suxiang Tong, et al. 2003. “A Novel Coronavirus Associated with Severe Acute Respiratory Syndrome..” *The New England Journal of Medicine* 348 (20) (May 15): 1953–1966.

Kuo, Lili, and Paul S Masters. 2002. “Genetic Evidence for a Structural Interaction Between the Carboxy Termini of the Membrane and Nucleocapsid Proteins of Mouse Hepatitis Virus..” *Journal of Virology* 76 (10) (May): 4987–4999.

Kuo, Lili, and Paul S Masters. 2003. “The Small Envelope Protein E Is Not Essential for Murine Coronavirus Replication..” *Journal of Virology* 77 (8)

(April): 4597–4608.

Kuo, Lili, and Paul S Masters. 2010. “Evolved Variants of the Membrane Protein Can Partially Replace the Envelope Protein in Murine Coronavirus Assembly..” *Journal of Virology* 84 (24) (December): 12872–12885.

Kuo, Lili, Kelley R Hurst, and Paul S Masters. 2007. “Exceptional Flexibility in the Sequence Requirements for Coronavirus Small Envelope Protein Function..” *Journal of Virology* 81 (5) (March): 2249–2262.

Künkel, F, and G Herrler. 1993. “Structural and Functional Analysis of the Surface Protein of Human Coronavirus OC43..” *Virology* 195 (1) (July): 195–202.

Lai, M M, and D Cavanagh. 1997. “The Molecular Biology of Coronaviruses..” *Advances in Virus Research* 48: 1–100.

Lai, M M, R S Baric, P R Brayton, and S A Stohlman. 1984. “Characterization of Leader RNA Sequences on the Virion and mRNAs of Mouse Hepatitis Virus, a Cytoplasmic RNA Virus..” *Proceedings of the National Academy of Sciences of the United States of America* 81 (12) (June): 3626–3630.

Lau, Susanna K P, Patrick C Y Woo, Cyril C Y Yip, Herman Tse, Hoi-Wah Tsoi, Vincent C C Cheng, Paul Lee, et al. 2006. “Coronavirus HKU1 and Other Coronavirus Infections in Hong Kong..” *Journal of Clinical Microbiology* 44 (6) (June): 2063–2071.

Lau, Susanna K P, Patrick C Y Woo, Kenneth S M Li, Yi Huang, Hoi-Wah Tsoi, Beatrice H L Wong, Samson S Y Wong, Suet-Yi Leung, Kwok-Hung Chan, and Kwok-Yung Yuen. 2005. “Severe Acute Respiratory Syndrome Coronavirus-Like Virus in Chinese Horseshoe Bats..” *Proceedings of the National Academy of Sciences of the United States of America* 102 (39) (September 27): 14040–14045.

Lecce, J G, M W King, and R Mock. 1976. “Reovirus-Like Agent Associated with Fatal Diarrhea in Neonatal Pigs..” *Infection and Immunity* 14 (3) (September): 816–825.

Lee, Wai-Ming, and Paul Ahlquist. 2003. “Membrane Synthesis, Specific Lipid Requirements, and Localized Lipid Composition Changes Associated with a Positive-Strand RNA Virus RNA Replication Protein..” *Journal of Virology* 77 (23) (December): 12819–12828.

Lewicki, Daniel N, and Thomas M Gallagher. 2002. “Quaternary Structure of

Coronavirus Spikes in Complex with Carcinoembryonic Antigen-Related Cell Adhesion Molecule Cellular Receptors.." *The Journal of Biological Chemistry* 277 (22) (May 31): 19727–19734.

Li, Fang. 2012. "Evidence for a Common Evolutionary Origin of Coronavirus Spike Protein Receptor-Binding Subunits.." *Journal of Virology* 86 (5) (March): 2856–2858.

Li, Wendong, Zhengli Shi, Meng Yu, Wuze Ren, Craig Smith, Jonathan H Epstein, Hanzhong Wang, et al. 2005. "Bats Are Natural Reservoirs of SARS-Like Coronaviruses.." *Science (New York, NY)* 310 (5748) (October 28): 676–679.

Li, Wenhui, Michael J Moore, Natalya Vasilieva, Jianhua Sui, Swee Kee Wong, Michael A Berne, Mohan Somasundaran, et al. 2003. "Angiotensin-Converting Enzyme 2 Is a Functional Receptor for the SARS Coronavirus.." *Nature* 426 (6965) (November 27): 450–454.

Liao, Y, Q Yuan, J Torres, J P Tam, and D X Liu. 2006. "Biochemical and Functional Characterization of the Membrane Association and Membrane Permeabilizing Activity of the Severe Acute Respiratory Syndrome Coronavirus Envelope Protein.." *Virology* 349 (2) (June 5): 264–275.

Lim, K P, and D X Liu. 2001. "The Missing Link in Coronavirus Assembly. Retention of the Avian Coronavirus Infectious Bronchitis Virus Envelope Protein in the Pre-Golgi Compartments and Physical Interaction Between the Envelope and Membrane Proteins.." *The Journal of Biological Chemistry* 276 (20) (May 18): 17515–17523.

.

Locker, J K, J K Rose, M C Horzinek, and P J Rottier. 1992. "Membrane Assembly of the Triple-Spanning Coronavirus M Protein. Individual Transmembrane Domains Show Preferred Orientation.." *The Journal of Biological Chemistry* 267 (30) (October 25): 21911–21918.

Lopez, Lisa A, Ambere J Riffle, Steven L Pike, Douglas Gardner, and Brenda G Hogue. 2008. "Importance of Conserved Cysteine Residues in the Coronavirus Envelope Protein.." *Journal of Virology* 82 (6) (March): 3000–3010.

Luo, Haibin, Dalei Wu, Can Shen, Kaixian Chen, Xu Shen, and Hualiang Jiang. 2006. "Severe Acute Respiratory Syndrome Coronavirus Membrane Protein Interacts with Nucleocapsid Protein Mostly Through Their Carboxyl Termini by Electrostatic Attraction.." *The International Journal of Biochemistry & Cell Biology* 38 (4): 589–599.

Luo, Haibin, Fei Ye, Kaixian Chen, Xu Shen, and Hualiang Jiang. 2005. "SR-Rich Motif Plays a Pivotal Role in Recombinant SARS Coronavirus Nucleocapsid Protein Multimerization.." *Biochemistry* 44 (46) (November 22): 15351–15358.

Luo, Z, and S R Weiss. 1998. "Roles in Cell-to-Cell Fusion of Two Conserved Hydrophobic Regions in the Murine Coronavirus Spike Protein.." *Virology* 244 (2) (May 10): 483–494.

Lustig, A, and A J Levine. 1992. *One Hundred Years of Virology*. *Journal of Virology*. Vol. 66.

Luytjes, W, P J Bredenbeek, A F Noten, M C Horzinek, and W J Spaan. 1988. "Sequence of Mouse Hepatitis Virus A59 mRNA 2: Indications for RNA Recombination Between Coronaviruses and Influenza C Virus.." *Virology* 166 (2) (October): 415–422.

Macneughton, M R, and H A Davies. 1978. "Ribonucleoprotein-Like Structures From Coronavirus Particles.." *The Journal of General Virology* 39 (3) (June): 545–549.

Maeda, J, A Maeda, and S Makino. 1999. "Release of Coronavirus E Protein in Membrane Vesicles From Virus-Infected Cells and E Protein-Expressing Cells.." *Virology* 263 (2) (October 25): 265–272.

Maeda, J, J F Repass, A Maeda, and S Makino. 2001. "Membrane Topology of Coronavirus E Protein.." *Virology* 281 (2) (March 15): 163–169.

Madan, Vanessa, Meritxell de Jesús García, Miguel A Sanz, and Luis Carrasco. 2005. "Viroporin Activity of Murine Hepatitis Virus E Protein.." *FEBS Letters* 579 (17) (July 4): 3607–3612.

Maier, Oana, Debra L Galan, Harald Wodrich, and Christopher M Wiethoff. 2010. "An N-Terminal Domain of Adenovirus Protein VI Fragments Membranes by Inducing Positive Membrane Curvature." *Virology* 402 (1) (June 20): 11–19.

Masters, P S. 1992. "Localization of an RNA-Binding Domain in the Nucleocapsid Protein of the Coronavirus Mouse Hepatitis Virus.." *Archives of Virology* 125 (1-4): 141–160.

McBride, Corrin E, and Carolyn E Machamer. 2010. "A Single Tyrosine in the Severe Acute Respiratory Syndrome Coronavirus Membrane Protein Cytoplasmic Tail Is Important for Efficient Interaction with Spike Protein.." *Journal of Virology* 84 (4) (February): 1891–1901.

McCown, Matthew F, and Andrew Pekosz. 2006. “Distinct Domains of the Influenza a Virus M2 Protein Cytoplasmic Tail Mediate Binding to the M1 Protein and Facilitate Infectious Virus Production.” *Journal of Virology* 80 (16) (August 1): 8178–8189.

McIntosh, K, J H Dees, W B Becker, A Z Kapikian, and R M Chanock. 1967. “Recovery in Tracheal Organ Cultures of Novel Viruses From Patients with Respiratory Disease..” *Proceedings of the National Academy of Sciences of the United States of America* 57 (4) (April): 933–940.

Mohandas, D V, and S Dales. 1991. “Endosomal Association of a Protein Phosphatase with High Dephosphorylating Activity Against a Coronavirus Nucleocapsid Protein..” *FEBS Letters* 282 (2) (May 6): 419–424.

Molenkamp, R, and W J Spaan. 1997. “Identification of a Specific Interaction Between the Coronavirus Mouse Hepatitis Virus A59 Nucleocapsid Protein and Packaging Signal..” *Virology* 239 (1) (December 8): 78–86.

Nakajima, Atsushi, Hideki Iijima, Markus F Neurath, Takashi Nagaishi, Edward E S Nieuwenhuis, Raktima Raychowdhury, Jonathan Glickman, et al. 2002. “Activation-Induced Expression of Carcinoembryonic Antigen-Cell Adhesion Molecule 1 Regulates Mouse T Lymphocyte Function..” *Journal of Immunology (Baltimore, Md : 1950)* 168 (3) (February 1): 1028–1035.

Narayanan, K, A Maeda, J Maeda, and S Makino. 2000. “Characterization of the Coronavirus M Protein and Nucleocapsid Interaction in Infected Cells..” *Journal of Virology* 74 (17) (September): 8127–8134.

Narayanan, K, and S Makino. 2001. “Cooperation of an RNA Packaging Signal and a Viral Envelope Protein in Coronavirus RNA Packaging..” *Journal of Virology* 75 (19) (October): 9059–9067.

Narayanan, Krishna, Kyongmin Hwang Kim, and Shinji Makino. 2003. “Characterization of N Protein Self-Association in Coronavirus Ribonucleoprotein Complexes..” *Virus Research* 98 (2) (December): 131–140.

Nelson, G W, and S A Stohlman. 1993. “Localization of the RNA-Binding Domain of Mouse Hepatitis Virus Nucleocapsid Protein..” *The Journal of General Virology* 74 (Pt 9) (September): 1975–1979.

Nelson, G W, S A Stohlman, and S M Tahara. 2000. “High Affinity Interaction Between Nucleocapsid Protein and Leader/Intergenic Sequence of Mouse Hepatitis Virus RNA..” *The Journal of General Virology* 81 (Pt 1) (January): 181–188.

Neuman, Benjamin W, Gabriella Kiss, Andreas H Kunding, David Bhella, M Fazil Baksh, Stephen Connelly, Ben Droese, et al. 2011. "A Structural Analysis of M Protein in Coronavirus Assembly and Morphology.." *Journal of Structural Biology* 174 (1) (April): 11–22.

Nguyen, V P, and B G Hogue. 1997. "Protein Interactions During Coronavirus Assembly.." *Journal of Virology* 71 (12) (December): 9278–9284.

Niemann, H, R Geyer, H D Klenk, D Linder, S Stirm, and M Wirth. 1984. "The Carbohydrates of Mouse Hepatitis Virus (MHV) A59: Structures of the O-Glycosidically Linked Oligosaccharides of Glycoprotein E1.." *The EMBO Journal* 3 (3) (March): 665–670.

Nieto-Torres, Jose L, Marta L DeDiego, Enrique Alvarez, Jose M Jiménez-Guardeño, Jose A Regla-Nava, Mercedes Llorente, Leonor Kremer, Shen Shuo, and Luis Enjuanes. 2011. "Subcellular Location and Topology of Severe Acute Respiratory Syndrome Coronavirus Envelope Protein.." *Virology* 415 (2) (July 5): 69–82.

Oostra, M, C A M De Haan, R J de Groot, and P J M Rottier. 2006. "Glycosylation of the Severe Acute Respiratory Syndrome Coronavirus Triple-Spanning Membrane Proteins 3a and M." *Journal of Virology* 80 (5) (March 1): 2326–2336.

Opstelten, D J, M J Raamsman, K Wolfs, M C Horzinek, and P J Rottier. 1995. "Envelope Glycoprotein Interactions in Coronavirus Assembly.." *The Journal of Cell Biology* 131 (2) (October): 339–349.

Ortego, Javier, Juan E Ceriani, Cristina Patiño, Juan Plana, and Luis Enjuanes. 2007. "Absence of E Protein Arrests Transmissible Gastroenteritis Coronavirus Maturation in the Secretory Pathway." *Virology* 368 (2) (November 25): 296–308.

Oshiro, L S, J H Schieble, and E H Lennette. 1971. "Electron Microscopic Studies of Coronavirus." *The Journal of General Virology* 12 (2) (August 1): 161–168.

Palokangas, H, M Ying, K Väänänen, and J Saraste. 1998. "Retrograde Transport From the Pre-Golgi Intermediate Compartment and the Golgi Complex Is Affected by the Vacuolar H+-ATPase Inhibitor Bafilomycin A1." *Molecular Biology of the Cell* 9 (12) (December 1): 3561–3578.

Parker, M M, and P S Masters. 1990. "Sequence Comparison of the N Genes of Five Strains of the Coronavirus Mouse Hepatitis Virus Suggests a Three Domain Structure for the Nucleocapsid Protein.." *Virology* 179 (1)

(November): 463–468.

Parry, Jane. 2003. "WHO Warns That Death Rate From SARS Could Reach 10%.." *BMJ (Clinical Research Ed.)*, May 10.

Payne, H R, and J Storz. 1988. "Analysis of Cell Fusion Induced by Bovine Coronavirus Infection.." *Archives of Virology* 103 (1-2): 27–33.

Peng, Guiqing, Dawei Sun, Kanagalaghatta R Rajashankar, Zhaohui Qian, Kathryn V Holmes, and Fang Li. 2011. "Crystal Structure of Mouse Coronavirus Receptor-Binding Domain Complexed with Its Murine Receptor.." *Proceedings of the National Academy of Sciences of the United States of America* 108 (26) (June 28): 10696–10701.

Pervushin, Konstantin, Edward Tan, Krupakar Parthasarathy, Xin Lin, Feng Li Jiang, Dejie Yu, Ardcharaporn Vararattanavech, Tuck Wah Soong, Ding Xiang Liu, and Jaume Torres. 2009. "Structure and Inhibition of the SARS Coronavirus Envelope Protein Ion Channel." *PLoS Pathogens* 5 (7) (July 1): e1000511.

Pratelli, A, A Tinelli, N Decaro, F Cirone, G Elia, S Roperto, M Tempesta, and C Buonavoglia. 2003. "Efficacy of an Inactivated Canine Coronavirus Vaccine in Pups.." *The New Microbiologica* 26 (2) (April): 151–155.

Raaben, Matthijs, Clara C Posthuma, Monique H Verheije, Eddie G Te Lintelo, Marjolein Kikkert, Jan W Drijfhout, Eric J Snijder, Peter J M Rottier, and Cornelis A M de Haan. 2010. "The Ubiquitin-Proteasome System Plays an Important Role During Various Stages of the Coronavirus Infection Cycle.." *Journal of Virology* 84 (15) (August): 7869–7879.

Raamsman, M J, J K Locker, A de Hooge, A A de Vries, G Griffiths, H Vennema, and P J Rottier. 2000. "Characterization of the Coronavirus Mouse Hepatitis Virus Strain A59 Small Membrane Protein E.." *Journal of Virology* 74 (5) (March): 2333–2342.

Ramajayam, R, Kian-Pin Tan, and Po-Huang Liang. 2011. "Recent Development of 3C and 3CL Protease Inhibitors for Anti-Coronavirus and Anti-Picornavirus Drug Discovery.." *Biochemical Society Transactions* 39 (5) (October): 1371–1375.

Rasband, W.S., ImageJ, U. S. National Institutes of Health, Bethesda, Maryland, USA, http://imagej.nih.gov/ij/, 1997-2011.

Risco, C, I M Antón, C Suñé, A M Pedregosa, J M Martín-Alonso, F Parra, J L Carrascosa, and L Enjuanes. 1995. "Membrane Protein Molecules of Transmissible Gastroenteritis Coronavirus Also Expose the Carboxy-

Terminal Region on the External Surface of the Virion.." *Journal of Virology* 69 (9) (September): 5269–5277.

Routledge, E, R Stauber, M Pfleiderer, and S G Siddell. 1991. "Analysis of Murine Coronavirus Surface Glycoprotein Functions by Using Monoclonal Antibodies.." *Journal of Virology* 65 (1) (January): 254–262.

Ruch, Travis R, and Carolyn E Machamer. 2011. "The Hydrophobic Domain of Infectious Bronchitis Virus E Protein Alters the Host Secretory Pathway and Is Important for Release of Infectious Virus.." *Journal of Virology* 85 (2) (January): 675–685.

Saikatendu, Kumar Singh, Jeremiah S Joseph, Vanitha Subramanian, Tom Clayton, Mark Griffith, Kin Moy, Jeffrey Velasquez, et al. 2005. "Structural Basis of Severe Acute Respiratory Syndrome Coronavirus ADP-Ribose-1''-Phosphate Dephosphorylation by a Conserved Domain of nsP3.." *Structure (London, England : 1993)* 13 (11) (November): 1665–1675.

Sawicki, S G, and D L Sawicki. 1990. "Coronavirus Transcription: Subgenomic Mouse Hepatitis Virus Replicative Intermediates Function in RNA Synthesis.." *Journal of Virology* 64 (3) (March): 1050–1056.

Sawicki, S G, and D L Sawicki. 2005. "Coronavirus Transcription: a Perspective.." *Current Topics in Microbiology and Immunology* 287: 31–55.

Schelle, Barbara, Nadja Karl, Burkhard Ludewig, Stuart G Siddell, and Volker Thiel. 2005. "Selective Replication of Coronavirus Genomes That Express Nucleocapsid Protein.." *Journal of Virology* 79 (11) (June): 6620–6630.

Schochetman, G, R H Stevens, and R W Simpson. 1977. "Presence of Infectious Polyadenylated RNA in Coronavirus Avian Bronchitis Virus.." *Virology* 77 (2) (April): 772–782.

Schultze, B, and G Herrler. 1992. "Bovine Coronavirus Uses N-Acetyl-9-O-Acetylneuraminic Acid as a Receptor Determinant to Initiate the Infection of Cultured Cells.." *The Journal of General Virology* 73 (Pt 4) (April): 901–906.

Seybert, A, A Hegyi, S G Siddell, and J Ziebuhr. 2000. "The Human Coronavirus 229E Superfamily 1 Helicase Has RNA and DNA Duplex-Unwinding Activities with 5'-to-3' Polarity.." *RNA (New York, NY)* 6 (7) (July): 1056–1068.

Shapiro, L H, R A Ashmun, W M Roberts, and A T Look. 1991. "Separate Promoters Control Transcription of the Human Aminopeptidase N Gene in

Myeloid and Intestinal Epithelial Cells.." *The Journal of Biological Chemistry* 266 (18) (June 25): 11999–12007.

Shih, Yi-Ping, Chia-Yen Chen, Shih-Jen Liu, Kuan-Hsuan Chen, Yuan-Ming Lee, Yu-Chan Chao, and Yi-Ming Arthur Chen. 2006. "Identifying Epitopes Responsible for Neutralizing Antibody and DC-SIGN Binding on the Spike Glycoprotein of the Severe Acute Respiratory Syndrome Coronavirus." *Journal of Virology* 80 (21) (November 1): 10315–10324.

Siddell, S. 1995. *The Coronaviridae*. Springer.

Sinha, A, H G Shen, S Schalk, N M Beach, Y W Huang, P G Halbur, X J Meng, and T Opriessnig. 2010. "Porcine Reproductive and Respiratory Syndrome Virus Infection at the Time of Porcine Circovirus Type 2 Vaccination Has No Impact on Vaccine Efficacy.." *Clinical and Vaccine Immunology : CVI* 17 (12) (December): 1940–1945.

Siu, Y L, K T Teoh, J Lo, C M Chan, F Kien, N Escriou, S W Tsao, et al. 2008. "The M, E, and N Structural Proteins of the Severe Acute Respiratory Syndrome Coronavirus Are Required for Efficient Assembly, Trafficking, and Release of Virus-Like Particles.." *Journal of Virology* 82 (22) (November): 11318–11330.

Sloots, Theo P, Peter McErlean, David J Speicher, Katherine E Arden, Michael D Nissen, and Ian M Mackay. 2006. "Evidence of Human Coronavirus HKU1 and Human Bocavirus in Australian Children.." *Journal of Clinical Virology : the Official Publication of the Pan American Society for Clinical Virology* 35 (1) (January): 99–102.

Snijder, Eric J, Peter J Bredenbeek, Jessika C Dobbe, Volker Thiel, John Ziebuhr, Leo L M Poon, Yi Guan, Mikhail Rozanov, Willy J M Spaan, and Alexander E Gorbalenya. 2003. "Unique and Conserved Features of Genome and Proteome of SARS-Coronavirus, an Early Split-Off From the Coronavirus Group 2 Lineage.." *Journal of Molecular Biology* 331 (5) (August 29): 991–1004.

Snijder, Eric J, Yvonne van der Meer, Jessika Zevenhoven-Dobbe, Jos J M Onderwater, Jannes van der Meulen, Henk K Koerten, and A Mieke Mommaas. 2006. "Ultrastructure and Origin of Membrane Vesicles Associated with the Severe Acute Respiratory Syndrome Coronavirus Replication Complex.." *Journal of Virology* 80 (12) (June): 5927–5940.

Spaan, W, H Delius, M Skinner, J Armstrong, P Rottier, S Smeekens, B A Van der Zeijst, and S G Siddell. 1983. "Coronavirus mRNA Synthesis Involves Fusion of Non-Contiguous Sequences.." *The EMBO Journal* 2 (10): 1839–

1844.

Spagnolo, J F, and B G Hogue. 2000. “Host Protein Interactions with the 3' End of Bovine Coronavirus RNA and the Requirement of the Poly(a) Tail for Coronavirus Defective Genome Replication..” *Journal of Virology* 74 (11) (June): 5053–5065.

Spencer, Kelly-Anne, Michael Dee, Paul Britton, and Julian A Hiscox. 2008. “Role of Phosphorylation Clusters in the Biology of the Coronavirus Infectious Bronchitis Virus Nucleocapsid Protein..” *Virology* 370 (2) (January 20): 373–381.

Stewart, Shaun M, Wai-Hong Wu, Erin N Lalime, and Andrew Pekosz. 2010. “The Cholesterol Recognition/Interaction Amino Acid Consensus Motif of the Influenza a Virus M2 Protein Is Not Required for Virus Replication but Contributes to Virulence.” *Virology* 405 (2) (September 30): 530–538.

Sturman, L S, and K V Holmes. 1977. “Characterization of Coronavirus II. Glycoproteins of the Viral Envelope: Tryptic Peptide Analysis..” *Virology* 77 (2) (April): 650–660.

Teoh, Kim-Tat, Yu-Lam Siu, Wing-Lim Chan, Marc A Schlüter, Chia-Jen Liu, J S Malik Peiris, Roberto Bruzzone, Benjamin Margolis, and Béatrice Nal. 2010. “The SARS Coronavirus E Protein Interacts with PALS1 and Alters Tight Junction Formation and Epithelial Morphogenesis.” *Molecular Biology of the Cell* 21 (22) (November 1): 3838–3852.

Thiel, V, and S G Siddell. 1994. “Internal Ribosome Entry in the Coding Region of Murine Hepatitis Virus mRNA 5..” *The Journal of General Virology* 75 (Pt 11) (November): 3041–3046.

Thorp, Edward B, Joseph A Boscarino, Hillary L Logan, Jeffrey T Goletz, and Thomas M Gallagher. 2006. “Palmitoylations on Murine Coronavirus Spike Proteins Are Essential for Virion Assembly and Infectivity..” *Journal of Virology* 80 (3) (February): 1280–1289.

Tong, Suxiang, Christina Conrardy, Susan Ruone, Ivan V Kuzmin, Xiling Guo, Ying Tao, Michael Niezgoda, et al. 2009. “Detection of Novel SARS-Like and Other Coronaviruses in Bats From Kenya..” *Emerging Infectious Diseases* 15 (3) (March): 482–485.

Tooze, J, and S A Tooze. 1985. “Infection of AtT20 Murine Pituitary Tumour Cells by Mouse Hepatitis Virus Strain A59: Virus Budding Is Restricted to the Golgi Region..” *European Journal of Cell Biology* 37 (May): 203–212.

Tooze, S A, J Tooze, and G Warren. 1988. “Site of Addition of N-Acetyl-Galactosamine to the E1 Glycoprotein of Mouse Hepatitis Virus-A59..” *The Journal of Cell Biology* 106 (5) (May): 1475–1487.

Torres, Jaume, Krupakar Parthasarathy, Xin Lin, Rathi Saravanan, Andreas Kukol, and Ding Xiang Liu. 2006. “Model of a Putative Pore: the Pentameric Alpha-Helical Bundle of SARS Coronavirus E Protein in Lipid Bilayers.” *Biophysical Journal* 91 (3) (August 1): 938–947.

Torres, Jaume, Uma Maheswari, Krupakar Parthasarathy, Lifang Ng, Ding Xiang Liu, and Xiandi Gong. 2007. “Conductance and Amantadine Binding of a Pore Formed by a Lysine-Flanked Transmembrane Domain of SARS Coronavirus Envelope Protein.” *Protein Science : a Publication of the Protein Society* 16 (9) (September 1): 2065–2071.

Tseng, Ying-Tzu, Shiu-Mei Wang, Kuo-Jung Huang, Amber I-Ru Lee, Chien-Cheng Chiang, and Chin-Tien Wang. 2010. “Self-Assembly of Severe Acute Respiratory Syndrome Coronavirus Membrane Protein..” *The Journal of Biological Chemistry* 285 (17) (April 23): 12862–12872.

Turner, Brian C, Erin M Hemmila, Nicole Beauchemin, and Kathryn V Holmes. 2004. “Receptor-Dependent Coronavirus Infection of Dendritic Cells..” *Journal of Virology* 78 (10) (May): 5486–5490.

Tyrrell, D A, M L Bynoe, and B Hoorn. 1968. “Cultivation of ‘Difficult’ Viruses From Patients with Common Colds..” *British Medical Journal* 1 (5592) (March 9): 606–610.

Ulasli, Mustafa, Monique H Verheije, Cornelis A M de Haan, and Fulvio Reggiori. 2010. “Qualitative and Quantitative Ultrastructural Analysis of the Membrane Rearrangements Induced by Coronavirus..” *Cellular Microbiology* 12 (6) (June): 844–861.

van der Hoek, Lia, Krzysztof Pyrc, Maarten F Jebbink, Wilma Vermeulen-Oost, Ron J M Berkhout, Katja C Wolthers, Pauline M E Wertheim-van Dillen, Jos Kaandorp, Joke Spaargaren, and Ben Berkhout. 2004. “Identification of a New Human Coronavirus..” *Nature Medicine* 10 (4) (April): 368–373.

Vennema, H, G J Godeke, J W Rossen, W F Voorhout, M C Horzinek, D J Opstelten, and P J Rottier. 1996. “Nucleocapsid-Independent Assembly of Coronavirus-Like Particles by Co-Expression of Viral Envelope Protein Genes..” *The EMBO Journal* 15 (8) (April 15): 2020–2028.

Verheije, Monique H, Marne C Hagemeijer, Mustafa Ulasli, Fulvio Reggiori, Peter J M Rottier, Paul S Masters, and Cornelis A M de Haan. 2010. “The

Coronavirus Nucleocapsid Protein Is Dynamically Associated with the Replication-Transcription Complexes.." *Journal of Virology* 84 (21) (November): 11575–11579.

Verma, Sandhya, Lisa A Lopez, Valerie Bednar, and Brenda G Hogue. 2007. "Importance of the Penultimate Positive Charge in Mouse Hepatitis Coronavirus A59 Membrane Protein.." *Journal of Virology* 81 (10) (May): 5339–5348.

Verma, Sandhya, Valerie Bednar, Andrew Blount, and Brenda G Hogue. 2006. "Identification of Functionally Important Negatively Charged Residues in the Carboxy End of Mouse Hepatitis Coronavirus A59 Nucleocapsid Protein.." *Journal of Virology* 80 (9) (May): 4344–4355.

Voss, Daniel, Susanne Pfefferle, Christian Drosten, Lea Stevermann, Elisabetta Traggiai, Antonio Lanzavecchia, and Stephan Becker. 2009. "Studies on Membrane Topology, N-Glycosylation and Functionality of SARS-CoV Membrane Protein.." *Virology Journal* 6: 79.

Wang, Jibin, Shouguo Fang, Han Xiao, Bo Chen, James P Tam, and Ding Xiang Liu. 2009. "Interaction of the Coronavirus Infectious Bronchitis Virus Membrane Protein with Beta-Actin and Its Implication in Virion Assembly and Budding.." *PloS One* 4 (3): e4908.

White, Tiana C, Zhengping Yi, and Brenda G Hogue. 2007. "Identification of Mouse Hepatitis Coronavirus A59 Nucleocapsid Protein Phosphorylation Sites.." *Virus Research* 126 (1-2) (June): 139–148.

Wilbur, S M, G W Nelson, M M Lai, M McMillan, and S A Stohlman. 1986. "Phosphorylation of the Mouse Hepatitis Virus Nucleocapsid Protein.." *Biochemical and Biophysical Research Communications* 141 (1) (November 26): 7–12.

Williams, R K, G S Jiang, and K V Holmes. 1991. "Receptor for Mouse Hepatitis Virus Is a Member of the Carcinoembryonic Antigen Family of Glycoproteins.." *Proceedings of the National Academy of Sciences of the United States of America* 88 (13) (July 1): 5533–5536.

Wilson, Lauren, Carolyn McKinlay, Peter Gage, and Gary Ewart. 2004. "SARS Coronavirus E Protein Forms Cation-Selective Ion Channels.." *Virology* 330 (1) (December 5): 322–331.

Wilson, Lauren, Peter Gage, and Gary Ewart. 2006. "Hexamethylene Amiloride Blocks E Protein Ion Channels and Inhibits Coronavirus Replication.." *Virology* 353 (2) (September 30): 294–306.

Woo, Patrick C Y, Susanna K P Lau, Chung-ming Chu, Kwok-Hung Chan, Hoi-Wah Tsoi, Yi Huang, Beatrice H L Wong, et al. 2005. "Characterization and Complete Genome Sequence of a Novel Coronavirus, Coronavirus HKU1, From Patients with Pneumonia.." *Journal of Virology* 79 (2) (January): 884–895.

Xu, H Y, K P Lim, S Shen, and D X Liu. 2001. "Further Identification and Characterization of Novel Intermediate and Mature Cleavage Products Released From the ORF 1b Region of the Avian Coronavirus Infectious Bronchitis Virus 1a/1b Polyprotein.." *Virology* 288 (2) (September 30): 212–222.

Ye, Ye, and Brenda G Hogue. 2007. "Role of the Coronavirus E Viroporin Protein Transmembrane Domain in Virus Assembly.." *Journal of Virology* 81 (7) (April): 3597–3607.

Yount, B, K M Curtis, and R S Baric. 2000. "Strategy for Systematic Assembly of Large RNA and DNA Genomes: Transmissible Gastroenteritis Virus Model.." *Journal of Virology* 74 (22) (November): 10600–10611.

Yount, Boyd, Mark R Denison, Susan R Weiss, and Ralph S Baric. 2002. "Systematic Assembly of a Full-Length Infectious cDNA of Mouse Hepatitis Virus Strain A59.." *Journal of Virology* 76 (21) (November): 11065–11078.

Yount, Boyd, Rhonda S Roberts, Amy C Sims, Damon Deming, Matthew B Frieman, Jennifer Sparks, Mark R Denison, Nancy Davis, and Ralph S Baric. 2005. "Severe Acute Respiratory Syndrome Coronavirus Group-Specific Open Reading Frames Encode Nonessential Functions for Replication in Cell Cultures and Mice.." *Journal of Virology* 79 (23) (December): 14909–14922.

Zelus, Bruce D, Jeanne H Schickli, Dianna M Blau, Susan R Weiss, and Kathryn V Holmes. 2003. "Conformational Changes in the Spike Glycoprotein of Murine Coronavirus Are Induced at 37 Degrees C Either by Soluble Murine CEACAM1 Receptors or by pH 8.." *Journal of Virology* 77 (2) (January): 830–840.

Zhou, M, and E W Collisson. 2000. "The Amino and Carboxyl Domains of the Infectious Bronchitis Virus Nucleocapsid Protein Interact with 3' Genomic RNA.." *Virus Research* 67 (1) (March): 31–39.

Ziebuhr, J. 2005. "The Coronavirus Replicase.." *Current Topics in Microbiology and Immunology* 287: 57–94.

Ziebuhr, J, and S G Siddell. 1999. "Processing of the Human Coronavirus 229E

Replicase Polyproteins by the Virus-Encoded 3C-Like Proteinase: Identification of Proteolytic Products and Cleavage Sites Common to Pp1a and Pp1ab.." *Journal of Virology* 73 (1) (January): 177–185.

Ziebuhr, J, E J Snijder, and A E Gorbalenya. 2000. "Virus-Encoded Proteinases and Proteolytic Processing in the Nidovirales.." *The Journal of General Virology* 81 (Pt 4) (April): 853–879.

APPENDIX A

OPTIMIZATION OF THE USE OF THE TETRA-CYSTEINE TAGGED E FOR USE IN CORRELATIVE LIGHT ELECTRON MICROSCOPY (CLEM) AND LIVE CELL IMAGING

INTRODUCTION

Correlative Light Electron Microscopy (CLEM) is a complex technique in microscopy that combines light and electron microscopy (Current protocols CLEM). Immunofluorescence provides invaluable information regarding the location of proteins in the cells, but a single fluorescing single spot may represent protein aggregates, trafficking vesicles or an entire organelle. Identification of the location of a protein in a cell requires ultrastructural information. This information can be gathered by performing thin section transmission electron microscopy on the same cells from where live-cell IF data has been collected. This allows one to observe the location of a protein and in the same cell determine at the ultrastructures that the protein is associated with. This method is called correlative light electron microscopy (CLEM). CLEM has successfully been used by other researchers to study the localization of GFP-tagged cellular proteins by live cell imaging, followed by thin section TEM analysis in the same cell.

Lumio ™ (Invitrogen) is a short 6 amino acid tetracysteine peptide (Cys-Cys-Xaa-Xaa-Cys-Cys) that can be appended to a protein without generally disrupting its structure or function. Lumio ™ labeling reagents are based on biarsenical labeling reagents bind to the tetracysteine tag when added to cells and under appropriate wavelength fluoresces with high specificity (Invitrogen.com). This allows *in vivo* live cell analysis of localization and trafficking of the protein. The LumioTM Green Labeling Reagent is based on the FlAsH reagent and is a non-fluorescent, biarsenical derivative of fluorescein. The reagent can fluoresce when bound to the tetracysteine tag and excited at 508 nm with an emission

maxima at 608 nm (Invitrogen.com). This reagent can be used for live cell imaging and has been used for flourescnece recovery after photobleaching (FRAP) analyses in our experiments. The Lumio Red Labeling Reagent is based on the ReAsH reagent and is a non-fluorescent, biarsenical derivative of the red fluorophore resorufin (Invitrogen.com). This reagent can fluoresce when bound to the tetra-cysteine tag and excited at 593 nm laser. It has emission maxima of 608 nm (Invitrogen.com). This reagent has the ability to release free radicals in the presence of bright light and photoconvert diaminobenzidine to an electron dense photoprecipitate (Gaietta et al. 2006)

. While the technology for photoconversion has been around for a while, this is the first system that used a small tag to fluorescently label a protein and use the same tag to combine light and electron microscopy. The project involved extensive use of the SOLS bioimaging facilities, including the Keck Bioimaging Lab confocal and EM microscopes. Establishment of this state-of-the-art imaging capability helped provide significant new information on the role of the E protein in coronavirus assembly. This powerful technology can be easily adapted for use in various projects. I have provided a generalized description of the methodology used to establish this technology during my graduate work.

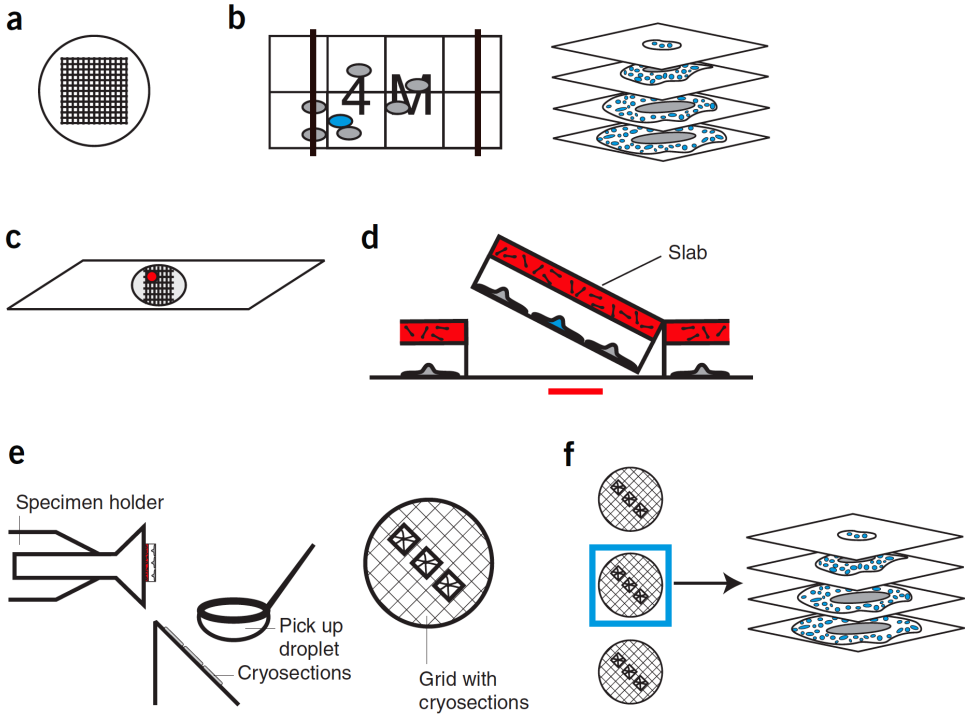

Figure 21: Protocol for Correlative Live Imaging and Electron Microscopy

Cells were grown in a glass bottomed gridded coverslip. Flourescent images were obtained of specific cells and the position of the cell on a grid was noted. Confocal images of specific cells were obtained. Flourescent signals were converted to electron dense precipitate. The coverslip was processed for electron microscopy and embedded in resin. Based on the grid position of the cell of interest, the cell was excised using a razor blade and ultra thin (70m) serial sections of the specific cells were obtained and electron micrographs were obtained.

Adapted with permission from Nature Methods 5, 973 - 980 (2008)

MATERIALS

1. 35mm Glass bottomed cell culture dish with gridded coverslip of No. 1 thickness (MatTek)
2. Dry lubricant spray (Electron Microscopy Sciences)
3. Glutaraldehyde (Sigma Aldrich)
4. Phosphate buffer pH 7.4
5. DTT (Sigma Aldrich)
6. Sodium Cacodylate buffer
7. Blocking buffer: 10 mM KCN, 10 mM aminotriazole, 0.01% hydrogen peroxide, 50 mM glycine in 0.1 M cacodylate buffer
8. Diaminobenzidine at 1mg/ml in blocking buffer
9. Cells
10. Tetracysteine tagged protein
11. Lumio Green or Lumio Red In Cell staining kit (Invitrogen)
12. Kim-Wipes
13. dH_20
14. 2% Osmium tetroxide (Electron Microscopy Sciences)
15. Eponate 12 resin (Electron Microscopy Sciences)
16. Laminar flow hood
17. Cell culture incubator (37 ^{0}C and 5% CO_2)
18. Confocal microscope with heated stage, humidifier and heated objective lens
19. Ultra Microtome

20. Transmission Electron microscope (Philips 80kV STEM)

METHODS

Initial preparation

1. Spray glass-bottomed coverslip with dry lubricant, allow to dry and wipe down twice with Kim wipe.
2. Place dish open in the laminar flow hood and expose to UV for atleast 90 minutes.
3. Seed susceptible cells at required density.
4. Infect or transfect cells with appropriately tagged virus or protein.
5. At specific time post infection or transfection, label the cells with the Lumio Green or Lumio Red reagent

Lumio Staining

1. Aspirate media and wash cells twice with any reduced serum media such as Opti-MEM.
2. Add Lumio Green or Lumio Red at a final concentration of 1mM to the cells.
3. Place immediately back in the in the incubator for 30 min to 1 hour depending on the level of expression of the tagged protein.
4. Aspirate media and wash cells twice with reduced serum media.
5. Add DTT at a final concentration of 1mM to the cells.
6. Place immediately back in the incubator for 10 min.
7. Repeat steps 5 and 6 atleast twice.
8. Refeed cells with complete media and allow cells to recover for 1 hour.

For Live Cell imaging and FRAP

1. Prepare the confocal microscope stage with the live cell imaging chamber.
2. Ensure that the chamber temperature, humidity and CO_2 levels are equilibrated for optimal cell survival.
3. Collect images using appropriate lasers (489 nm for Lumio Green and 545 nm for Lumio Red).
4. Adjust laser power, pin-hole opening, detection gain to ensure best signal-to –noise ratio.
5. For live cell imaging, ensure that the temperature, humidity and CO_2 levels are maintained constant throughout the experiment.
6. For FRAP analysis, measure a pre-bleach image using low laser power and a completely open pin-hole.
7. Choose a specific region for photo bleaching such that the bleached volume is an insignificant portion of the total signal volume using the high laser power to ensure complete photo bleaching.
8. This is important for Lumio stained samples because unlike GFP tagged proteins, the total amount of stained protein remains the same throughout the experiment.
9. Immediately upon bleaching collect images using pre-bleach settings with very short intervals such as 1- 5 seconds.
10. Analyze the mobility fraction as the ratio of the recovered intensity over the bleached density.

For Correlative Live and Electron Microscopy (CLEM)

1. Only Lumio Red or ReAsH is capable of photoconversion and must be used for CLEM.
2. Capture live cell images as described above.
3. Obtain the location of the cell in the gridded coverslip using phase contrast or DIC imaging.
4. Keep careful record of fluorescent images and their position on the gridded coverslip.
5. Once all fluorescent images are obtained, photoconversion is carried out.
6. Aspirate media and wash cells twice in Phosphate buffer pH 7.4.
7. Fix cells in 2% glutaraldehyde sodium cacodylate buffer at room temperature for 1 hour. Ensure that the cells are not disturbed during the process of fixation.
8. Aspirate the fixative and wash cells in blocking buffer.
9. Incubate at room temperature for 10 minutes.
10. Replace blocking buffer with freshly prepared 1mg/ml diaminobenzidine in blocking buffer.
11. Carry our photoconversion using a 75W Xenon lamp without neutral density filters focused through the 10X objective.
12. Capture the photoconverted images of previously images cells using the position of the cells recorded from the gridded coverslip.

Processing for electron microscopy

1. Aspirate the photoconversion buffer from the cells.

2. Wash cells twice in water.
3. Add 0.1 M Osmium tetroxide to the dish and incubate at room temperature for 1 hour
4. Wash cells twice in water.
5. Dehydrate cells in increasing concentration of acetone for 10 minutes each.
6. Complete hydration with 100 % acetone three times for 10 minutes each.
7. Resin infiltration:
    a. Make up fresh Eponate 12 resin (medium hard)
    b. Make increasing concentrations of Eponate- 12 in acetone (25, 50, 70 %) and treat the cells for 8 hours each. At this time, the cells are placed on a rocker to allow even resin distribution.
    c. Treat the cells with 100 % resin 3X for 12 hours each.
8. Place dish in 65 ^{0}C incubator for 48 hours.
9. Once polymerization is complete, freeze the dish -20 ^{0}C for 10 minutes.
10. Detach the resin from the dish.
11. An image of the gridded coverslip will be transferred with the detached resin, along with the cells.
12. Cut out individual cells observed using the location of the cell on the gridded coverslip.
13. Place the individual cells on resin blocks using Superglue and allow to set overnight.
14. Trim and section the cells using an ultramicrotome at 60-70 nm thickness.
15. Collect serial sections and observe samples in the electron microscope.